NOVEL THERAPEUTIC FOR RESPIRATORY SYNCYTIAL VIRUS

DEVELOPMENT OF NOVEL PEPTIDE MIMETIC THERAPEUTICS FOR RESPIRATORY SYNCYTIAL VIRUS

By CHRISTOPHER K.W. CHIANG, B.Sc.

A Thesis Submitted to the School of Graduate Studies in Partial Fulfillment of the Requirements for the Degree Master of Science

McMaster University © Copyright by Christopher Chiang, July 2017

DESCRIPTIVE NOTE

McMaster University MASTER OF SCIENCE (2017) Hamilton, Ontario (Medical Science)

TITLE: Development of Novel Peptide Mimetic Therapeutics for Respiratory Syncytial Virus

AUTHOR: Christopher Chiang, B.Sc. (McMaster University)

SUPERVISOR: Dr. James Mahony

NUMBER OF PAGES: xix, 96

LAY ABSTRACT

Respiratory syncytial virus is a respiratory illness that is one of the leading causes of childhood hospitalization worldwide. RSV infects almost all infants at least once by the age of two. It can also repeatedly infect individuals throughout their lives, which puts the elderly and individuals with weak immune, cardiac or pulmonary systems at risk. There are also no approved vaccines or antiviral treatments available to prevent or combat a RSV infection, which highlights the pressing need for the development of new antiviral drugs. This thesis focuses on developing and evaluating the efficacy of two different antiviral peptides, which both target and disrupt the formation of the viral machinery required for the replication of the RSV genome.

ABSTRACT

Background: Respiratory syncytial virus (RSV) is one of the leading causes of acute lower respiratory tract infection and childhood hospitalization worldwide. However, there are currently no vaccines or antivirals available to prevent or treat RSV infections. Of the 11 proteins encoded by RSV's negative-sense single-stranded RNA genome, the nucleoprotein, phosphoprotein, and large polymerase interact through well characterized domains to form the RNA-dependent RNA polymerase complex. This polymerase complex is essential for viral replication and virulence, which makes it an excellent antiviral target. Previous studies have shown that the nucleoprotein-phosphoprotein interaction of the polymerase complex can be disrupted by synthetic peptides of the last 21 C-terminal ($P_{220-241}$) or the first 29 N-terminal (P_{1-29}) amino acids of the phosphoprotein.

Objective: The Mahony lab has also previously demonstrated that $P_{220-241}$ conjugated to a maltose binding protein (MBP) and HIV-1 Tat cell penetrating peptide (CPP) could inhibit up to 90% of RSV A replication *in vitro*. However, the bacterial derived MBP is immunogenic. This study builds on these findings by developing and evaluating the efficacy of a $P_{220-241}$ peptide mimetic conjugated to human thioredoxin (hTrx) carrier protein and a P_{1-29} peptide mimetic conjugated to MBP.

Methods and Results: Inverse PCR and In-Fusion® cloning was used to clone a hTrx-$P_{220-241}$ plasmid, which was then expressed as a recombinant protein and purified by affinity chromatography for functional analysis. HTrx-$P_{220-241}$ was shown to specifically interact with RSV nucleoprotein in a glutathione S-transferase (GST) pull down assays and it could

successfully enter into LLC-MK2 cells. However, upon challenge with RSV A, LLC-MK2 cells that were incubated with increasing concentrations of hTrx-$P_{220-241}$ did not inhibit RSV A replication when assessed by indirect immunofluorescence microscopy. The MBP-P_{1-29} construct did not exhibit any significant cytotoxicity in LLC-MK2 cells nor BEAS-2B cells. Upon challenge with RSV A, LLC-MK2 cells and BEAS-2B cells pre-treated with MBP-P_{1-29} demonstrated a dose-dependent inhibition of RSV replication *in vitro*, with a percent inhibition of infection of 80% and 60% respectively. Furthermore, MBP-P_{1-29} also reduced the release of infectious progeny virion by up to 74% in LLC-MK2 cells and 34% in BEAS-2B cells.

Conclusion: Phosphoprotein peptide mimetics targeting essential nucleoprotein-phosphoprotein interaction are a promising approach in the development of therapeutic treatments for RSV. In this study, a $P_{220-241}$ peptide mimetic conjugated to a human thioredoxin scaffold protein was not able to inhibit RSV A replication while a P_{1-29} peptide attached to a maltose binding protein was effective in reducing RSV replication *in vitro*. Thus, further studies are required to evaluate a P_{1-29} peptide mimetic against different RSV A and B strains and to find an appropriate human carrier protein to attach it to.

Acknowledgements

I would first like to thank my research supervisor, Dr. James Mahony, for providing me with the opportunity to conduct innovative research in his cutting edge laboratory. Over the span of four years, you have been a great mentor teaching me about the scientific process and how to meticulously plan each experiment. Your passion for research and your fervent curiosity have taught me the importance of reading and incorporating new discoveries in the scientific literature to my project. I am very fortunate to have been under your tutelage and I am grateful for all the knowledge and lifelong skills you have instilled upon me. I would also like to thank my committee members, Dr. Kjetil Ask and Dr. Marek Smieja. Your diverse academic backgrounds and research specialties have provided me with thoughtful guidance and advice as well as the importance of considering the clinical challenges and implications of my research.

I am also honoured to have spent the last four years working and learning alongside many academically talented and bright students. They have continuously challenged me to become a better researcher and a better individual while providing me with a positive and fun environment to grow in. I would like to extend special thanks to Dr. David Bulir who has been an inspiration and a tremendous source of help in my project. He has always strongly encouraged me to critically analyze my experiments and has always been there to answer both science and life questions. Dr. Christopher Stone has always been a great role model and a source of entertainment. I would like to thank Sylvia Chong who has always been very understanding about the lab members' inability to keep essential reagents stocked and our unique standards of cleanliness. I would also like to extend a special mention to

Dan Jang who has always been a pleasure to talk to and has always considered me as his second son. I would also like to thank my fellow graduate students Steven Liang, Zachariah Scinocca, Samantha Mihalco, and Jordan Nelson. We shared many jokes, worries, and food adventures as well as entertaining scientific and philosophical discussions. I am also grateful to other members of the lab who have contributed to my years of pleasurable lab experience: Jodi Gilchrist, Kathy Luinstra, Lucas Penny, Karanbir Brar, Chae Muhn, Steven Zhang, Kimberly Lau, Heather Gunter, Albert Choe, Karishma Manji, Harsukh Kaur, Kenneth Mwawasi, and Jerry Wang.

Finally, I owe my deepest gratitude to my family and friends who have been my pillar of support throughout my Master's degree and life in general. My father and mother, Lee and Gina, and my brother, Albert, have always provided me with kind words of encouragement and monthly care packages, which have always been welcomed and greatly appreciated. I could not do it without their continual support and I hope to continue making them proud as I move onto the next chapter in my life.

This thesis is dedicated to my parents, Lee and Gina, and my older brother, Albert

TABLE OF CONTENTS

List of Abbreviations……...xiii

List of Figures…….xvii

List of Tables……..xviii

Declaration of Academic Achievement…….….xix

Chapter 1 – Introduction and Thesis Objectives……...…1

1.1 Respiratory Syncytial Virus History and Overview……2

1.2 Respiratory Syncytial Virus Clinical Features and Epidemiology……..3

1.3 Respiratory Syncytial Virus Transmission and Seasonality……5

1.4 Respiratory Syncytial Virus Taxonomy and Antigenic Diversity……...7

1.5 Respiratory Syncytial Virus Genome……..8

1.6 Respiratory Syncytial Virus Replication and Life Cycle……...11

1.7 Current Treatment Options – Vaccines…….16

1.8 Current Treatment Options – Pharmaceutical Options……..18

1.9 Antiviral Target: The nucleoprotein-phosphoprotein interaction in the RNA-dependent RNA polymerase……23

1.10 The Use of Peptide Mimetics as Novel Antiviral Therapeutics……...25

1.11 The Mutated Human Thioredoxin Carrier Protein……..26

1.12 Thesis Objectives……27

Chapter 2 – Materials and Methods……28

2.1 Development of peptide mimetic expression vectors

2.1.1 Primer Design for Peptide Mimetic Constructs and Primer Resuspension……...29

2.1.2 Genetic Cloning of Expression Vectors using Inverse Polymerase Chain Reaction and the In-Fusion® Cloning System…….....29

2.2 Chemically Competent *Escherichia coli*

2.2.1 Preparation of Chemically Competent *Escherichia coli* ……..31

2.2.2 Transformation into *E. coli* Strains……...31

2.3 Expression and Affinity Purification of Protein

2.3.1 Expression and Purification of Recombinant Human Thioredoxin……32

2.3.2 Expression and Purification of Recombinant MBP-$P_{220-241}$ and MBP-P_{1-29}……...34

2.4 Sodium Dodecyl Sulfate Polyacrylamide Gel Electrophoresis…….....34

2.5 Analysis by Western Blot…….35

2.6 Quantification of Protein Concentration……...36

2.7 Glutathione S-transferase (GST) Pulldown Assay……...37

2.8 Cell Culture

2.8.1 Cell Culture - Passaging Cells……...38

2.8.2 Cell Culture – Seeding Plates…….....39

2.9 Assessment of Cellular Uptake of Recombinant Proteins……....39

2.10 Concentration of Proteins Using Trichloroacetic Acid Precipitation……40

2.11 Propagation Respiratory Syncytial Virus Subtype A…….41

2.12 Determination of Propagated Respiratory Syncytial Virus Titer……...41

2.13 Viral Inhibition Assay Using Indirect Immunofluorescence Microscopy……..42

2.14 Assessing Protein Toxicity with PrestoBlue® Reagent Cell Viability Assay……....43

2.15 Assessing RSV Progeny Release Using Indirect Immunofluorescence Microscopy.44

2.16 Statistical Analysis……..….45

Chapter 3 – Results……..46

3.1 The development and assessment of the antiviral activity of hTrx-$P_{220-241}$

3.1.1 Development of recombinant hTrx-$P_{220-241}$……....47

3.1.2 Expression and affinity purification of hTrx-$P_{220-241}$……..49

3.1.3 hTrx-$P_{220-241}$ interacts with full length RSV nucleoprotein……....51

3.1.4 Uptake of hTrx-$P_{220-241}$ into LLC-MK2 cells…….53

3.1.5 Inhibition of RSV A replication by hTrx-$P_{220-241}$……55

3.2 Development and evaluation of the novel MBP-P_{1-29} peptide mimetic

3.2.1 Genetic Cloning, Protein expression and Affinity purification of MBP-P_{1-29}…….57

3.2.2 Uptake of MBP-P_{1-29} into LLC-MK2 cells……59

3.2.3 The effect of MBP-P_{1-29} on LLC-MK2 cell viability…….60

3.2.4 Inhibition of RSV A infection in LLC-MK2 cells by MBP-P_{1-29}……..61

3.2.5 The effect of MBP-P_{1-29} on BEAS-2B cell viability……...63

3.2.6 Inhibition of RSV A infection in BEAS-2B cells by MBP-P_{1-29}…….64

3.2.7 Inhibition of progeny virus release by MBP-P_{1-29}……..66

Chapter 4 – Discussion……68

4.1 The development and assessment of the efficacy of hTrx-$P_{220-241}$

4.1.1 Interaction between hTrx-$P_{220-241}$ and N protein…….69

4.1.2 Uptake of hTrx-$P_{220-241}$ into LLC-MK2 cells…….69

4.1.3 Inhibition of RSV replication by hTrx-$P_{220-241}$……..……71

4.2 Development and evaluation of the efficacy of MBP-P_{1-29} peptide mimetic

4.2.1 The effect of MBP-P_{1-29} on cell viability……72

4.2.2 The inhibition of RSV replication by MBP-P_{1-29}……73

4.3 Future directions

4.3.1 Future directions – binding kinetics and immunoprecipitation of hTrx-$P_{220-241}$ and N…….74

4.3.2 Future directions – testing MBP-P_{1-29} in other RSV strains……...75

4.3.3 Future directions – attaching MBP-P_{1-29} on a human carrier protein……..75

4.3.4 Future directions – mode of therapeutic drug delivery……...76

4.4 Closing remarks……77

Chapter 5 – References……79

Chapter 6 – Appendix……...92

Table 6.1: Forward and Reverse Primers used in Inverse PCR……...93

Figure 6.2 Overview of the Inverse PCR and In-Fusion® Cloning System Process Using $P_{220-241}$ as an example……..94

Figure 6.3 Boxcar Diagrams of Recombinant Proteins Used in This Study……95

Figure 6.4 Amino Acid Alignment of RSV A and RSV B Phosphoproteins……..96

LIST OF ABBREVIATIONS

9R – Nine Arginine

APS – Ammonium Persulfate

BSA – Bovine Serum Albumin

BEAS-2B – Human Lung Bronchus Epithelial Cells

CPP – Cell Penetrating Peptide

CTL – Cytotoxic T Lymphocyte

DNA – Deoxyribonucleic Acid

DMEM – Dulbecco's Modified Eagle Medium

EDTA – Ethylenediaminetetraacetic Acid

Em - Emission

Ex - Excitation

F_0 – Inactive Precursor of Fusion Protein

F_1 – Active Subunit of Fusion Protein

F_2 – Active Subunit of Fusion Protein

FBS – Fetal Bovine Serum

Fc region – Fragment Crystallisable Region

FDA – Food and Drug Administration

FI – Formalin-inactivated

FITC – Fluorescein Isothiocyanate

FPLC – Fast Protein Liquid Chromatography

F protein – Fusion Glycoprotein

GAGs – Glycosaminoglycans

GE – Gene-end

GLP-1 – Glucagon-like Peptide 1

GS – Gene-start

GST – Glutathione S-transferase

GTP – Guanosine-5'-triphosphate

G protein – Attachment Glycoprotein

HEp-2 – Human HeLa Contaminant Carcinoma Cells

HIV – Human Immunodeficiency Virus

hTrx – Human Thioredoxin

IMPDH – Inosine Monophosphate Dehydrogenase

IPTG – Isopropyl β-D-1-thiogalactopyranoside

kDa – Kilodalton

Ka – Association Equilibrium Constant

LB – Luria-Bertani Broth

Le – Leader

LLC-MK2 – Rhesus Monkey Kidney Cells

LRTI – Lower Respiratory Tract Infection

L protein – Large Polymerase Subunit

MBP – Maltose Binding Protein

mRNA – Messenger RNA

M protein – Matrix Protein

M2 protein – Matrix Protein 2

N° – Wildtype Monomeric, RNA-free Nucleoprotein

N^{mono} – Monomeric, RNA-free Nucleoprotein Mutant (K170A/R185A)

NLS – Nuclear Localisation Signal

NS1 – Non-Structural Protein 1

NS2 – Non-Structural Protein 2

N protein – Nucleoprotein

OD – Optical Density

P_{1-29} – First 29 N-terminal Amino Acids of Phosphoprotein

$P_{220-241}$ – Last 21 C-terminal Amino Acids of Phosphoprotein

PBS – Phosphate Buffered Saline

PBST – Phosphate Buffered Saline + 0.1% Tween-20

PCR – Polymerase Chain Reaction

PICU – Paediatric Intensive Care Unit

PMSF – Phenylmethylsulfonyl Fluoride

P protein - Phosphoprotein

RCT – Randomized Control Trial

RdRp – RNA-dependent RNA Polymerase

RFU – Relative Fluorescent Unit

RIPA – Radioimmunoprecipitation Assay

RNA – Ribonucleic Acid

RPM – Revolutions Per Minute

RSV – Respiratory Syncytial Virus

SDS – Sodium Dodecyl Sulfate

SDS-PAGE – Sodium Dodecyl Sulfate Polyacrylamide Gel Electrophoresis

SH – Small Hydrophobic Protein

SOC – Super Optimal Broth with Catabolic Repression

SPR – Surface Plasmon Resonance

TAE – Tris, Acetic Acid, EDTA buffer

TCA – Trichloroacetic Acid

TEMED – Tetramethylethylenediamine

Th – T Helper

Tr - Trailer

US – United States

USD – United States Dollars

x g – Centrifugal Force

LIST OF FIGURES

Figure 3.1.1: DNA agarose gel of inverse PCR-generated human thioredoxin products

Figure 3.1.2: Purification of hTrx-$P_{220-241}$

Figure 3.1.3: Interaction of MBP-$P_{220-241}$ or hTrx-$P_{220-241}$ with GST-N

Figure 3.1.4: Uptake of hTrx-$P_{220-241}$ and MBP-$P_{220-241}$ by LLC-MK2 cells

Figure 3.1.5: Inhibition of RSV A by MBP-$P_{220-241}$ and hTrx-$P_{220-241}$

Figure 3.2.1: Cloning and purification of MBP-P_{1-29}

Figure 3.2.2: Uptake of MBP-P_{1-29} into LLC-MK2 cells

Figure 3.2.3: Effect of MBP-P_{1-29} on LLC-MK2 cell viability

Figure 3.2.4: Inhibition of RSV A infection in LLC-MK2 cells by MBP-P_{1-29}

Figure 3.2.5: Effect of MBP-P_{1-29} on BEAS-2B cell viability

Figure 3.2.6: Inhibition of RSV A infection in BEAS-2B cells

Figure 3.2.7: MBP-P_{1-29} inhibits viral progeny production

Figure 6.2: Inverse PCR and In-Fusion® Cloning System process using $P_{220-241}$ as an example

Figure 6.3: Boxcar diagrams of recombinant proteins used in this study

Figure 6.4: Amino acid alignment of RSV A and RSV B phosphoproteins

LIST OF TABLES

Table 6.1: Forward and Reverse Primers used in Inverse PCR

DECLARATION OF ACADEMIC ACHIEVEMENT

Christopher K.W. Chiang performed all of the experiments described in the thesis except for:

1. Cloning of HisMBP-NLS-$P_{220-241}$ and GST-N was performed by Dr. David Bulir.
2. The stock of RSV A Long strain used in this thesis was provided by Sylvia Chong.

CHAPTER 1 - INTRODUCTION

INTRODUCTION

1.1 Respiratory Syncytial Virus History and Overview

Human respiratory syncytial virus (RSV) is one of the most important causes of acute lower respiratory tract infection (LRTI) and is one of the leading causes of childhood hospitalization worldwide (Nair et al., 2017; Stensballe, Devasundaram, & Simoes, 2003). RSV was first isolated in 1956 by Morris and his colleagues as chimpanzee coryza agent during an epizootic outbreak of coughing, sneezing, and nasal discharge in a colony of chimpanzee (Blount, Morris, & Savage, 1956). It was later isolated from humans and renamed to respiratory syncytial virus due to the characteristic formation of syncytia, pseudo giant cells (Chanock et al., 1962).

Respiratory syncytial virus infects approximately 70% of infants during the first year of life and almost all children have been infected at least once by the age of two (Glezen, Taber, Frank, & Kasel, 1986). Individuals can also be repeatedly infected throughout their lives, which make the elderly and individuals with compromised immune, pulmonary or cardiac systems highly susceptible to viral infection (Hall, Simőes, & Anderson, 2013). In 2005, RSV accounted for over 30 million new acute lower respiratory infections worldwide in children below the age of five, which resulted in over 3.4 million hospitalizations for severe cases (Nair et al., 2010). While the majority of individuals successfully recover, up to 199,000 children younger than the age of five passed away from RSV-related complications with 99% of these cases taking place in developing countries (Nair et al., 2010). In the year 2000, the annual medical cost for all RSV-associated

hospitalizations and medical encounters for children less than five years old in the United States alone totaled to approximately $652 million USD (Paramore, Ciuryla, Ciesla, & Liu, 2004). Furthermore, from 1997 to 2000 in the United States, the total annual RSV-associated expenses were approximately $2.6 billion for infant hospitalizations and an additional $1 billion for treating elderly patients (Falsey, Hennessey, Formica, Cox, & Walsh, 2005; Leader & Kohlhase, 2003). RSV therefore poses both a significant medical and economic burden.

1.2 Respiratory Syncytial Virus Clinical Features and Epidemiology

Most children infected with RSV are symptomatic and present with lower respiratory tract complications (Hall et al., 2013). Preterm infants with RSV may experience apnea, irritability or tiredness (Eiland, 2009). Apnea is prevalent in 1.2% - 23.8% of all neonatal cases and may appear before other respiratory symptoms (Ralston & Hill, 2009). However, this symptom does not appear in subsequent RSV infections (Hall et al., 2013). Infected children commonly experience wheezing, bronchiolitis or pneumonia (Hall et al., 2013). RSV infection typically begins in the nasopharynx and clinically manifests as an upper respiratory tract infection with complications including coryza, congestion, cough, and low grade fever (Hall et al., 2013; La Via, Marks, & Stutman, 1992). Between two to five days, viral infection can progress into the lower respiratory tract infection and infants typically present with tachypnea, coryza, labored breathing, pharyngitis, sneezing, and wheezing (Eiland, 2009; Hall et al., 2013; La Via et al., 1992). RSV symptoms typically peak at five days post infection and clear up after seven to ten

days, but the cough may remain for up to four weeks due to slowly recovering ciliated cells (Eiland, 2009; Hall et al., 2013). Although most patients successfully recover, approximately 0.5% to 1.5% of hospitalized patients pass away as a result of RSV related complications (La Via et al., 1992). On the other hand, RSV infection in older children and adults typically present with congestion, cough, fever, sinusitis, and otitis media (Eiland, 2009; Hall et al., 2013). However, in elderly adults, a diagnosis of RSV often arises due to a worsening of co-morbid health conditions like chronic obstructive pulmonary disease (Hall et al., 2013).

Furthermore, patients with a RSV infection may also present with concurrent or secondary bacterial infections, which may exacerbate the severity of the respiratory illness (Hishiki et al., 2011). Preterm infants with RSV have an increased risk of acquiring a concurrent bacterial infection, which is associated with longer hospitalization stays, increased recovery times, and admittance to the paediatric intensive care unit (PICU) (Brealey, Sly, Young, & Chappell, 2015; Resch, Gusenleitner, & Mueller, 2007). Moreover, up to 40% of infants admitted to PICU have a bacterial co-infection and remain on ventilator support for longer compared to infants only infected with RSV (Kneyber et al., 2005; Thorburn, Harigopal, Reddy, Taylor, & van Saene, 2006). In these infants, the bacterial infections often occurs in the lower respiratory tract and is most commonly caused by *Haemophilus influenzae*, *Streptococcus pneumoniae* or *Moraxella catarrhalis* (Hishiki et al., 2011). It also thought that RSV facilitates bacterial colonization and growth by decreasing bacterial clearance and increasing bacteria adherence to respiratory epithelial cells (Brealey et al., 2015). Following a RSV infection, individuals may be susceptible to

secondary bacterial infection due to the body suppressing inflammatory responses to prevent further damage and promote healing to occur (Brealey et al., 2015; Hussell & Cavanagh, 2009). Finally, severe RSV infection in infants is also significantly associated with recurrent wheezing and asthma later in life where the greater the severity of RSV bronchiolitis experienced, the greater the risk of getting asthma (Wu & Hartert, 2011).

1.3 Respiratory Syncytial Virus Transmission and Seasonality

RSV is a highly transmissible disease with a basic reproduction number, the average number of secondary infections produced from one infected person in an uninfected population, ranging between one and seven (Drysdale, Green, & Sande, 2016; A. Weber, Weber, & Milligan, 2001). It can be spread when individuals inhale airborne virus-containing particle droplets released by a sneeze, cough, or breath. Although RSV aerosol particles can traverse through the air, epidemiological studies suggest it is an uncommon method of infection (Hall et al., 2013; Lindsley et al., 2010). RSV is primarily spread when individuals come in contact with infectious respiratory secretions on environmental surfaces upon which the inoculum enter through the nose, eyes, and respiratory tract (Hall & Douglas, 1981; Hall et al., 2013; Lindsley et al., 2010). Respiratory secretions of RSV can remain infectious on non-porous countertops for up to 6 hours while it can only persist for approximately 30 minutes on cloth, paper tissues and skin (Hall & Douglas, 1981). The prolonged survival times increase the risk of RSV transmission especially in a hospital environment.

Nosocomial spread of RSV is a significant concern in pediatric wards and in vulnerable patient populations with compromised immune, pulmonary or cardiac systems (Bont, 2009; Hall et al., 2013). Nosocomial infection accounts for approximately six to ten percent of hospital RSV cases and increases the treatment cost for community-acquired RSV by 30.5% (Bont, 2009; Jacobs et al., 2013; Simon et al., 2008; Tuan et al., 2015). Nosocomial infection in high-risk infants result in severe disease progression, poor clinical outcomes, and possibly even death (Bont, 2009; Simon et al., 2008). However, cases of nosocomial RSV infection can be reduced by 39 – 67% by following strict infection control practices such as proper hand washing, the use of personal protective equipment, and timely isolation of RSV-infected infants (Drysdale et al., 2016; Hall, Geiman, Douglas, & Meagher, 1978; Karanfil et al., 1999).

As RSV is a highly seasonal virus, there are periods of time marked with little activity and distinct outbreaks with sharp activity over the course of two to four months (Weber, Mulholland, & Greenwood, 1998). In temperate or Mediterranean climates, RSV outbreaks mainly occur from November to April in the Northern Hemisphere and from March to October in the Southern Hemisphere (Hall et al., 2013; M. W. Weber et al., 1998). There is variability in the timing of RSV outbreaks (Mullins, Lamonte, Bresee, & Anderson, 2003). For example, the RSV season in the southern regions of the United States started significantly earlier and lasted longer while the Midwest region began later and were shorter compared to the rest of the US (Mullins et al., 2003). Furthermore, there is variation in the timing of RSV seasons within geographic regions, which suggest that the timing of seasonal outbreaks are specific to communities (Mullins et al., 2003). For instance, in the

state of Connecticut in the USA, peak timings of seasonal RSV epidemics differed by up to four weeks between different counties (Noveroske, Warren, Pitzer, & Weinberger, 2016). On the other hand, seasonality of RSV epidemics in the tropics are less consistent (Hall et al., 2013). In tropical and subtropical climates with seasonal rainfalls, community outbreaks typically peaked one to two months after the onset of the rainy season while other tropical regions vary from year to year (Hall et al., 2013; Weber et al., 1998). Thus, community-specific data are required for accurate prediction of RSV outbreaks, which can be used to guide immune prophylaxis treatment and infection control strategies (Hall et al., 2013).

1.4 Respiratory Syncytial Virus Taxonomy and Antigenic Diversity

Respiratory syncytial virus belongs to the order *Mononegavirales* (Afonso et al., 2016). It originally belonged to the *Paramyxoviridae* family, but was re-categorized into the *Pneumoviridae* family and the *Orthopneumovirus* genus in 2016 (Afonso et al., 2016; Chang & Dutch, 2012). The other member within the *Pneumoviridae* family is metapneumovirus (Afonso et al., 2016). RSV has two major antigenic subtypes: A and B (Sullender, 2000). RSV subtype A viruses include the laboratory strain Long and A2 viruses while subtype B contains the West Virginia and CH-18537 strain (Sullender, 2000). The largest antigenic and genetic diversity between subtype A and B occurs in the attachment glycoprotein, the G protein (Sullender, 2000). Between RSV subtype A strains, there is a 94% amino acid similarity between the attachment glycoproteins. (Johnson, Spriggs, Olmsted, & Collins, 1987). In contrast, there is only a 53% similarity between

RSV subtype A and B where the majority of the amino acid differences lies in the ectodomain of the G protein (Johnson et al., 1987). Both RSV subtype A and B can be found circulating in the yearly RSV epidemics; however, it is possible that one of the subtypes may predominate over the other (Sullender, 2000). Furthermore, these dominant viruses are genetically different each year, which may contribute to how RSV can repeatedly infect individuals throughout their lives (Cane, Matthews, & Pringle, 1994; Sullender, 2000). In the United States, RSV A is typically associated with higher hospitalization rates compared to RSV B, which suggests that RSV A may be associated with greater disease severity and virulence compared to RSV B (Jafri, Wu, Makari, & Henrickson, 2013).

1.5 Respiratory Syncytial Virus Genome

Respiratory syncytial virus is an enveloped, non-segmented, negative-sense, single stranded RNA virus (Collins et al., 2013). Its genome is composed of ten genes, which encode for eleven different proteins (González, Bueno, Carreño, Riedel, & Kalergis, 2012). There is a 44 nucleotide leader (Le) sequence at the 3' end and a 155 nucleotide trailer (Tr) sequence at the 5' end of the RSV genome (Mink, Stec, & Collins, 1991). Before each gene is a gene-start (GS) motif that directs gene transcription and at the end of each gene is a gene-end (GE) motif, which is responsible for transcription termination and polyadenylation (Kuo, Grosfeld, Cristina, Hill, & Collins, 1996).

The RSV genome encodes eight structural proteins found in both virions and virus-infected cells as well as two non-structural proteins found only in virus-infected cells (Ruuskanen & Ogra, 1993). There are two surface glycoproteins, the fusion (F) protein and attachment (G) protein (Ruuskanen & Ogra, 1993). They contain the major determinants of RSV antigenicity, and induce neutralizing and protective antibody responses (Ogra, 2004; Ruuskanen & Ogra, 1993). The G protein is a glycoslated type II transmembrane protein, which consists of a N-terminal cytoplasmic domain (residues 1-37), a non-cleaved hydrophobic signal (residues 38-63), and an ectodomain (residues 64-298) (Teng, Whitehead, & Collins, 2001). It is produced either as a full length transmembrane protein or a secreted N-terminally truncated protein (Teng et al., 2001). It is highly glycosylated with N- and O-linked carbohydrate chains where the number of each vary between different RSV strains (Teng et al., 2001). The G protein mediates viral attachment to host cells, improves cell-to-cell fusion, and enhances virion assembly or release (Ruuskanen & Ogra, 1993; Techaarpornkul, Barretto, & Peeples, 2001). Secreted G protein also protects RSV-infected cells from neutralizing antibodies by acting as an antigen decoy and inhibiting antibody-mediated antiviral activity of Fc receptor leukocytes (Bukreyev, Yang, & Collins, 2012). The F protein is a type I integral membrane protein that is initially synthesized as an inactive precursor, F_0, which moves toward the cell surface (Collins, Huang, & Wertz, 1984). However, RSV F_0 does not reach the cell surface (Bolt, Pedersen, & Birkeslund, 2000). Three F_0 monomers form a trimer and each of the monomers are cleaved by furin proteases to produce physiologically active, disulfide-bonded F_1 and F_2 subunits (Bolt et

al., 2000). These active subunits direct viral penetration and syncytium formation in RSV-infected cells (Ogra, 2004).

There are also three envelope-associated structural proteins, which include the small hydrophobic (SH) protein, the matrix (M) protein, and M2 protein (Ruuskanen & Ogra, 1993). The SH protein is another surface glycoprotein, which forms the viral coat together with the F and G proteins (Bawage, Tiwari, Pillai, Dennis, & Singh, 2013). Through molecular modeling and molecular dynamics simulation, the SH protein was predicted to be a viroporin, which alters cellular membrane fluidity to facilitate viral progeny release and to inhibit apoptosis in host cells during the course of infection (Araujo et al., 2016). This would enable virus-infected cells to survive longer resulting in more viral replication and an increase in virulence (Araujo et al., 2016). The M protein plays two key roles throughout the course of RSV infection (Ghildyal, Jans, Bardin, & Mills, 2012). Early on in the infection process, the M protein is translocated into the host cell nucleus to inhibit host cell transcription (Ghildyal et al., 2012). Following this, the M protein traffick back to the cytoplasm to assist in virion formation (P. Collins et al., 2013; Ghildyal et al., 2012). Finally, the two M2 proteins, M2-1 and M2-2, are produced from two overlapping open reading frames of M2's messenger RNA (mRNA) (Bermingham & Collins, 1999). Both M2-1 and M2-2 function as transcription factors where M2-1 is a transcription anti-termination factor while M2-2 is thought to induce the switch from transcription to RNA replication (Bermingham & Collins, 1999; P. Collins et al., 2013).

The last three structural proteins, in conjunction with M2-1 and M2-2 cofactors, form the RNA dependent RNA polymerase and consists of the nucleoprotein (N),

phosphoprotein (P), and the large polymerase (L) subunit (Ghildyal et al., 2012; Ogra, 2004). The N protein binds the RSV genome and antigenome to form a helical nucleocapsid and is used as the template for RNA synthesis (Collins et al., 2013; Tawar et al., 2009). The P protein is a major co-factor that mediates the interactions between the N, L, and M2-1 proteins within the nucleocapsid-polymerase complex (Collins et al., 2013). As a part of the nucleocapsid complex, the L protein associates with the P and N proteins to transcribe and replicate the RSV genome (Tawar et al., 2009). There are also two nonstructural proteins, NS1 and NS2, which are found only in infected cells and are not present in the RSV virion (Ogra, 2004; Ruuskanen & Ogra, 1993). Both NS1 and NS2 help to increase viral load and increase virulence by interfering with host innate immune responses such as inhibiting apoptosis, and inhibiting interferon induction and signalling (Bitko et al., 2007; Collins et al., 2013; Spann, Tran, & Collins, 2005).

1.6 Respiratory Syncytial Virus Replication and Life Cycle

RSV infection first begins with the attachment of infectious virion to target cells, which is largely mediated by the G protein (Ghildyal et al., 2012). Through electrostatic interactions, the positively charged heparin binding domain in the ectodomain of the G protein, located between $^{184}A \rightarrow T^{198}$ for RSV subgroup A and $^{183}K \rightarrow K^{197}$ for subgroup B, interacts with negatively charged sulfate groups present on heparan sulfate glycosaminoglycans (GAGs) (Feldman, Hendry, & Beeler, 1999). Interestingly, a cold-passaged respiratory syncytial virus B1 *cp-52*/2B5 (*cp*-52) that lacked the G and SH glycoprotein remained infectious and replicated to high titers, which suggest that the G

protein is not required for infectivity (Karron et al., 1997). Although the G protein is not required for RSV infection, viruses lacking the G protein have decreased cellular attachment, released virions less efficiently, and had a lower infectivity (Techaarpornkul et al., 2001). Thus, G protein binding to highly sulfated forms of heparan sulfate GAGs may confer a selective advantage to enable RSV to easily spread and attach to neighbouring cells (Feldman et al., 1999). Furthermore, studies have demonstrated that the F glycoprotein can also independently interact with heparin/heparan sulfate and can direct cellular attachment in the absence of the G protein through a heparan sulfate-like molecule, such as chondroitin sulfate B (Feldman, Audet, & Beeler, 2000). Further experiments have shown that the G protein accounts for 50% of all RSV binding, 25% is attributed to the F protein, and the last 25% by GAG-independent binding facilitated by the F protein (Techaarpornkul, Collins, & Peeples, 2002).

After attachment to target cells, the F protein directs the fusion of the cell and viral membranes leading to the release of the nucleocapsid into the host cell cytoplasm (Ghildyal et al., 2012). On the virion membrane, the F protein trimer is in a metastable, prefusion conformation (McLellan, Ray, & Peeples, 2013). The N-terminus of each F_1 subunit contains a group of hydrophobic residues, called the fusion peptide, which bind to cell surface receptors on the target cell membrane (Collins et al., 1984; McLellan et al., 2013). Nucleolin, as a part of a 500 kDa protein complex of membrane proteins and glycosylphosphatidylinositol-linked proteins, is thought to be the F protein's cell surface receptor (Mastrangelo & Hegele, 2013). Three molecules of nucleolin bind one F protein prefusion trimer to initiate the refolding of the F protein into its postfusion state, after which

nucleolin is no longer required (Mastrangelo & Hegele, 2013). In its postfusion form, the F protein trimer folds upon itself to bring the target cell and virion membranes close together to initiate membrane fusion (McLellan et al., 2013). However, as nucleolin is present on all cells, it is difficult to explain the restricted tropism of RSV to the respiratory tract (Mastrangelo & Hegele, 2013). Thus, it is possible that RSV tropism is derived from a combination of local environment factors, interaction of multiple receptors and co-receptors, and other molecules (Mastrangelo & Hegele, 2013).

Fusion of the cell and viral membrane causes the release of the nucleocapsid into the cytoplasm where viral RNA transcription and replication occurs (Ghildyal et al., 2012). RNA synthesis occurs in cytoplasmic inclusion bodies containing the N, P, L, M2-1, and possibly the M protein (Ghildyal et al., 2012). The P protein interacts with the N protein, which enables it to specifically bind viral RNA to form a nucleocapsid complex (Ghildyal et al., 2012). The P protein also acts as a polymerase cofactor mediating the interaction between L and the N-RNA complex (Ghildyal et al., 2012). Transcription is initiated when the the L protein binds to the promoter on the 3’ leader sequence on the RNA genome and transcription progresses sequentially in the direction of the 5’ trailer sequence (Cowton, McGivern, & Fearns, 2006). As the RNA-dependent RNA polymerase (RdRp) complex moves along the genome, it gets activated and inactivated by gene-start and gene-end signals respectively (Kuo et al., 1996). After being activated by a GS motif, the polymerase continues transcribing until a GE signal is reached, even if it encounters a second GS motif (Kuo et al., 1996). Conversely, when polymerase activity is terminated by a GE signal, the polymerase only re-initates RNA transcription upon receiving another GS signal (Kuo et

al., 1996). Furthermore, the M2-1 protein associates with the polymerase complex, through its interaction with P, to ensure no premature transcription termination occurs (Cowton et al., 2006; Ghildyal et al., 2012). Upon reaching a GE signal, the polymerase terminates transcription, polyadenylates the newly synthesized mRNA, and releases the mRNA without dissociating the polymerase from the template (Cowton et al., 2006). The polymerase then scans for the next GS signal downstream or upstream, as in the case of the gene encoding for the L protein, of the GE signal to re-initiate RNA transcription, which commences with the capping and methylation of the 5' end of the mRNA (Cowton et al., 2006; Fearns & Collins, 1999). The end result of transcription is the production of ten monocistronic, capped, methylated and polyadenylated mRNA (Cowton et al., 2006). As the polymerase tends to dissociate between gene segments, genes at the 5' end of the genome are transcribed less frequently than genes located at the 3' end (Cowton et al., 2006; Kuo et al., 1996). This gene expression arrangement enables the production of proteins, such as NS1 and NS2, that are required in large amounts (Cowton et al., 2006).

After transcription, the RSV mRNA are translated by host cell machinery (Cowton et al., 2006). Currently, it is not known what triggers the switch between RNA trancription to replication (Cowton et al., 2006). One model proposes that the switch occurs when a sufficient amount of N protein is produced to protect the newly synthesized RNA while another study proposes the M2-2 protein is responsible for inducing the switch 12-15 hours post infection (Bermingham & Collins, 1999). Nonetheless, replication of the RSV genome begins when the polymerase binds to the Le region on the 3' end of the genome and generates a full length, positive-sense antigenome (Cowton et al., 2006). The antigenome

acts as the template to synthesize the negative-sense RNA genome, which is concurrently encapsidated by the N protein (Cowton et al., 2006). The association between the nascent RNA and the N protein allows the polymerase to read through GE signals during the replication process (Cowton et al., 2006).

Following the replication process, the nucleocapsid complex and other viral proteins move to the apical cell surface where virion assembly and budding take place on lipid raft-enriched domains (Ghildyal et al., 2012). The M protein associates with the nucleocapsid complex by binding to the M2-1 protein, which silences RNA synthesis (Ghildyal et al., 2012). It also enables the nucleocapsid complex to bind to actin and be transported by the microfilament network to the site of virion assembly (Ghildyal et al., 2012; Jeffree et al., 2007; Ulloa, Serra, Asenjo, & Villanueva, 1998). Simultaneously, the F and G proteins are transported by the endoplasmic reticulum and Golgi apparatus via the glycoprotein secretory pathway to the site of virion assembly on the plasma membrane (Ghildyal et al., 2012). All of the components of the nucleocapsid complex (N, P, L, M, and M2-1) and envelope glycoprotein complex (SH, F, and G) assemble on detergent insoluble lipid rafts of the plasma membrane (Ghildyal et al., 2012; Marty, Meanger, Mills, Shields, & Ghildyal, 2003). The current mechanism underlying the budding process has not been fully elucidated, but it is thought to be driven by the F and M proteins (Ghildyal et al., 2012). One model suggest that the cytoplasmic tail of the F protein functions as a catalyst for the budding process (Baviskar, Hotard, Moore, & Oomens, 2013). The F protein cytoplasmic tail facilitates the incorporation of previously assembled inclusion bodies and the F protein into filaments near the plasma membrane (Baviskar et al., 2013).

Dimerization and oligomerization of the M protein induces the curvature of the cell membrane needed for budding and the release of the virion (Förster, Maertens, Farrell, & Bajorek, 2015; Ghildyal et al., 2012). Mutations disrupting M protein dimerization prevents the formation of viral filaments on the plasma membrane and prevents the release of virus particles (Förster et al., 2015).

1.7 Current Treatment Options – Vaccines

To date, there is no commercially licensed vaccine available to prevent RSV infection, which is also partly due to strict regulations placed after the failure of the first formalin-inactivated (FI) RSV vaccine trial in the 1960s (Killikelly, Kanekiyo, & Graham, 2016; Kim et al., 1969). Although the alum precipitated FI-RSV stimulated high levels of serum antibodies, it failed to confer protective immunity and paradoxically increased the severity of illness following natural RSV infection (Kim et al., 1969). Unfortunately, two FI-RSV vaccine recipients died from bacterial pneumonia complications following RSV infection (Killikelly et al., 2016). Follow up research revealed that formalin treatment of RSV altered the epitopes on the F glycoprotein, which resulted in the production of binding antibodies lacking neutralizing and fusion inhibiting activity (Murphy & Walsh, 1988). Consequently, high titers of antibodies bound to nonprotective epitopes on the F protein and formed immune complexes in the lungs, which may have enhanced the severity of the disease (Murphy & Walsh, 1988). Autopsy results revealed that the lumen of large bronchi contained large quantities of neutrophils, macrophages, and giant cells while small bronchi were infiltrated with neutrophils, lymphocytes and low amounts of eosinophils (Porter,

Prince, Yim, & Curtis, 2001). Moreover, the FI-RSV vaccine induced a strong T helper (Th) 2 biased response without Th1 involvement (Sawada & Nakayama, 2016). This induced high levels of Th2-associated cytokines and chemokines, which resulted in an inflammatory response (Sawada & Nakayama, 2016). However, low levels of cytotoxic T lymphocyte (CTL) activity result in poor elimination of RSV-infected cells (Sawada & Nakayama, 2016). In order to provide complete protection against RSV infection, there needs to be a balance between Th1 and Th2-mediated responses to produce cellular immunity and neutralizing antibodies (Sawada & Nakayama, 2016).

In designing the perfect RSV vaccine candidate, a number of factors needs to be considered. Vaccines can potentially be developed to target either young infants, infants between four to six months old, pregnant women, or the elderly (Anderson, 2013). Young infants would naturally benefit the most from a RSV vaccine (Anderson, 2013). However, the young infants' immature immune system and residual maternal antibodies may interfere with the development of a robust immune response following vaccination (Anderson, 2013; Murata, 2009; Schickli, Dubovsky, & Tang, 2009). In consideration of the first FI-RSV vaccine, the safety profile of new RSV vaccine candidates must also be carefully evaluated to ensure it does not result in enhanced RSV disease (Murata, 2009; Schickli et al., 2009). Vaccines also should not induce a Th2 polarized response, which would recruit high levels of eosinophils, neutrophils and lymphocytes into the lungs and cause inflammation and bronchoconstriction (Schickli et al., 2009). Furthermore, the RSV vaccines should not affect the safety and efficacy of routine childhood vaccinations such as, but not limited to, hepatitus B, pertussis, and poliovirus vaccines (Schickli et al., 2009). Although infants

older than six months have less maternal antibodies and a more mature immune system, they are still susceptible to enhanced RSV disease (Anderson, 2013; Haynes, 2013). Meanwhile, there are concerns about vaccinating pregnant women and its effect on the developing fetus (Haynes, 2013). Finally, it may challenging to induce a robust immune response in the elderly population due to pre-existing RSV immunity and immunosenescence (Anderson, 2013; Haynes, 2013; McElhaney, 2009; Murata, 2009).

1.8 Current Treatment Options – Pharmaceutical Options

Currently, infants hospitalized with a RSV infection are provided with supportive treatments to maintain adequate oxygenation and given intravenous fluids to maintain hydration status (Krilov, 2011). Treatment plans targeting the inflammatory responses triggered by RSV and or inhibiting viral activity have not shown significant benefits (Krilov, 2011). Randomized control trials (RCT) using either β-adrenergic bronchodilators, such as salbutamol and albuterol, or α-adrenergic bronchodilators, such as epinephrine and adrenaline, for the treatment of viral bronchiolitis have not shown consistent clinical benefits (American Academy of Pediatrics Subcommittee on Diagnosis and Management of Bronchiolitis, 2006). A RCT conducted by Gadomski et al (1994) found no significant difference between outpatient infant groups treated with either nebulized albuterol or placebo in the management of bronchiolitis while Dobson et al (1998) demonstrated nebulized albuterol therapy did not attenuate the severity of the illness nor enhance recovery for infants presenting with severe, acute bronchiolitis (American Academy of Pediatrics Subcommittee on Diagnosis and Management of Bronchiolitis, 2006; Dobson et

al., 1998; Gadomski et al., 1994). On the other hand, studies have shown that patients treated with α-adrenergic agents displayed short-term improvements in clinical score, oxygen saturation, respiratory rate at 60 minutes, and heart rate at 90 minutes (American Academy of Pediatrics Subcommittee on Diagnosis and Management of Bronchiolitis, 2006; Kristjánsson, Lødrup Carlsen, Wennergren, Strannegård, & Carlsen, 1993; Menon, Sutcliffe, & Klassen, 1995). Yet, these α-adrenergic agents do not significantly impact the overall course of the illness or the length of the patients' hospital stay (American Academy of Pediatrics Subcommittee on Diagnosis and Management of Bronchiolitis, 2006; Wainwright et al., 2003). Despite the lack of RCT evidence, clinical experience suggest that some infants show clinical improvement after nebulized bronchodilator treatments (American Academy of Pediatrics Subcommittee on Diagnosis and Management of Bronchiolitis, 2006). In such cases, clinical responses should be evaluated and bronchodilator treatments should only be continued if there is documented clinical improvement (American Academy of Pediatrics Subcommittee on Diagnosis and Management of Bronchiolitis, 2006). Other pharmaceutical treatments, including corticosteroids, have also failed to demonstrate sufficient clinical benefit in the management of acute RSV LRTIs (Krilov, 2011). Corneli et al (2007) evaluated the effectiveness of a single oral dose of dexamethasone in 600 children with acute, moderate-to-severe bronchiolitis and found there was no significant reduction in hospital admissions, improvement in respiratory status nor duration of hospitalization compared to infants given a placebo (Corneli et al., 2007). These findings were substantiated by a collective review of 17 studies, containing a total of 2,596 children, by the Cochrane Collaboration, which

found no clinically significant effect of systemic or inhaled glucocorticoids on respiratory rate, oxygen saturation, hospital admission rates, length of hospitalisation, subsequent visits, or readmission rates (Corneli et al., 2007; Fernandes et al., 2013).

Currently, the only clinically approved antiviral drug for the treatment of RSV LRTIs is ribavirin (Krilov, 2011). Ribavirin is a synthetic guanosine analog, which is effective against both DNA and RNA viruses, including RSV (Beaucourt & Vignuzzi, 2014). There have been several direct and indirect mechanisms of action that have been proposed to explain ribavirin's antiviral activity (Beaucourt & Vignuzzi, 2014). There are three direct mechanisms that propose that ribavirin can directly inhibit viral RNA dependent RNA polymerase activity, can interfere with RNA capping activity, and can increase mutation rates in viral genome through base pairing with both cytosine and uracil leading to the production of less fit viruses (Beaucourt & Vignuzzi, 2014; Franchetti & Grifantini, 1999; Graci & Cameron, 2006). Indirectly, ribavirin inhibits inosine monophosphate dehydrogenase (IMPDH), which leads to a depletion of intracellular guanosine-5'-triphosphate (GTP) levels (Beaucourt & Vignuzzi, 2014). Viruses require guanosine nucleotides to replicate their genome, thus a depletion of GTP may significantly reduce viral replication (Franchetti & Grifantini, 1999; Thomas, Ghany, & Liang, 2012). Lowering GTP pools may also facilitate the activity of ribavirin triphosphate in introducing mutations and or acting as a polymerase inhibitor (Thomas et al., 2012). Ribavirin may also have indirect immunomodulatory effects as unphosphorylated ribavirin can induce a Th1 polarized response over a Th2 response to clear virus-infected cells (Franchetti & Grifantini, 1999; Thomas et al., 2012). However, ribavirin is not widely used in the

treatment of RSV LRTIs due to a combination of its marginal clinical benefits, high costs, prolonged aerosol administration, and risks of secondary exposure and harm to healthcare providers (Krilov, 2011). It may still be used to effectively treat young infants and severely immunocompromised patients, such as hematopoietic stem cell recipients and lung transplant patients, at risk of mortality from RSV infection (Burrows et al., 2015; Krilov, 2011; Shah & Chemaly, 2011).

Besides ribavirin, palivizumab (Synagis) is used as prophylactic treatment for RSV (Bawage et al., 2013; Krilov, 2011). Palivizumab is a humanized monoclonal antibody targeting RSV's fusion glycoprotein that is administered intramuscularly on a monthly basis throughout the RSV season (Krilov, 2011). Early clinical trials demonstrated the effectiveness of palivizumab prophylaxis in reducing RSV hospitalization by 78% for premature infants, 39% reduction for infants with chronic lung disease, and a 45% reduction in RSV hospitalizations for infants with hemodynamically significant congenital heart disease (Feltes et al., 2003; IMpact-RSV Study Group, 1998). Palivizumab is currently approved by the US Food and Drug Administration (FDA) for high-risk infants, but cost considerations limit its use to infants with high risk of severe RSV infection and only during the RSV season (Bawage et al., 2013; Krilov, 2011). Motavizumab is a second-generation monoclonal antibody derived from palivizumab and has a higher affinity for RSV compared to palivizumab (Bawage et al., 2013; Krilov, 2011). Motavizumab was shown to achieve noninferiority compared to palivizumab in preventing RSV hospitalization and was demonstrated to be superior to palivizumab in reduction of outpatient RSV-specific LRTI (Carbonell-Estrany et al., 2010). However, it was not

approved by the US FDA because of mild cutaneous reactions and its development has since been discontinued (Krilov, 2011; Mejias, Garcia-Maurino, Rodriguez-Fernandez, Peeples, & Ramilo, 2017).

Currently, there are a number of novel RSV antivirals in development, such as the Gilead fusion inhibitor, GS-5806, and Alios' ALS-008176 (Mejias & Ramilo, 2015). GS-5806 is an oral small molecule inhibitor that targets RSV's fusion glycoprotein and blocks viral envelope fusion with host cells (DeVincenzo et al., 2014; Samuel et al., 2015). GS-5806 is currently in Phase-II clinical trials and has been effective in reducing both viral loads and clinical manifestations of RSV in adults upon challenge with RSV (DeVincenzo et al., 2014; Mejias & Ramilo, 2015). ALS-008176 is an oral cytidine nucleoside analog that enters respiratory tract epithelial cells, phosphorylated to a nucleoside triphosphate, and inhibits RSV replication by chain termination (DeVincenzo et al., 2015). A proof-of-concept clinical trial found that ALS-008176 reduced viral load, peak viral load, duration of viral shedding, and the severity of RSV in 23 patients compared to a placebo (DeVincenzo et al., 2015). Due to the small sample size, more clinical trials are needed to evaluate the efficacy of ALS-008176 (DeVincenzo et al., 2015). Another promising therapeutic antiviral against RSV is Ablynx's ALX-0171 (Mejias et al., 2017). It is made of three identical single variable chain antibody domains joined together by flexible linker peptides, which binds and inhibits pre-fusion and post-fusion conformations of RSV's F protein (Mejias et al., 2017). Preliminary results from a Phase I/IIa clinical trial has demonstrated that ALX-0171 could reduce viral loads and reduce clinical severity of

infants hospitalized with RSV compared to a placebo (Moses, Zeldin, & De Fougerolles, 2016).

1.9 Antiviral Target: The nucleoprotein-phosphoprotein interaction in the RNA-dependent RNA polymerase

Previously, it was mentioned that the formation of the RdRp complex is essential for the replication of the RSV genome and it is mainly composed of the N, P, L, M2-1, and M2-2 proteins (Ghildyal et al., 2012; Tawar et al., 2009). Furthermore, the N, P, and L proteins form the minimal replication complex where deletion of any of the these viral proteins would abrogate viral RNA replication (Yu, Hardy, & Wertz, 1995).

Of these viral proteins, the interaction between the N and P protein is well characterized in the scientific literature. The P protein functions as a polymerase cofactor facilitating the interaction between the L protein and helical nucleocapsid (Collins et al., 2013). Initial studies demonstrated that the C-terminal end of the P protein interacted with the N protein and deletion of the P protein's last six amino acids disrupted this interaction (García-Barreno, Delgado, & Melero, 1996). Further evidence was provided by a synthetic peptide of the last 21 C-terminal amino acids (residues 220-241) of the P protein that could displace the N protein from N-P complexes (García-Barreno et al., 1996). Interestingly, this region also overlaps with the P protein's L-binding domain, which spans amino acids 216 to 239 (Sourimant et al., 2015). Another study demonstrated that the last nine C-terminal residues of P protein were sufficient for binding the N protein (Tran et al., 2007). However,

not all of the residues within this region participate in N protein binding and this is shown by the mutation of Serine-237 (García-Barreno et al., 1996). Mutation of Serine-237, a casein kinase II phosphorylation site required for transcription, to alanine or threonine abrogated its function, but did not affect N protein binding (García-Barreno et al., 1996; Mazumder & Barik, 1994). Nonetheless, the last four residues of P protein must be present for the interaction to take place (Tran et al., 2007). Amongst these four residues, the first three residues (L238, E239, and D240) interact with the surface of the N protein through electrostatic interactions while only the last C-terminal residue, F241, fits within the actual hydrophobic binding pocket of N protein (Ouizougun-Oubari et al., 2015).

During replication, newly synthesized RNA requires encapsidation by the N protein for protection (Galloux et al., 2015). The P protein can also act as a chaperone protein to maintain the N protein in a monomeric, RNA-free form (N°), which prevents the N protein from non-specifically binding to cellular RNA or self-oligomerization (Galloux et al., 2015). The domains mediating this interaction are the last ten C-terminal amino acids and the first 29 N-terminal amino acids of the P protein (P_{1-29}) (Galloux et al., 2015). However, the former binds poorly to N° and can be disrupted by the binding of P_{1-29} to N° (Galloux et al., 2015). GST pulldown and deletion mapping experiments have identified residues F4, E7, F8, G10, F20, L21, E22, I24, and K25 on P protein as being critical for binding N° and maintaining polymerase activity (Galloux et al., 2015). Furthermore, overexpression of a synthetic P_{1-29} peptide was shown to reduce viral RNA synthesis by up to 50% in a RSV minireplicon experiment, which further highlights its role as a novel potential antiviral target (Galloux et al., 2015). However, the effect of P_{1-29} was not assessed *in vitro*.

1.10 The Use of Peptide Mimetics as Novel Antiviral Therapeutics

Peptide mimetics, also referred to as peptidomimetics, is a broad term to describe compounds or modified peptides that act as replacements for peptide-based enzyme substrates, inhibitors, ligands for receptors, and other biomolecules (Olson et al., 1993). Therapeutic peptide mimetics are typically less than 50 amino acids in length and are based on naturally occurring peptide hormones or parts of proteins (McGregor, 2008). They can be used as protein-protein inhibitors to outcompete and disrupt the interactions between their target protein and its native, full-length protein counterpart (Cochran, 2000; Mason, 2010). Compared to small molecule inhibitors, peptide mimetics possess a number of advantages including the ability to disrupt essential protein-protein interactions, having target affinity, and having target specificity (McGregor, 2008). Peptide mimetics are often non-immunogenic and their small size (<5 kDa) enables them to penetrate deep into tissues (McGregor, 2008). However, their use is limited by their short half-life due to rapid clearance from circulation and degradation by serum and tissue proteases (McGregor, 2008). This can be remedied by conjugating the peptide mimetic to a carrier protein, such as human serum albumin, or to an antibody fragment crystallisable (Fc) domain to exploit its half-life extension mechanism (McGregor, 2008; Werle & Bernkop-Schnürch, 2006). Peptide mimetics can also be used to target intracellular proteins by conjugating it to cell penetrating peptides (CPP) (McGregor, 2008).

Recently, there are a number of therapeutic peptide mimetics that have been developed for the treatment and management of diseases. For human immunodeficiency

virus (HIV), there is a CCR5 and CD4 co-receptor fusion peptide mimetic that targets HIV-1 gp120 glycoprotein and inhibits HIV entry into cells expressing these receptors (Kwong et al., 2011). Other examples include The Medicines Company's hirudin-based thrombin inhibitor, Angiomax, and Amylin's glucagon-like peptide-1 (GLP-1) drug, Exanatide (McGregor, 2008). The Mahony laboratory has also previously developed a RSV phosphoprotein peptide mimetic, which consists of the last 21 C-terminal amino acids of the phosphoprotein ($P_{220-241}$) conjugated to an *Escherichia coli* maltose binding protein (MBP), a polyhistidine tag, and a cell penetrating peptide derived from the HIV-1 Tat nuclear localisation signal (NLS). Previous graduate students in the Mahony laboratory have demonstrated that HisMBP-NLS-$P_{220-241}$ inhibited RSV replication by approximately 90% *in vitro* (unpublished data).

1.11 The Mutated Human Thioredoxin Carrier Protein

Given that bacterial MBP may induce an immune response in humans and animals, a human carrier protein would be ideal to conjugate $P_{220-241}$ to. One potential candidate is the human thioredoxin scaffold protein. Dr. Groner's laboratory in Frankfurt, Germany has recently developed a bacterially-expressed human thioredoxin (hTrx) protein with a cell penetrating peptide (Borghouts, Kunz, Delis, & Groner, 2008). This human thioredoxin scaffold protein was mutated to remove all five cysteine residues in order to acquire monomeric products upon protein purification and conjugated to a nine arginine (9R) CPP to enable transduction across biological membranes (Borghouts et al., 2008). Due to its prior success, hTrx appears to be an ideal human carrier protein.

1.12 Thesis Objectives

Given the Mahony laboratory's prior success working with a HisMBP-NLS-$P_{220-241}$ peptide mimetic, I had two main objectives in my Master's thesis. My first objective was to address the issue of MBP's immunogenicity by conjugating the therapeutic $P_{220-241}$ peptide mimetic onto the mutated human thioredoxin carrier protein. I hypothesized that this new recombinant RSV peptide mimetic would be comparable to its predecessor's, HisMBP-NLS-$P_{220-241}$, ability to interact with full-length RSV nucleoprotein and inhibit RSV replication *in vitro*. In this thesis, $P_{220-241}$ would be cloned onto a human thioredoxin carrier protein with a 9R CPP and a polyhistidine tag to form His_{10}-9R-S-hTrx-9R-$P_{220-241}$. My second objective was to expand on the work done on a synthetic P_{1-29} peptide mimetic by evaluating its efficacy in inhibiting RSV *in vitro*. I hypothesized that P_{1-29} conjugated to a HisMBP-NLS protein would be able inhibit RSV replication *in vitro* to a similar extent as reported by Galloux and colleagues in their RSV minireplicon assay. Due to the variety of complex recombinant peptide mimetics used, MBP-NLS-$P_{220-241}$ will be referred to as MBP-$P_{220-241}$, His_{10}-9R-S-hTrx-9R-$P_{220-241}$ will be referred to as hTrx-$P_{220-241}$, and HisMBP-NLS-P_{1-29} will be referred to as MBP-P_{1-29} in the rest of this thesis.

CHAPTER 2 –
MATERIALS AND METHODS

MATERIALS AND METHODS

2.1.1 Primer Design for Peptide Mimetic Constructs and Primer Resuspension

All the primers used in this thesis were designed to be compatible with the ligation-independent In-Fusion® Cloning System, which requires a region containing a 15 base pair overlap and is further discussed in **Section 4.1.1**. The 15 base pair overlap region is generated by designing the forward primer to have the first 15 nucleotides at their 5' end to be complementary to the first 15 nucleotides at the 5' end on the reverse primer and vice versa. All the primers ordered were shipped as lyophilized reagents, which were resuspended in UltraPure™ DNase/RNase-Free Distilled Water (Invitrogen) to a final concentration of 100 μM. A working stock of primers to be used in inverse Polymerase Chain Reaction (PCR) was made by diluting the primer stock concentration to 20 μM. An overview of all the primers used in this thesis can be found in the table in **Section 6.1**.

2.1.2 Cloning of Expression Vectors using Inverse Polymerase Chain Reaction and the In-Fusion® Cloning System

The template plasmids used to generate expression vectors for hTrx-$P_{220-241}$ and MBP-P_{1-29} were the mutated human thioredoxin carrier protein (hTrx Δcys5) in a pET-30 vector (kindly provided by Dr. Bernd Groner) and MBP-$P_{220-241}$ expression vector respectively. The inverse PCR and In-Fusion cloning is described in detail with figures in **Section 6.2**. Briefly, the hTrx Δcys5 vector was amplified using inverse PCR according to the manufacturer's protocol and primer set A in **Section 6.1** to insert the nucleotide

sequence for the last 21 C-terminal amino acids of the RSV phosphoprotein (EKLNNLEGNDSDNDLSLEDF) after the nine arginine CPP. The resulting PCR products to be analyzed by agarose gel electrophoresis were mixed at a 4:1 ratio with 5X DNA loading dye (50% w/v sucrose, 0.05 M Ethylenediaminetetraacetic acid [EDTA], 0.1% Bromophenol Blue, 4 M Urea, pH 7.0) and loaded onto a 0.6% agarose-ethidium bromide gel, which was placed in a gel tank containing 1x TAE buffer (40 mM Tris, 20 mM Acetate, 1 mM EDTA). The PCR products were electrophoresed at 140 V for 45 minutes using the PowerBac Basic Power Supply (BioRad) and visualized under ultraviolet light (UV) using the Gel Doc Ez Image (BioRad). The PCR products of the correct size were excised and purified using the Geneaid™ Gel/PCR DNA Fragments Extraction Kit as per the manufacturer's protocol. The linearized plasmid was circularized using the In-Fusion® Cloning System (Thermofisher Scientific Inc.) and was transformed into *Escherichia coli* DH5α chemically competent cells (New England Biolabs, Ipswich MA) as described in **Section 2.2.2**. The resulting plasmid was used as the template vector in another round of inverse PCR and In-Fusion® cloning using primer set B in **Section 6.1** using the same method described above. The MBP-$P_{1\text{-}29}$ plasmid containing the sequences for the first 29 N-terminal amino acids of RSV phosphoprotein (MEKFAPEFHGEDANNRATKFLE SIKGKFT) in reverse orientation was constructed using the method described above and using the MBP-$P_{220\text{-}241}$ plasmid as the initial template and primer set C. Boxcar diagrams of the final constructs are illustrated in **Section 6.3**.

2.2.1 Preparation of Chemically Competent *E. coli*

The various *E. coli* strains used in this thesis were DH5α, BL21 (DE), and Rosetta (DE3). Chemically competent *E. coli* were prepared by first growing the specific strain in 5 mL Luria-Bertani broth (LB) (1% w/v tryptone, 0.5% w/v yeast extract, 1% w/v NaCl) at 37°C and 250 RPM overnight. The overnight bacterial culture was used to inoculate 100 mL of fresh LB in a 1:100 ratio and grown until an ocular density at 600 nm (OD_{600}) of 0.5 was attained. The cells were cooled on ice for 15 minutes and pelleted by centrifugation at 3000 RPM for 10 minutes at 4°C. The supernatant was aspirated, the bacterial pellet was resuspended in ice cold 10 mM $MgSO_4$, and kept on ice for 30 minutes. It was then pelleted at 3000 RPM for 10 minutes at 4°C and the supernatant was aspirated. The pellet was resuspended in ice cold 50 mM $CaCl_2$ and incubated on ice for 30 minutes before being pelleted by centrifugation once again. Finally, the cells were resuspended in ice cold 50 mM $CaCl_2$ with 15% v/v glycerol, aliquoted, flash frozen, and stored at -80°C until further use.

2.2.2 Transformation into *E. coli* strains

Plasmids containing peptide mimetic constructs were added to chemically competent *E. coli* cells and incubated on ice for 30 minutes. The cells were heat shocked in a 42°C water bath for 45 seconds followed by a five minute incubation on ice. The cells were then grown in Super Optimal Broth with Catabolic repression (SOC medium) (2% w/v tryptone, 0.5% w/v yeast extract, 8.56 mM NaCl, 2.5 mM KCl, 10 mM $MgCl_2$, 10 mM $MgSO_4$, and 20 mM glucose] for 1 hour at 37°C. The cells were plated on LB plates

containing 1.5% agar and either 30 µg/mL of kanamycin for recombinant human thioredoxin constructs or 100 µg/mL of ampicillin for MBP- P_{1-29} using sterile glass beads. Plates were incubated at 37°C overnight. Colonies from successful transformants were selected from the LB agar plates and grown in 5 mL of LB with either 30 µg/mL of kanamycin or 100 µg/mL ampicillin overnight in a shaking incubator at 37°C and 250 RPM. *E. coli* glycerol stocks were made by mixing 200 µL of the overnight bacterial cultures in a 1:1 ratio with sterile 50% v/v glycerol and stored at -80°C until later use. Expression plasmids were purified from the remaining overnight bacterial culture using a Geneaid™ High-speed plasmid minikit according to the manufacturer's protocol and sent to MOBIX laboratory at McMaster University for sequencing. MBP-$P_{220-241}$, hTrx-$P_{220-241}$ and MBP-P_{1-29} were transformed and grown in *E. coli* Rosetta (DE3).

2.3.1 Expression and Affinity Purification of Recombinant Human Thioredoxin

Bacterial expression and purification of recombinant human thioredoxin constructs was performed as described by Borghouts et al. (2008). A 40 mL overnight culture of the recombinant human thioredoxin protein was inoculated into 2 L of LB containing 30 µg/mL of kanamycin and 33 µg/mL of chloramphenicol. The bacterial cultures were grown in a shaking incubator at 37°C and 250 RPM. When the OD_{600} was approximately 0.6, protein expression in the bacterial cultures were induced with the addition of 0.2 mM isopropyl β-D-1-thiogalactopyranoside (IPTG) for 4 hours at 30°C and 250 RPM. The cells were then harvested at 12,000 x g using a Sorvall® RC-5B refrigerated centrifuge for 5 minutes at 4°C. The cell pellets were resuspended in 20 mL of Urea Buffer 1 (8 M urea, 500 mM

NaCl, and 10 mM imidazole in Phosphate Buffered Saline [PBS], pH 7.5). The cells were lysed by sonication, six times at 25 Watts for 20 seconds with 30 second rest intervals each time. The cell lysate was centrifuged at 42,000 x g at 25°C for 45 minutes. The supernatant was filtered through a 0.22 µM filter (Millipore).

The recombinant human thioredoxin proteins were purified using a Gene-Q pump and Fast Protein Liquid Chromatography (FPLC) with the AKTA FPLC (GE Healthcare). Using the Gene-Q pump, the filtered supernatant in Urea Buffer 1 was loaded into a His-Trap™ column charged with 100 mM of $NiCl_2$ and washed with Urea Buffer 1. Recombinant human thioredoxin proteins were then eluted off the His-Trap™ column using an elution gradient of 80 mM to 300 mM imidazole established using Urea Buffer A (8 M urea, 500 mM NaCl, 80 mM imidazole in PBS, pH 7.5) and Urea Buffer B (8 M urea, 500 mM NaCl, 300 mM imidazole in PBS, pH 7.5) on the AKTA FPLC. The eluted protein was dialyzed and refolded overnight in 125 volumes of L-arginine-HCl refolding buffer (400 mM L-arginine monohydrochloride, 500 mM NaCl and 10% v/v glycerol in PBS, pH 7.5) at 4°C [except for His_{10}-G-9R-S-hTrx-9R-$RSVP_{220-241}$ which was dialyzed overnight at 25°C]. Then, 0.25 buffer volume of the dialysis buffer was replaced with PBS + 10% glycerol every 2 hours for a total of 4 times. Finally, the purified protein solution was filtered through a 0.22 µM filter (Nalgene). A small sample of the protein was analyzed on a SDS-PAGE gel to determine its purity while the rest was stored at -80°C until later use.

2.3.2 Expression and Affinity Purification of MBP- $P_{220-241}$ and MBP- P_{1-29}

A 100 mL overnight culture of recombinant MBP protein was inoculated into 6 L of LB containing 100 µg/mL of ampicillin. The bacterial cultures were grown in a shaking incubator at 37°C and 250 RPM. At an OD_{600} of approximately 0.6, protein expression in the bacterial cultures were induced with the addition of 0.2 mM IPTG at 25°C and was shaken at 250 RPM for 4 hours. The cells were harvested at 12,000 x g using a Sorvall® RC-5B refrigerated centrifuge for 5 minutes at 4°C. The cell pellets were resuspended in 20 mL of Urea Buffer 1 and lysed by sonication, six times at 25 Watts for 20 seconds with 30 second rest intervals each time. The cell lysate was centrifuged at 42,000 x g at 25°C for 45 minutes. The supernatant was filtered through a 0.22 µM filter (Millipore) and purification of the protein via the AKTA FPLC was performed as described in **Section 2.3.1**. The purified protein was buffer exchanged with a HiPrep 26/10 Desalting Column (GE Healthcare) into sterile PBS + 10% glycerol. The purified protein solution was filtered through a 0.22 µM filter and concentrated through an Amicon® Ultra-15 Centrifugal Filter (Millipore) at 3500 RPM at 4°C for 30 minutes to an hour. A small sample of the protein was analyzed on a SDS-PAGE gel to determine its purity while the rest was stored at -80°C until future use.

2.4. Sodium Dodecyl Sulfate Polyacrylamide Gel Electrophoresis

Protein samples were dissolved in 5x Laemmli buffer (4% w/v SDS, 100 mM Tris pH 7.0, 2 mM EDTA, 10% v/v glycerol, 0.002% w/v bromonophenol blue, 12.5% v/v β-

mercaptoethanol) and boiled at 95°C for 10 minutes on a heating block before being run on either a 12% or a 16% polyacrylamide gel. The resolving gel portion of the polyacrylamide gel was made with 375 mM Tris-HCl pH 6.8, 0.1% (v/v) sodium dodecyl sulfate (SDS), 0.4% (v/v), Tetramethylethylenediamine (TEMED), 12% (v/v) Acryl/Bis-Acryl, and 0.1% (v/v) ammonium persulfate (APS). The stacking portion of the polyacrylamide gel was made using 5% (v/v) Acryl/Bis-Acryl, 100 mM Tris-HCl pH 8.7, 0.1% (v/v) SDS, 0.1%(v/v) APS, and 0.4% (v/v) TEMED. The solidified gels were placed in mini-PROTEAN Tetra Cell (Bio-Rad) with SDS-PAGE running buffer (0.1% SDS, 192 mM glycine, 25 mM Tris pH 9.5). Protein samples were loaded into the wells and separated by electrophoresis through the stacking gel at 80V for 20 minutes and then separated by electrophoresis through the resolving gel at 120V for 80 minutes. A small amount of BLUelf Prestained Protein Ladder (FroggaBio) was also ran to determine the approximate size of protein samples.

2.5 Analysis by Western Blot

The polyacrylamide gel from **Section 2.4** was transferred onto a nitrocellulose membrane using the iBlot Gel Transfer Device (Invitrogen™). The nitrocellulose membrane was blocked with 5% skim milk powder in PBS + 0.1% Tween-20 (PBST) for 30 minutes at room temperature on an orbital shaker. The nitrocellulose membrane was then incubated with a primary antibody in 5% skim milk powder in PBST for 45 minutes at room temperature on an orbital shaker at 60 RPM. The primary antibodies used in this

thesis were a mouse anti-His antibody (Sigma) at a 1:10,000 dilution, a mouse anti-GST antibody (Sigma-Aldrich) at a 1:5,000 dilution, and a mouse anti-α-tubulin (GenScript) at a 1:5,000 dilution. To remove non-specifically bound antibodies, the membrane was washed three times with PBST for 5 minute intervals each time on an orbital shaker at 80 RPM. The membrane was then incubated with a goat anti-mouse antibody conjugated to horse radish peroxidase (Sigma) at a 1:5,000 dilution in 5% skim milk powder in PBST for 45 minutes at room temperature on an orbital shaker at 60 RPM. The membrane was once again washed three times and incubated with a chemiluminescence solution (Pierce) for a minute. The membrane was exposed to CL-XPosure™ (Thermofisher) film paper in the dark room and developed using the Konica SRX-101A Tabletop Photo Processor.

2.6. Quantification of Protein Concentration

A Bradford protein assay was used to determine the concentration of purified protein. A standard curve was generated using various concentrations of Bovine Serum Albumin (BSA) in dialysis buffer (after 4th PBS + 10% glycerol exchange) for human thioredoxin proteins or PBS + 10% glycerol for recombinant MBP constructs: 0 mg/mL, 0.2 mg/mL, 0.6 mg/mL, 1.0 mg/mL, and 1.5 mg/mL. Aliquots of purified protein and all the protein standards were mixed with 127.5 µL of DC™ Protein Reagent A (BioRad) and 1 mL of DC™ Protein Reagent B (BioRad) in a cuvette. The absorbance at a wavelength of 750 nm was read for all the standard curve and protein samples using an Ultrospec 4300 pro UV/Visible spectrophotometer and was plotted using Microsoft Excel 2013. A line of

best fit was created using the absorbance of the standard curve protein samples and the concentration of the human thioredoxin protein was extrapolated from this line of best fit.

2.7 Glutathione S-transferase (GST) Pulldown Assay

The expression plasmids for recombinant GST proteins (GST-N and GST) were transformed into *E. coli* Rosetta (DE3) cells. The bacteria were grown in a shaking incubator at 37°C and 250 RPM. At OD_{600} of approximately 0.6, the bacterial cultures were cooled on ice and induced with 0.2 mM IPTG for three hours in a shaking incubator at 25°C and 250 RPM. The cells were harvested at 12,000 x g using a Sorvall® RC-5B refrigerated centrifuge for 5 minutes at 4°C. The cell pellets were resuspended in 15 mL of PBST with a protease inhibitor tablet (Pierce) and lysed by sonication, six times at 25 Watts for 20 seconds with 30 second rest intervals each time. The cell lysates were centrifuged at 42,000 x g at 4°C for 45 minutes and the supernatants were filtered through a 0.22 µM filter.

Ten millilitres of GST-N cell lysate and a 1:10 dilution of GST cell lysate in PBST were each incubated with 200 µL of Glutathione High Capacity Magnetic Agarose Beads (Sigma-Aldrich) and nutated for 1 hour at 4°C. The beads were then pelleted at 3000 RPM for 5 minutes and the supernatant was removed by aspiration. The beads were washed once with 10 mL of PBST, pelleted by centrifugation at 3,000 RPM for 5 minutes, and the supernatant was removed. The beads were blocked with 10 mL of 5% BSA in PBST while nutating for 1 hour at 4°C. The beads were pelleted at 3,000 RPM for 5 minutes and all but 2 mL of supernatant was removed by aspiration. Aliquots of 250 µL of GST-N-bound beads

and GST-bound beads were placed in 1.5 mL Eppendorf tubes and mixed with 750 µL of either MBP-$P_{220-241}$ (in triplicates) or hTrx-$P_{220-241}$ (in triplicates) cell lysates. The beads were then nutated for 2 hours at 25°C. The beads were then washed seven times with a warm high salt wash buffer (20 mM Tris-HCl, 500 mM KCl, 0.1% Triton X-100, pH 7.4) on a magnetic NucliSENS miniMag® machine. After the final wash, the beads were then resuspended in 50 µL of Laemmli buffer and heated at 95°C for 10 minutes. The samples were then ran on a 12% SDS-PAGE gel and analyzed by Western Blot as previously described in **Section 2.5.**

2.8.1 Cell Culture – Passaging Cells

LLC-MK2 cells (rhesus monkey kidney cells), BEAS-2B cells (human bronchus epithelial lung cells), and HEp-2 cells (Human HeLa contaminant carcinoma cells) were obtained from ATCC. All the cell lines were propagated using Dulbecco's Modified Eagle Medium (DMEM) (Gibco) containing 10% v/v fetal bovine serum (FBS) in 25 cm^2 or 75 cm^2 tissue culture flasks (Greiner Bio-One) in a 37°C and 5% CO_2 incubator. When the cells in the flask developed a fully confluent monolayer, the cells were passaged into a new flask at a ratio of 1:3 to 1:10 in DMEM + 10% FBS. The old media was removed aseptically by aspiration and the monolayers were washed once with 1 mL of 0.05% Trypsin-EDTA (Invitrogen) to remove any of the remaining old media. The monolayers were then incubated with 1 mL of Trypsin-EDTA for 25 cm^2 flask or 3 mL of Trypsin-EDTA for 75 cm^2 flask for approximately 3 to 5 minutes or until cells are detached from the flask in a 37°C and 5% CO_2 incubator. The cells were then resuspended in DMEM + 10% FBS to

inhibit trypsin activity and added to a new tissue culture flask, which was then incubated at 37°C and 5% CO_2.

2.8.2 Cell Culture – Seeding Plates

LLC-MK2 or BEAS-2B cells were treated with Trypsin-EDTA and detached from the flask as described in **Section 2.8.1**. The trypsin activity was inhibited by the addition of DMEM + 10% FBS and cells were pelleted by centrifugation at 500 x g for 5 minutes. The media was aseptically aspirated and the cells were thoroughly resuspended in 5 mL of DMEM + 10% FBS. A small amount of cells were mixed in a 1:1 ratio with 0.4% Trypan Blue and 20 µL were loaded onto a dual chamber cell counter counting slide (BioRad). The cells were counted using a TC20™ Automated Cell Counter (BioRad). Cells were seeded at various cell densities on either a 6 well plate or 96 well plate and incubated at 37°C and 5% CO_2 for either overnight, 24 or 48 hours.

2.9 Assessment of Cellular Uptake of Recombinant Proteins

LLC-MK2 cells in DMEM + 10% FBS were seeded into a 6 well plate at a cell density of 1,000,000 cells and left to attach in a 37°C and 5% CO_2 incubator overnight. The cells were washed once with DMEM. The cells were then incubated with either 20 µM of recombinant human thioredoxin proteins or 20 µM MBP-$P_{220-241}$ in DMEM at 37°C and 5% CO_2 for either 0 hours, 2 hours or 4 hours. At each respective time point, the media was aseptically aspirated and the wells were washed twice with PBS. The wells were treated with acid wash buffer (0.2 M glycine, 0.15 M NaCl, pH 3.0) for five minutes. The acid

wash buffer was aseptically aspirated, cells were washed with PBS, and then incubated with 1 mL of radioimmunoprecipitation assay (RIPA) buffer (Thermofisher) with 1 mM EDTA, 1 mM Phenylmethylsulfonyl fluoride (PMSF), and crushed protease inhibitor tablets (Pierce) for 10 minutes at room temperature. The wells were scraped with a cell scraper and lysates were incubated on ice for 10 minutes. The lysates were clarified by centrifugation at 16,000 x g for 15 minutes at 4°C. A sample of the supernatant was re-suspended in 5x Laemmli buffer and heated at 95°C for 10 minutes prior to being run on a 12% or 16% SDS-PAGE gel. The gel was analyzed by Western blot using mouse anti-His and mouse anti-α-tubulin antibodies using the method previously outlined in **Section 2.5**.

2.10 Concentration of Proteins Using Trichloroacetic Acid Precipitation

The remaining supernatant in **Section 2.9** was concentrated using trichloroacetic acid (TCA) precipitation in a 1.5 mL Eppendorf tube. TCA was added to the supernatant samples to a final concentration of 10% v/v and was incubated on ice for 10 minutes. The precipitated protein was pelleted at 16,000 x g for 5 minutes at 4°C on a bench top centrifuge. The pellet was washed with ice cold acetone and incubated in a -80°C freezer for 1 hour. The precipitated protein was pelleted at 16,000 x g for 10 minutes at 4°C and the supernatant was discarded. The acetone wash was repeated once more. The supernatant was discarded and the precipitated protein pellet was dried in a 37°C incubator with the Eppendorf tube with the lid left open for 10 minutes. The pellet was resuspended in 5x Laemmli buffer, boiled at 95°C for 15 minutes, and analyzed on a polyacrylamide gel as described in **Section 2.4 and 2.5**.

2.11 Propagation of Respiratory Syncytial Virus Subtype A

A 1 mL frozen aliquot of a clinical sample of RSV A Long strain of unknown titer was obtained from the St. Joseph's Hospital clinical virology laboratory. The virus aliquot was thawed and added to a fully confluent monolayer of HEp-2 cells in a T25 flask. The virus was allowed to adsorb for 4 hours in a 37°C and humidified 5% CO_2 incubator and rocked every 15 minutes to redistribute the inoculum. After 4 hours, virus adsorption was stopped with the addition of 4 mL of REFEED medium and the flask was incubated at 37°C and 5% CO_2 for 7-8 days. The virus was harvested by scraping off the entire monolayer using a cell scraper and the cell lysate was transferred into a falcon tube containing sterile glass beads. The tube was vortexed twice for 30 seconds each time and then centrifuged at 500 x g for 5 minutes to pellet cellular debris. The supernatant was then passed through a 0.22 μM filter, divided into 100 - 500 μL aliquots, and stored at -80°C until future use.

2.12 Determination of Propagated Respiratory Syncytial Virus Titer

The titer of RSV was determined by making 1:10 serial dilutions of the frozen virus aliquots in REFEED medium and 100 μL of each dilution was added to a 96 well plate containing confluent LLC-MK2 cells. The plate was centrifuged at 1,500 x g for 30 minutes and then incubated at 37°C and 5% CO_2 for 30 minutes. The viral medium in the wells were aseptically aspirated, replaced with REFEED medium, and incubated for 48 hours at 37°C and 5% CO_2. The media in the wells were then aseptically aspirated and washed twice with PBS before being fixed with ice cold methanol for 20 minutes at room temperature.

The wells were washed twice with PBST and blocked with 5% BSA in PBST for one hour at 37°C and 5% CO_2. The wells were washed twice with PBST, and treated with 1:1,000 dilution of RSV anti-fusion protein (Abcam) in 5% BSA in PBST for one hour at 37°C and 5% CO_2. The wells were washed seven times with PBST to remove non-specifically bound protein, and treated with a 1:200 dilution of goat anti-mouse-FITC antibody (Cedarlane) in 5% BSA in PBST for one hour in the dark at 37°C and 5% CO_2. The wells were washed seven times with PBST and incubated with 0.05% Evan's Blue reagent for 20 minutes at room temperature. The wells were washed twice with PBST and visualized with an Evos Light Microscope. The overall virus titer was determined by counting the total number of infected cells (cells showing green fluorescence) per monolayer multiplied by its respective dilution factor.

2.13 Assessing Viral Inhibition Using Indirect Immunofluorescence Microscopy

LLC-MK2 cells or BEAS-2B cells in DMEM + 10% FBS were seeded into a 96 well plate at a cell density of 40 000 cells/well and placed in a 37°C and 5% CO_2 incubator overnight for cells to attach. For the MBP-$P_{220-241}$ and hTrx-$P_{220-241}$ experiment, the cells were washed once with DMEM and incubated with either 0 µM, 10 µM, or 20 µM of hTrx-$P_{220-241}$ or 20 µM of MBP-$P_{220-241}$ in 100 µL of DMEM in a 37°C and 5% CO_2 incubator for 2 hours. For MBP-P_{1-29}, the cells were washed once with DMEM and incubated with either 0 µM, 20 µM, 40 µM, 80 µM, or 120 µM of MBP- P_{1-29} in 100 µL of DMEM in a 37°C and 5% CO_2 incubator for 2 hours. The media on the cells were then aseptically aspirated and replaced with 100 µL RSV A in REFEED medium, centrifuged at 1,500 x g

for 30 minutes, and incubated at 37°C and 5% CO_2 for 30 minutes. The viral medium was then aseptically aspirated out and replaced with either DMEM for no virus or peptide treated wells, DMEM for 0 µM of peptide treated wells or their respective peptide conditions. The 96 well plate was then incubated in a 37°C and 5% CO_2 incubator for 2 days and then visualized using indirect immunofluorescence microscopy as described in **Section 2.12**. Pictures of representative, random fields of view at 10x magnification for each experimental condition were taken on the Evos Light microscope. Percent inhibition (PI) calculations were made by comparing the average number of RSV-infected cells in the virus only wells (V) with the number of virus-infected cells in each of the various peptide conditions (P): PI = [(V-P)/V] x 100%.

2.14 Assessing Protein Toxicity with PrestoBlue® Reagent Cell Viability Assay

LLC-MK2 cells or BEAS-2B cells were seeded in a 96 well plate at 10,000 cells/well in DMEM + 10% FBS and incubated at 37°C and 5% CO_2 overnight for cells to attach. The cells were washed once in DMEM + 10% FBS before being treated with either 100 µL of DMEM + 10% FBS, MBP-$P_{1\text{-}29}$ in DMEM + 10% FBS or 2 mg/mL of cycloheximide in DMEM + 10% FBS and incubated at 37°C and 5% CO_2 for 0, 1, 2, and 3 days. At each time point, the wells were washed once with DMEM + 10% FBS before being incubated with 100 µL of 1:10 dilution of PrestoBlue® Reagent in DMEM + 10% FBS for 20 minutes at 37°C and 5% CO_2. 100 µL of PrestoBlue® Reagent was then transferred into a 96 well black polystyrene microplate (Greiner Bio-one) and relative fluorescent unit (RFU) readings were taken at an excitation wavelength (Ex) of 535 nm and

an emission wavelength (Em) of 615 nm using a SpectraMax Gemini EM plate reader. The wells were washed once with DMEM + 10% FBS and the respective experimental media solutions were added to each well and incubated at 37°C and 5% CO_2 until the next time point.

2.15 Assessing RSV Progeny Virus Release Using Indirect Immunofluorescence Microscopy

LLC-MK2 cells or BEAS-2B cells in DMEM + 10% FBS were seeded into a 96 well plate at a cell density of 40,000 cells per well and placed in a 37°C and 5% CO_2 incubator for two days for cells to attach. The cells were washed once with DMEM and incubated with either 0 µM, 80 µM, or 120 µM of MBP- $P_{1\text{-}29}$ in 100 µL of DMEM in a 37°C and 5% CO_2 incubator for 2 hours. The media on the cells were then aseptically aspirated and replaced with 100 µL RSV A in REFEED medium, centrifuged at 1,500 x g for 30 minutes, and incubated at 37°C and 5% CO_2 for 30 minutes. The viral medium was then aseptically aspirated out and replaced with either DMEM for no virus or peptide treated wells, DMEM for 0 µM of peptide treated wells or their respective peptide conditions. The 96 well plate was then incubated in a 37°C and 5% CO_2 incubator for 2 days. The supernatant from these wells were then taken, diluted 1:1 in DMEM media, and used to infect another set of 96 well plates containing LLC-MK2 or BEAS-2B cells respectively. The plates were centrifuged at 1500 x g for 30 minutes and incubated at 37°C and 5% CO_2 for 30 minutes. The supernatants in the wells were aseptically aspirated and replaced with DMEM. The cells were incubated at 37°C and 5% CO_2 for two days and then

visualized using indirect immunofluorescence microscopy as described in **Section 2.12**. Percent inhibition (PI) calculations were made by comparing the average number of RSV-infected cells in the virus only wells (V) with the number of virus-infected cells in each of the various peptide conditions (P): PI = [(V-P)/V] x 100%.

2.16 Statistical Analyses

All of the statistical analyses were performed using the GraphPad Prism® version 7.00 (GraphPad Software Inc, USA) and the data was presented as mean ± standard deviation. A one-way analysis of variance (ANOVA) followed by a *post hoc* Dunnett's test comparison was used to compare the peptide groups with the virus-only treated groups. A p value < 0.05 was determined to be significant for all tests. $P > 0.05$ (not shown), $P < 0.001$ (***), and $P < 0.0001$ (****).

CHAPTER 3 – RESULTS

RESULTS

3.1 Development and assessment of the antiviral activity of hTrx-$P_{220-241}$

3.1.1 Development of recombinant hTrx-$P_{220-241}$

In this study, the activity of novel RSV peptides will be compared to the previously tested MBP-$P_{220-241}$. The recombinant MBP-$P_{220-241}$ was originally cloned by Dr. David Bulir and all the experiments for this construct was completed by Jordan Nelson. The MBP carrier protein was chosen to increase the solubility of $P_{220-241}$ and to allow the protein to be expressed in *E. coli* (Sun, Tropea, & Waugh, 2011). The construct contained a HIV-1 Tat CPP to provide MBP-$P_{220-241}$ with the ability to enter into cells. The $P_{220-241}$ peptide mimetic was cloned onto the C-terminal end of this construct after the HIV-1 Tat CPP. A boxcar diagram of this construct is depicted in **Section 6.3**.

Due to the immunogenicity of the bacterial MBP carrier, a human carrier protein would be more preferable. The mutated human thioredoxin scaffold protein was chosen based on a number of favourable biophysical properties. Since it was based on the native human thioredoxin protein, it would likely not be immunogenic in humans. Furthermore, the mutations introduced to eliminate the cysteine residues (hTrx Δcys5) resulted in a loss of biological function and led to the purification of large quantities of monomeric protein from bacterial cultures (Borghouts et al., 2008). In addition, the hTrx construct also contained a polyarginine CPP, which enabled the anticancer peptide aptamers developed by Borghouts et al. (2008) to successfully enter into cells (Borghouts et al., 2008). Thus, owing to its prior success, the hTrx scaffold protein appeared as an ideal carrier protein for the $P_{220-241}$ peptide. To mimic the arrangement of MBP-$P_{220-241}$ construct and the need for

the F241 residue of $P_{220-241}$ to be exposed, the $P_{220-241}$ peptide mimetic was cloned on the C-terminal end of hTrx Δcys5 after the 9R CPP.

A pET-30 vector containing hTrx Δcys5 composed of two polyhistidine tags, an S-tag, and a 9R cell penetrating peptide (His_6-S-hTrx Δcys5-9R-His_{10}) was kindly provided by Dr. Bernd Groner in Frankfurt, Germany. It was used as the initial template in an inverse PCR reaction to produce a linearized plasmid containing $P_{220-241}$ (the PCR primers are listed in **Section 6.1**). The resulting PCR products were analyzed on a 0.6% agarose-ethidium bromide gel alongside a 1 Kb plus DNA ladder (**Figure 3.1.1.A**). The desired PCR product was approximately 6,000 base pairs in length, which was purified by gel extraction and the plasmid was circularized using the In-Fusion® cloning system. Subsequently, this newly constructed plasmid was used as the template to clone an extended polyhistidine tag (His_{10}) and a second 9R CPP onto the N-terminus of the hTrx protein in place of the hexaHis tag to form His_{10}-9R-S-hTrx-9R-$P_{220-241}$ using the method described in **Section 2.1.2**. The final plasmid was sent to Mobix laboratory at McMaster University for DNA Sanger sequencing to confirm the DNA sequence.

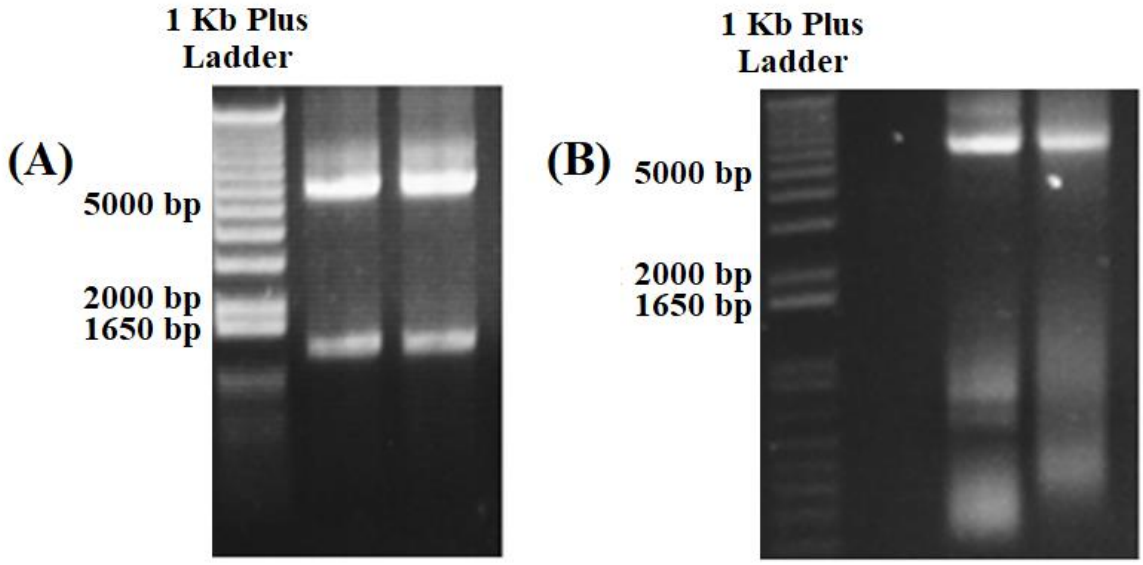

Figure 3.1.1: DNA agarose gel of inverse PCR-generated human thioredoxin products. 0.6% agarose gels analyzing the size of linearized plasmids that were generated using inverse PCR using primers encoding the nucleotide sequence for either $P_{220-241}$ or His_{10}-9R. The agarose gels were analyzed on the Quantity One program of the BioRad GelDoc™ XR+ system. The left lane on each agarose gel corresponds to a 1 Kb plus DNA ladder that were ran alongside two replicate inverse PCR samples and the approximate size of the PCR products were determined by comparison with the ladder. (A) Inverse PCR products of His_6-S-hTrx-9R-$RSVP_{220-241}$ generated by inverse PCR. (B) Inverse PCR products of His_{10}-9R-S-hTrx-9R-$RSVP_{220-241}$.

3.1.2 Expression and affinity purification of hTrx-$P_{220-241}$

The plasmid containing hTrx-$P_{220-241}$ was transformed into *E. coli* Rosetta (DE3), grown up in a 2 L bacterial culture, and purified by affinity chromatography on the AKTA FPLC according to the method described in **Section 2.3.1**. The purified product was run on a 16% SDS-PAGE gel and analyzed by Western Blot using a mouse anti-His antibody and goat anti-mouse-horseradish peroxidase antibody to confirm protein expression and to

assess for the presence of breakdown products (**Figure 3.1.2**). The predicted size of hTrx-$P_{220-241}$ was approximately 21.8 kilodaltons (kDa) as predicted by the ExPasy Compute Isoelectric Point/Molecular Weight tool.

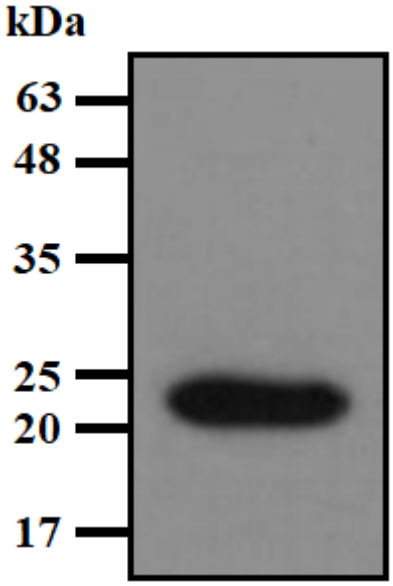

Figure 3.1.2: Purification of hTrx-$P_{220-241}$. HTrx-$P_{220-241}$ was grown in 2 L bacterial cultures and affinity purified using its polyhistidine tag and the AKTA FPLC. The purified protein was dialyzed overnight into an L-arginine hydrochloride refolding buffer and then into PBS + 10% glycerol. A small sample of the purified protein was run on a 16% SDS-PAGE gel and analyzed by Western Blot using a mouse α His antibody. A BLUelf prestained protein ladder (with the indicated molecular weight in kDa) was run alongside the protein sample and it was used to determine the approximate molecular weight of the purified protein. HTrx-$P_{220-241}$ (right) appear as a monomeric product with no visible breakdown products. The theoretical molecular weight of hTrx-$P_{220-241}$ was predicted to be 21.8 kDa by the ExPasy Compute pI/Mw tool.

3.1.3 hTrx-$P_{220-241}$ interacts with full length RSV nucleoprotein

Prior to evaluating the antiviral activity of hTrx-$P_{220-241}$, it was essential to confirm that hTrx-$P_{220-241}$ can interact with RSV nucleoprotein. Tran et al. (2007) demonstrated that the last nine C-terminal amino acids of phosphoprotein were sufficient to interact with GST-tagged N protein (GST-N) (Tran et al., 2007). Furthermore, a previous graduate student in Dr. Mahony's laboratory showed that MBP-$P_{220-241}$ could bind to GST-N in a GST pulldown assay. Thus, the interaction between hTrx-$P_{220-241}$ and GST-N was assessed in a GST pulldown assay using MBP-$P_{220-241}$ as a positive control while GST alone was used as a negative control. GST and GST-N bound to magnetic glutathione-agarose beads were used as bait proteins while MBP-$P_{220-241}$ and hTrx-$P_{220-241}$ were used as the prey proteins. Cell lysates from *E. coli* expressing GST-N and GST were bound to magnetic glutathione-agarose beads, blocked with 5% BSA in PBST, and incubated with either MBP-$P_{220-241}$ or hTrx-$P_{220-241}$ lysates (in triplicates). The beads were then washed with a high salt wash buffer to remove non-specific interactions, re-suspended in Laemmli buffer, and boiled at 95°C for 10 minutes to elute the protein off the beads. The samples were ran on a 12% SDS-PAGE gel and analyzed by Western blot using either a mouse anti-His or mouse anti-GST antibody. Both MBP-$P_{220-241}$ and hTrx-$P_{220-241}$ specifically interacted with GST-N, but did not interact with GST (**Figure 3.1.3.A** and **Figure 3.1.3.C**). An anti-GST antibody was used as a loading control.

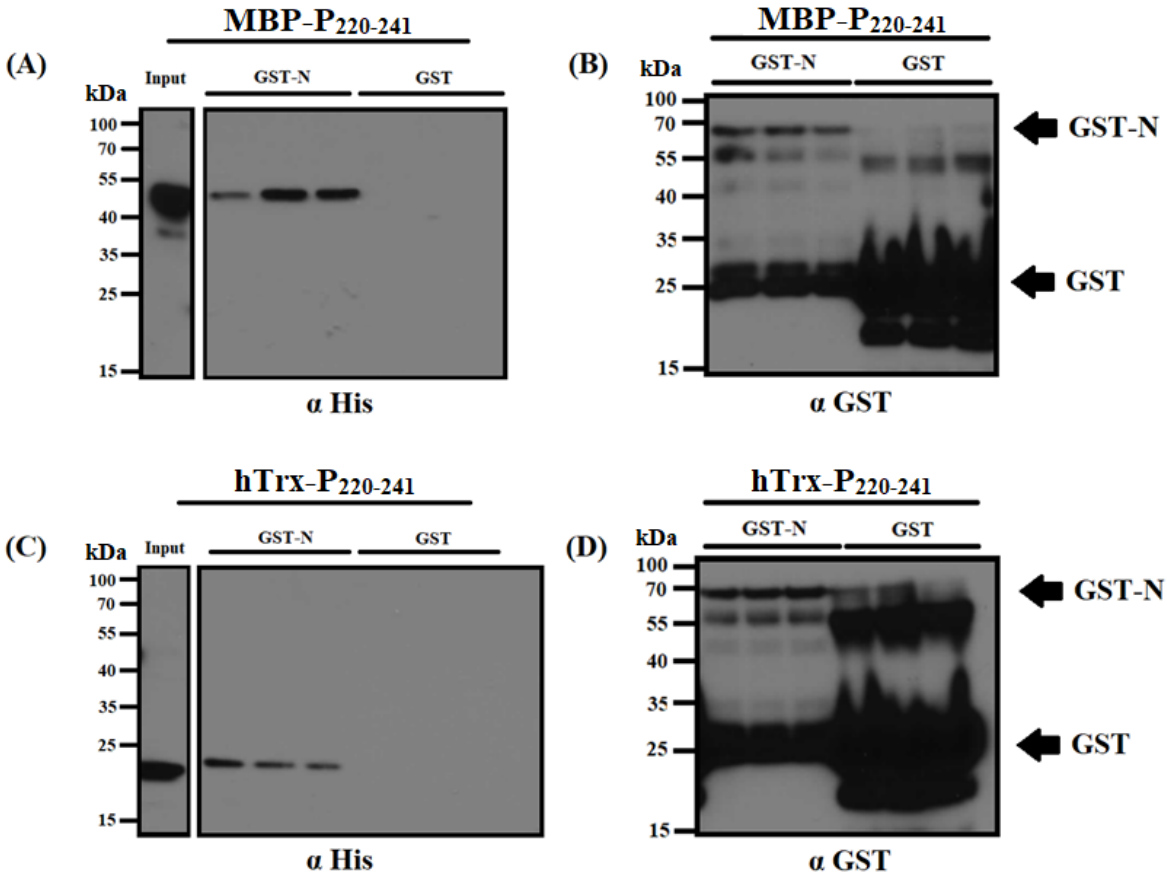

Figure 3.1.3: Interaction of MBP-P$_{220-241}$ or hTrx-P$_{220-241}$ with GST-N. Cell lysates containing GST or GST-N (bait proteins) were bound to magnetic glutathione-agarose beads for 1 hour while nutating and then blocked with 5% w/v BSA in PBST for 1 hour while nutating. These beads were then incubated with either MBP-P$_{220-241}$ or hTrx-P$_{220-241}$ (prey proteins) at 25°C for 2 hours and then washed seven times with 25°C high salt wash buffer for 15 seconds each on a magnetic NucliSENS miniMag® with 1 second spin intervals. The beads were then resuspended in Laemmli buffer and boiled at 95°C. The samples were ran on a 12% SDS-PAGE gel and analyzed by Western Blot using either a mouse α His antibody or a mouse α GST antibody. To the left of all the figures is a prestained protein ladder that was run alongside protein samples. (A) The input control (left) depicted the size of MBP-P$_{220-241}$ prey protein. From left to right, the wells after the input control were elution fractions of GST-N bound beads (in triplicates) and GST bound beads (in triplicates). (B) The protein samples in (a) were analyzed using a mouse α-GST antibody as a loading control. (C) The input control (left) depicted the size of hTrx-P$_{220-241}$ prey protein. From left to right, the wells after the input control were elution fractions of GST-N bound beads (in triplicates) and GST bound beads (in triplicates). (D) The protein samples in (c) were analyzed using a mouse α-GST antibody as a loading control.

3.1.4 Uptake of hTrx-$P_{220-241}$ into LLC-MK2 cells

After confirming that hTrx-$P_{220-241}$ interacts with the N protein, the next step was to investigate whether or not hTrx-$P_{220-241}$ can be taken up into LLC-MK2 cells. In designing hTrx-$P_{220-241}$, a second 9R CPP was added to the N-terminus of the peptide mimetic as previous experiments with only the 9R adjacent to $P_{220-241}$ was not taken up into cells (data not shown). Without intracellular localization, hTrx-$P_{220-241}$ would not be able to bind N protein in RSV-infected cells nor disrupt the formation of the essential RdRp complex. Thus, this is a crucial experiment prior to testing hTrx-$P_{220-241}$ for antiviral activity. Furthermore, MBP-$P_{220-241}$ was previously demonstrated to be successfully taken up into LLC-MK2 cells in as little as ten minutes.

LLC-MK2 cells were seeded into a six well plate and incubated with either media, hTrx Δcys5, MBP-$P_{220-241}$ or hTrx-$P_{220-241}$ for two or four hours. The cells were then washed with PBS, treated with an acid buffer wash to remove exogenously bound protein, and lysed with RIPA buffer. Lysates were collected, pelleted by centrifugation, and the supernatants were collected for further processing. The supernatants were TCA precipitated, run on a SDS-PAGE gel, and analyzed by Western blot using a mouse α-His antibody. HTrx Δcys5 served as a positive uptake control, media served as the negative control, and a mouse anti-α-tubulin antibody served as a loading control. Surprisingly, MBP-$P_{220-241}$ did not get taken up into LLC-MK2 cells (**Figure 3.1.4.A**) and MBP-$P_{220-241}$ uptake results of the previous student could not be replicated. However, hTrx-$P_{220-241}$ did get taken up by LLC-MK2 cells (**Figure 3.1.4.C**).

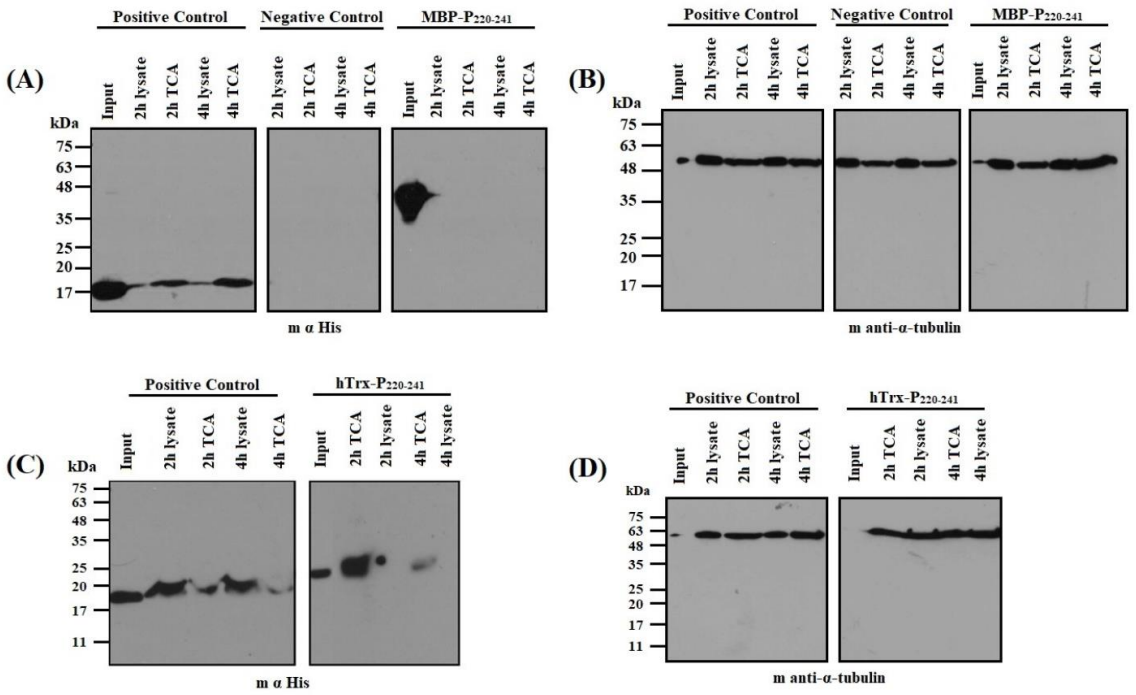

Figure 3.1.4: Uptake of hTrx-P$_{220-241}$ and MBP-P$_{220-241}$ by LLC-MK2 cells. LLC-MK2 cells in a 6 well plate were incubated with either 20 μM of a positive uptake control (hTrx Δcys), DMEM with no peptide, 20 μM of MBP-P$_{220-241}$ or 20 μM hTrx-P$_{220-241}$ for 2 or 4 hours. At each time point, cell monolayers were washed twice with PBS and once with an acid wash buffer to remove exogenously bound protein. Cells were lysed with RIPA buffer and the cellular debris were pelleted by centrifugation. The supernatants were taken, a small amount of it was stored, and the rest were TCA precipitated to concentrate the protein. The samples were resuspended in Laemmli buffer, boiled, ran on a 12% SDS-PAGE gel and analyzed by Western Blot using a mouse α-His antibody for (A) and (C) or mouse anti-α-tubulin antibody for (B) and (D). To the left of each figure is a prestained protein ladder that was run alongside protein samples and used to determine approximate size of protein bands. (A) Western blot of MBP-P$_{220-241}$ cell lysate samples with positive and negative uptake controls. The input are purified proteins used in the uptake experiment and indicate the size of the protein. (B) Lysates from MBP-P$_{220-241}$ uptake experiment were analyzed with anti-α-tubulin antibody as a loading control. (C) Western blot of hTrx-P$_{220-241}$ lysate samples with positive and negative uptake controls. The input are purified proteins used in the uptake experiment and represent the size that the proteins should appear as. (D) Lysates from hTrx-P$_{220-241}$ uptake experiment were analyzed with anti-α-tubulin antibody as a loading control.

3.1.5 Inhibition of RSV A replication by hTrx-$P_{220-241}$

One of the main objectives in this thesis was to evaluate the efficacy of hTrx-$P_{220-241}$ in inhibiting RSV replication *in vitro*. Historical data from Dr. Mahony's laboratory demonstrated that 20 μM MBP-$P_{220-241}$ could inhibit RSV A replication. Considering that hTrx-$P_{220-241}$ could interact with the N protein and could enter into cells, I hypothesized that hTrx-$P_{220-241}$ would inhibit RSV replication. Fully confluent monolayers of LLC-MK2 cells in a 96 well plate were pre-incubated with MBP-$P_{220-241}$ or hTrx-$P_{220-241}$. The cells were then infected with RSV A and incubated with either MBP-$P_{220-241}$ or hTrx-$P_{220-241}$ for 48 hours before being visualized with indirect immunofluorescent microscopy using an anti-RSV fusion protein antibody and a goat anti-mouse-FITC antibody (**Figure 3.1.5.A**). The controls used in this experiment were wells treated with no virus and no peptide, and wells infected only with RSV. The number of infected cells per monolayer were counted (**Figure 3.1.5.B**) and percent inhibition was calculated using the formula described in **Section 2.13**. Compared to a virus only control, MBP-$P_{220-241}$ inhibited RSV replication by approximately 50.6% at 20 μM while hTrx-$P_{220-241}$ inhibited RSV A replication by approximately 7.7% at 20 μM and 4.0% at 10 μM (**Figure 3.1.5.C**). Higher concentrations of hTrx-$P_{220-241}$ could not be tested due to visible cytotoxicity above 20 μM. Since MBP-$P_{220-241}$ demonstrated antiviral activity, it must have been taken up by cells in **Section 3.1.4**, but it was not detected perhaps due to the cleavage of the polyhistidine tag.

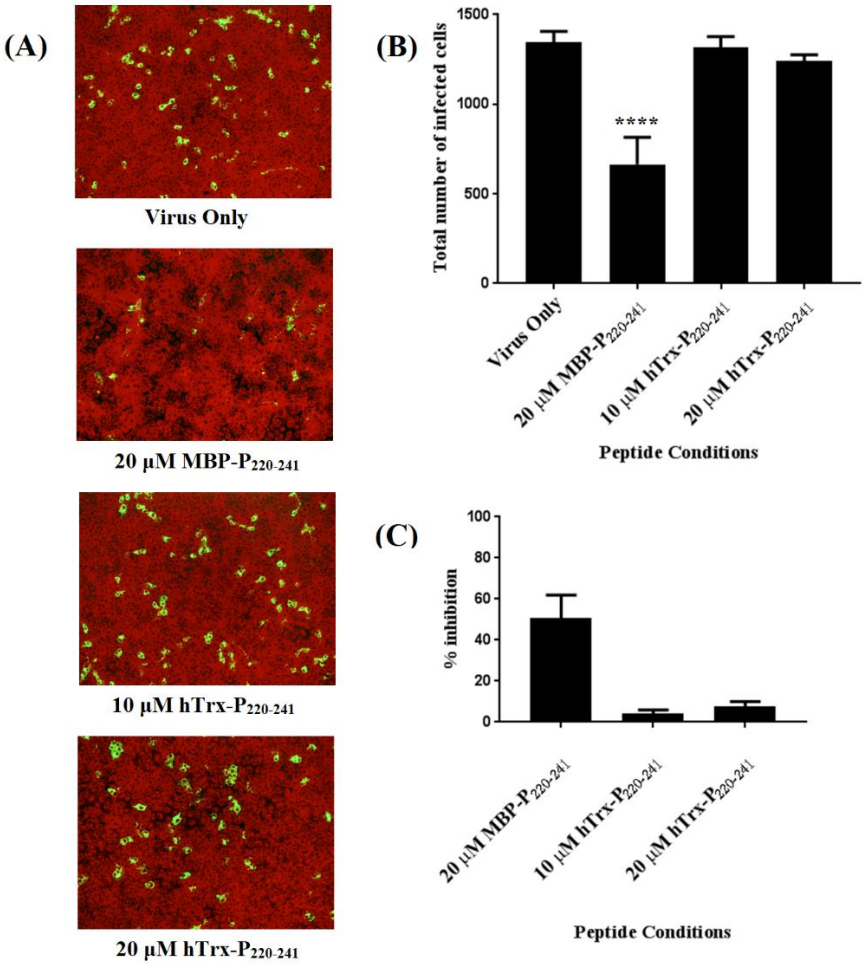

Figure 3.1.5: Inhibition of RSV A infection by MBP-$P_{220-241}$ and hTrx-$P_{220-241}$. LLC-MK2 cells were treated with 20 µM MBP-$P_{220-241}$, 10 µM hTrx-$P_{220-241}$ or 20 µM hTrx-$P_{220-241}$ prior to being infected with RSV A for 48 hours. The cells were fixed with methanol and visualized using indirect immunofluorescence microscopy using a mouse anti-RSV fusion protein antibody and goat anti-mouse-FITC. (A) Representative, random fields of view of stained LLC-MK2 monolayers were taken by an Evos light microscope at 10x magnification. Virus-infected cells stained green (FITC) and non-infected cells were stained red. (B) The mean of the total number of RSV-infected cells in wells treated with 20 µM MBP-$P_{220-241}$, 10 µM hTrx-$P_{220-241}$ or 20 µM hTrx-$P_{220-241}$ (in triplicates) were plotted. The error bars represent one standard deviation from the mean. The statistical significance was calculated using one-way ANOVA followed by a *post hoc* Dunnett's test comparison, which compared the peptide groups with the virus-only treated groups. **** indicates a p value <0.0001 (C) Percent inhibition of RSV infection by MBP-$P_{220-241}$ and hTrx-$P_{220-241}$ compared to virus only control. Error bars represent one standard deviation from the mean.

3.2 Development and evaluation of the novel MBP-P_{1-29} peptide mimetic

3.2.1 Genetic Cloning, Protein Expression and Affinity Purification of MBP-P_{1-29}

Since hTrx-$P_{220-241}$ did not inhibit RSV replication, the next objective was to design and assess the antiviral activity of a novel P_{1-29} peptide mimetic *in vitro*. Previous studies have demonstrated that P_{1-29} could interact with the N protein and that a P_{1-29} synthetic peptide could reduce RNA replication by approximately 50% in a minigenome replicon assay (Galloux et al., 2015). To build on these findings, I hypothesized that P_{1-29} conjugated to MBP and a CPP would be able to inhibit RSV replication *in vitro*. Using inverse PCR and the In-Fusion® cloning system, the nucleotide sequence of P_{1-29} was inserted on the C-terminus of a MBP-NLS vector after the HIV-1 Tat CPP to generate MBP-P_{1-29} (the corresponding primers used are listed in **Section 6.1**). To ensure P_{1-29} was in proper orientation, the amino acid sequence was reversed so that the first amino acid, methionine, was now the last amino acid. A boxcar diagram is shown in **Section 6.3**.

The MBP-P_{1-29} plasmid was then transformed into *E. coli* Rosetta and purified according to the method described in **Section 2.3.2**. The purified product was run on a 12% SDS-PAGE gel and analyzed by Western Blot using a mouse anti-His antibody and goat anti-mouse-horseradish peroxidase antibody to confirm protein expression and to assess for the presence of breakdown products (**Figure 3.2.1.B**). The predicted size of MBP-P_{1-29} was approximately 50.7 kDa using the online ExPasy Compute Isoelectric Point/Molecular Weight tool.

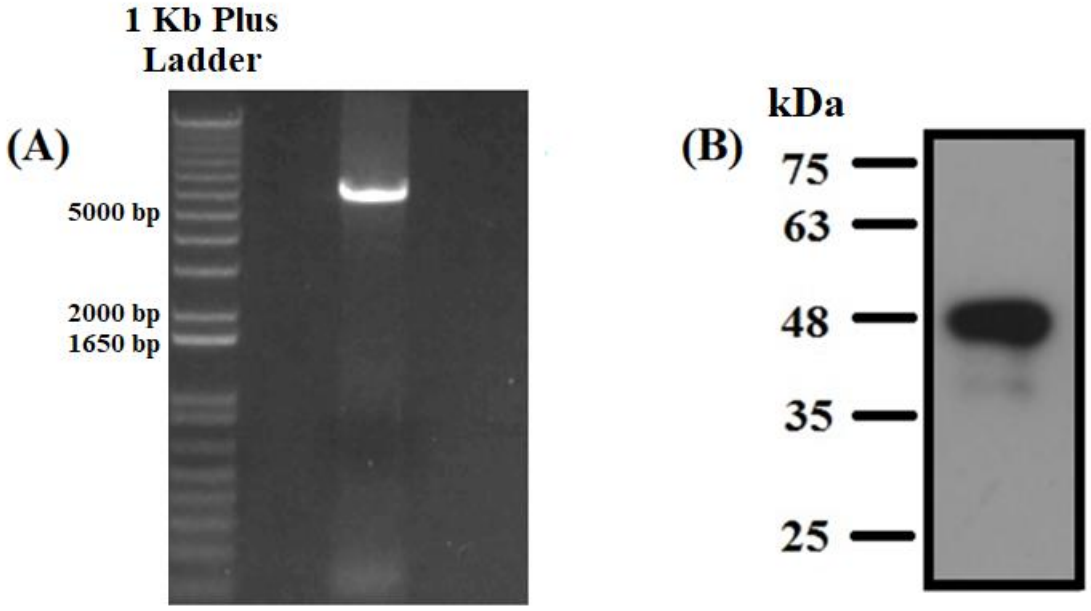

Figure 3.2.1: Cloning and purification of MBP-P_{1-29}. (A) **Agarose gel of MBP-P_{1-29} inverse PCR products.** A 0.6% agarose gel analyzing the size of MBP-P_{1-29} linearized plasmid that was generated using inverse PCR and primers encoding for the nucleotide sequence of P_{1-29}. The agarose gels were analyzed on the Quantity One program of the BioRad GelDoc™ XR+ system. The left lane on each agarose gel corresponds to a 1 Kb plus DNA ladder that were ran alongside PCR samples and the approximate size of PCR products were determined by comparison with the ladder. The predicted size of the plasmid was 6000 base pairs. (B) **Western blot of MBP-P_{1-29}.** MBP-P_{1-29} was grown in bacterial cultures and affinity purified using its polyhistidine tag and the AKTA FPLC. The protein was buffer exchanged into PBS + 10% glycerol, filtered, and concentrated. A small sample of the protein was run on a 12% SDS-PAGE gel and analyzed by Western blot using a mouse α His antibody. A prestained protein ladder (with the indicated molecular weight in kDa) was run alongside the protein sample to determine the approximate molecular weight of the purified protein. The theoretical molecular weight of MBP-P_{1-29} was predicted to be 50.7 kDa by the ExPasy Compute pI/Mw tool.

3.2.2 Uptake of MBP-P_{1-29} into LLC-MK2 cells

In designing MBP-P_{1-29}, a HIV-1 Tat nuclear localisation signal was chosen as the CPP to facilitate cellular uptake. Without intracellular localization, it would not be possible to assess the antiviral activity of MBP-P_{1-29}. The cellular uptake assay was performed as described in **Section 3.1.4**. MBP-P_{1-29} was successfully taken up into cells after both two and four hours (**Figure 3.2.2.A**).

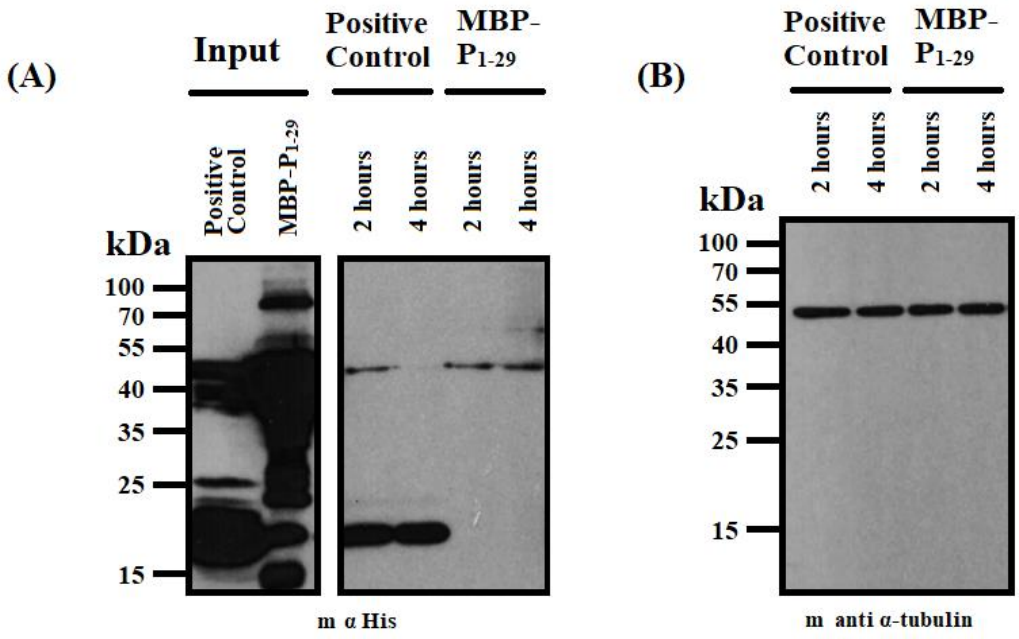

Figure 3.2.2: Uptake of MBP-P_{1-29} by LLC-MK2 cells. LLC-MK2 cells in a 6 well plate were incubated with either 20 μM of a positive uptake control (hTrx Δcys) or 50 μM of MBP-P_{1-29} for 2 and 4 hours. At each time point, cell monolayers were washed twice with PBS, once with an acid wash buffer, and PBS once more to remove exogenously bound protein. Cells were lysed with a RIPA buffer cocktail containing protease inhibitors and the cellular debris were pelleted by centrifugation. The supernatants were taken and mixed with Laemmli buffer, boiled, and ran on a 12% SDS-PAGE gel. The gels were analyzed by Western Blot. To the left of each figure is a prestained protein ladder that was run alongside protein samples and used to determine approximate size of protein bands. (A) Western blot of MBP-P_{1-29} cell lysate samples with a positive uptake control. The input wells are purified proteins used in the uptake experiment and indicate the size of the protein. (B) Lysates from MBP-P_{1-29} uptake experiment were analyzed with an anti-α-tubulin antibody as a loading control.

3.2.3 The effect of MBP-P_{1-29} on LLC-MK2 cell viability

Prior to testing for antiviral activity, it was important to ensure that MBP-P_{1-29} does not exhibit any cytotoxicity. PrestoBlue reagent is a resazurin-based dye that provides a fluorescence measurement that is proportional to the total number of metabolically active cells (Fields & Lancaster, 1993; Xu, McCanna, & Sivak, 2015). At Day 0, an under confluent monolayer of LLC-MK2 cells in a 96 well plate were incubated with 1:10 dilution of PrestoBlue reagent in media and relative fluorescent unit (RFU) measurements were conducted at an excitation wavelength of 535 nm and an emission wavelength of 615 nm. The monolayers were then washed twice with media and incubated with either media, MBP-P_{1-29} or cycloheximide. After 24 hours, the experimental conditions were aspirated, PrestoBlue readings were taken, and the experimental media conditions were replaced. This was repeated twice more every 24 hours. The positive control were wells incubated with media. The negative control was cycloheximide, which is an inhibitor of protein synthesis in eukaryotic cells (Schneider-Poetsch et al., 2010). Over the period of three days, there appeared to be no significant difference between media and 120 μM MBP-P_{1-29}-treated cells (**Figure 3.2.3**) indicating that this concentration of peptide was not toxic. However, 160 μM MBP-P_{1-29}-treated cells showed a decrease in RFU over time indicating its toxicity at this concentration. Cycloheximide-treated cells displayed relatively consistent RFU measurements over the course of 72 hours indicating no cell division.

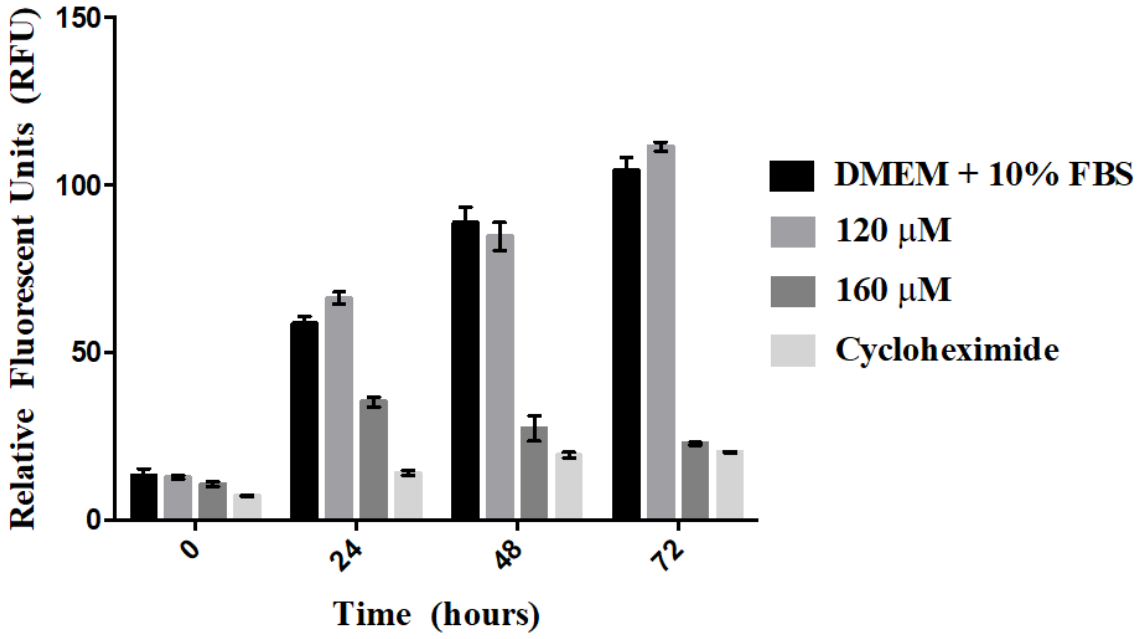

Figure 3.2.3: Effect of MBP-P_{1-29} on LLC-MK2 cell viability. An under confluent monolayer of LLC-MK2 cells in a 96 well plate were treated (in triplicates) with either DMEM+10% FBS media, 120 μM MBP-P_{1-29}, 160 μM MBP-P_{1-29} or 2 mg/mL cycloheximide in DMEM + 10% FBS for 0, 24, 48, and 72 hours. At each time point, the media was aspirated and the wells were treated with PrestoBlue® Reagent in DMEM + 10% FBS for 20 minutes at 37°C and 5% CO_2. The media was then transferred to a 96 well black plate and relative fluorescent unit (RFU) measurements were taken by a fluorimeter at an excitation wavelength of 535 nm and emission wavelength of 615 nm. The mean of the RFU measurements from the three replicates were plotted. Error bars represent one standard deviation from the mean.

3.2.4 Inhibition of RSV A infection in LLC-MK2 cells by MBP-P_{1-29}

One of the central goals of this thesis was to assess the antiviral properties of the novel MBP-P_{1-29} peptide *in vitro*. This inhibition assay was performed as described in **Section 2.10** and **Section 3.1.5**. Compared to a virus only control, MBP-P_{1-29} inhibited RSV A replication in a dose-dependent manner: approximately 80.6% at 120 μM, 71.7% at 80 μM, 56.9% at 40 μM, and 32.7% at 20 μM (**Figure 3.2.4.C**).

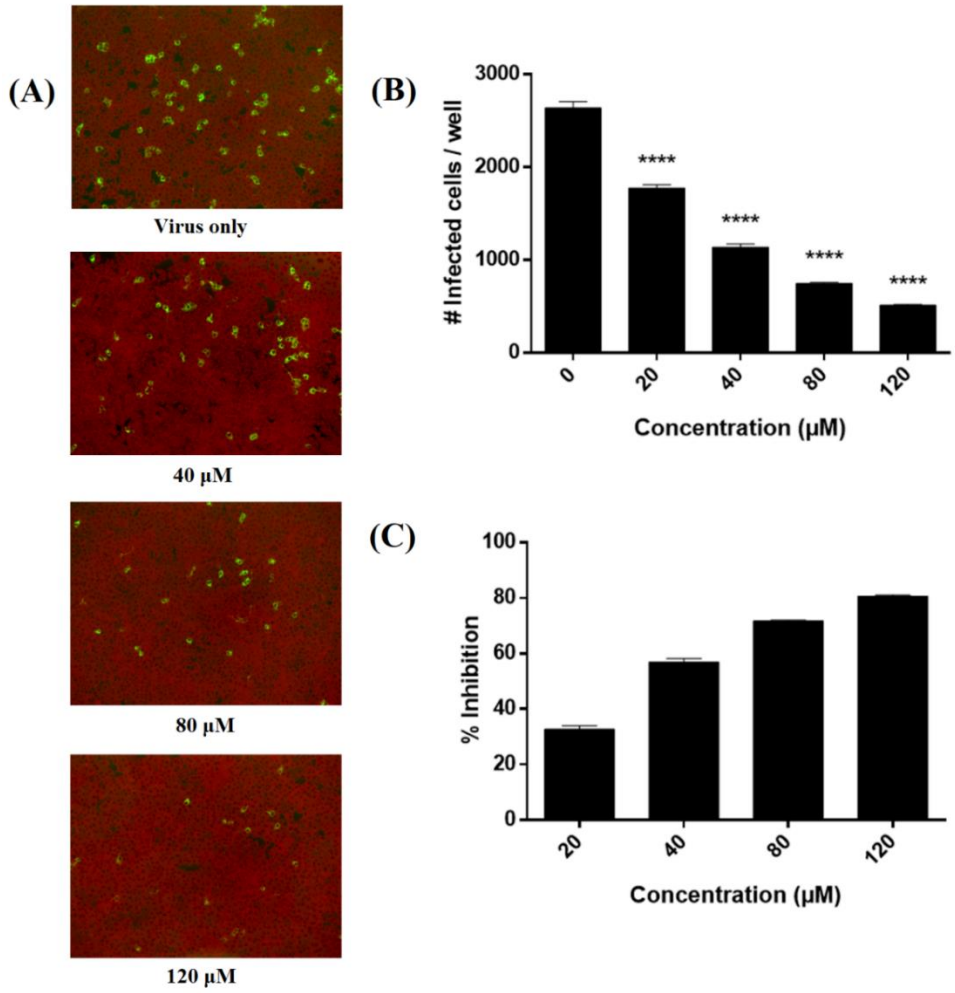

Figure 3.2.4: Inhibition of RSV A infection in LLC-MK2 cells by MBP-P_{1-29}. LLC-MK2 cells were treated with increasing doses of MBP-P_{1-29} prior to being infected with RSV A for 48 hours. The cells were fixed with methanol and visualized using indirect immunofluorescence microscopy using a mouse anti-RSV fusion protein antibody and goat anti-mouse-FITC. (A) Representative, random fields of view of stained LLC-MK2 monolayers were taken by an Evos light microscope at 10x magnification. Virus-infected cells stained green (FITC) and non-infected cells were stained red. (B) The mean of the total number of RSV-infected cells in wells treated with either 0, 20, 40, 80, or 120 µM of MBP-P_{1-29} (in triplicates) were plotted. The error bars represent one standard deviation from the mean and the statistical significance was calculated using one-way followed by a *post hoc* Dunnett's test comparing the peptide groups with the virus-only treated groups. **** indicates a p value <0.0001 (C) Percent inhibition of RSV infection by MBP-P_{1-29} compared to virus only control. Error bars represent one standard deviation from the mean.

3.2.5 The effect of MBP-P_{1-29} on BEAS-2B cell viability

To confirm that the antiviral activity of MBP-P_{1-29} is not limited specifically to LLC-MK2 cells, I tested MBP-P_{1-29} on a human bronchus epithelial cell line, BEAS-2B cells. First, I investigated whether or not MBP-P_{1-29} was toxic to this cell line using the PrestoBlue® reagent cell viability assay described in **Section 2.15** and **Section 3.2.3**. The controls used in the experiment were once again wells treated with media or 2mg/mL cycloheximide. Over the span of 72 hours, there was no statistically significant difference between media and 120 μM MBP-P_{1-29}-treated cells in BEAS-2B cells (**Figure 3.2.5**). Cycloheximide-treated cells displayed relatively consistent RFU measurements over the span of 72 hours.

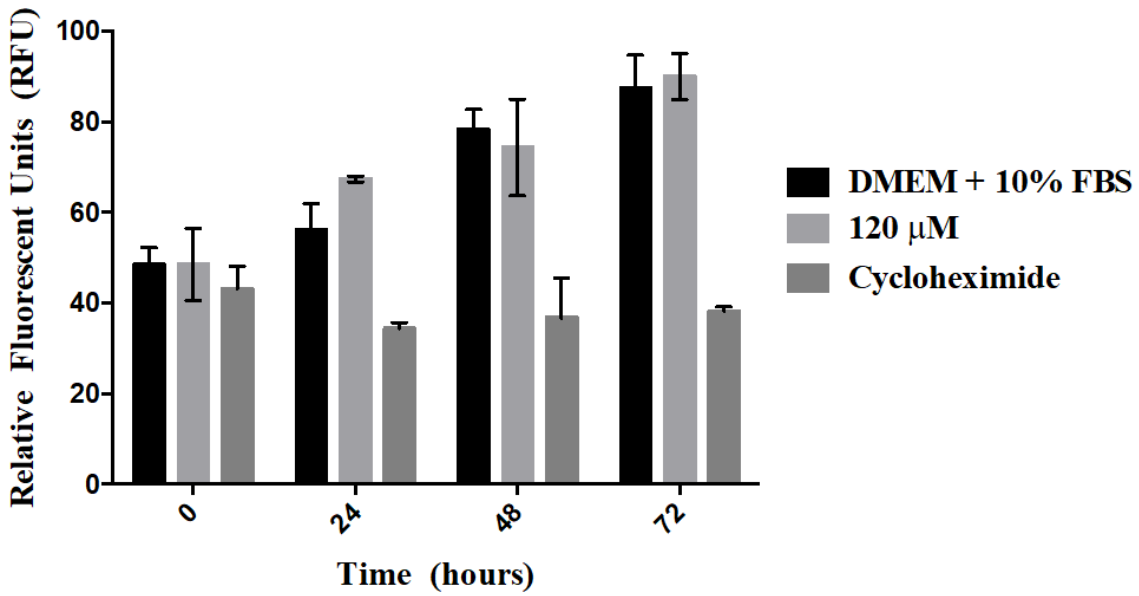

Figure 3.2.5: Effect of MBP-P_{1-29} on BEAS-2B cell viability. An under confluent monolayer of BEAS-2B cells in a 96 well plate were treated (in triplicates) with either DMEM+10% FBS media, 120 μM MBP-P_{1-29}, or 2 mg/mL cycloheximide in DMEM + 10% FBS for 0, 24, 48, and 72 hours. At each time point, the media was aspirated and the wells were treated with PrestoBlue® Reagent in DMEM + 10% FBS for 20 minutes at 37°C and 5% CO_2. The media was then transferred to a 96 well black plate and relative fluorescent unit (RFU) measurements were taken by a fluorimeter at an excitation wavelength of 535 nm and emission wavelength of 615 nm. The mean of the RFU measurements from the three replicates were plotted. Error bars represent one standard deviation from the mean.

3.2.6 Inhibition of RSV A infection in BEAS-2B cells by MBP-P_{1-29}

Next, the ability of MBP-P_{1-29} to inhibit RSV infection in BEAS-2B cells was tested. The inhibition assay was performed as described in **Section 2.10** and **Section 3.1.5**. Compared to a virus only control, MBP-P_{1-29} inhibited RSV A replication by approximately 60% at 120 μM, 44.4% at 80 μM, 24% at 40 μM and 13.3% at 20 μM (**Figure 3.2.6.C**).

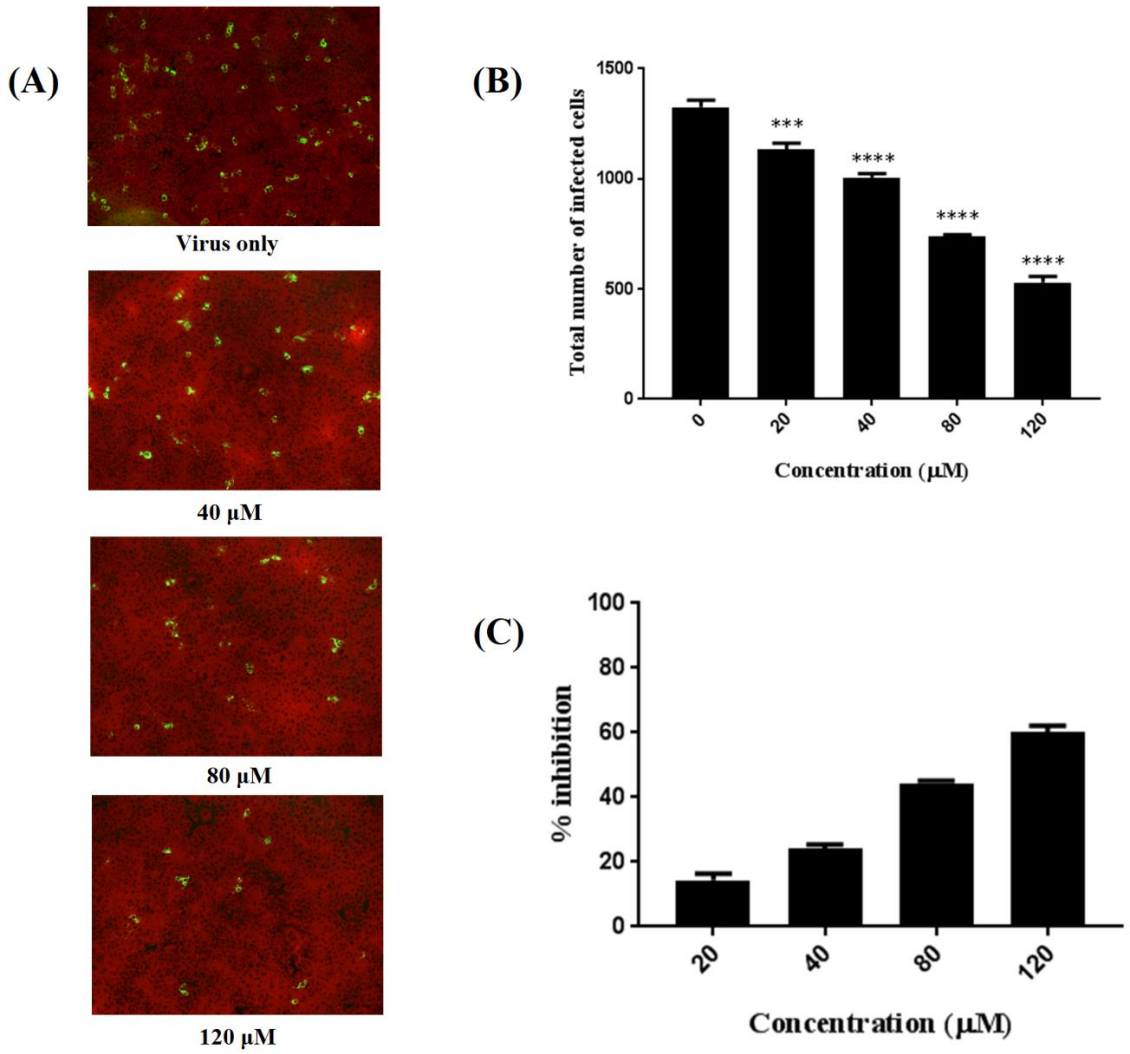

Figure 3.2.6: Inhibition of RSV A infection in BEAS-2B cells by MBP-P_{1-29}. BEAS-2B cells were treated with increasing doses of MBP-P_{1-29} prior to being infected with RSV A for 48 hours. The cells were fixed with methanol and visualized using indirect immunofluorescence microscopy using a mouse anti-RSV fusion protein antibody and goat anti-mouse-FITC. (A) Representative, random fields of view of stained LLC-MK2 monolayers were taken by an Evos light microscope at 10x magnification. Virus-infected cells stained green (FITC) and non-infected cells were stained red. (B) The mean of the total number of RSV-infected cells in wells treated with either 0, 20, 40, 80, or 120 µM of MBP-P_{1-29} (in triplicates) were plotted. The error bars represent one standard deviation from the mean and the statistical significance was calculated using one-way ANOVA followed by a *post hoc* Dunnett's test comparing the peptide groups with the virus-only treated groups. *** indicates a p value < 0.001, **** indicates a p value <0.0001 (C) Percent inhibition of RSV infection by MBP-P_{1-29} compared to virus only control. Error bars represent one standard deviation from the mean.

3.2.7 Inhibition of progeny virus release by MBP-P_{1-29}

After evaluating MBP-P_{1-29}'s effect on viral replication, I investigated whether or not this inhibition would translate to a reduction in the number of viable progeny RSV virus released. To do so, fully confluent monolayers of LLC-MK2 cells or BEAS-2B cells in a 96 well plate were pre-incubated with increasing concentrations of MBP-P_{1-29} or media. The cells were then infected with RSV A and incubated again with their respective media conditions for 48 hours. The supernatants were then taken, diluted 1:1 in fresh media, and used to infect new 96 well plates containing either LLC-MK2 or BEAS-2B cells respectively. The cells were visualized by indirect immunofluorescence microscopy, the total number of infected cells per monolayer were counted, and percent inhibition was calculated. The controls used in this experiment were wells treated with no virus and no peptide, and wells infected only with RSV. In LLC-MK2 cells, there was approximately a 74.5% reduction in viral progeny release at 120 μM and 31.4% reduction of progeny virus release at 80 μM (**Figure 3.2.7.A**). Meanwhile, in BEAS-2B cells, there was a 34.7% reduction of progeny virus release at 120 μM and 19.3% reduction in progeny virus release at 80 μM (**Figure 3.2.7.B**).

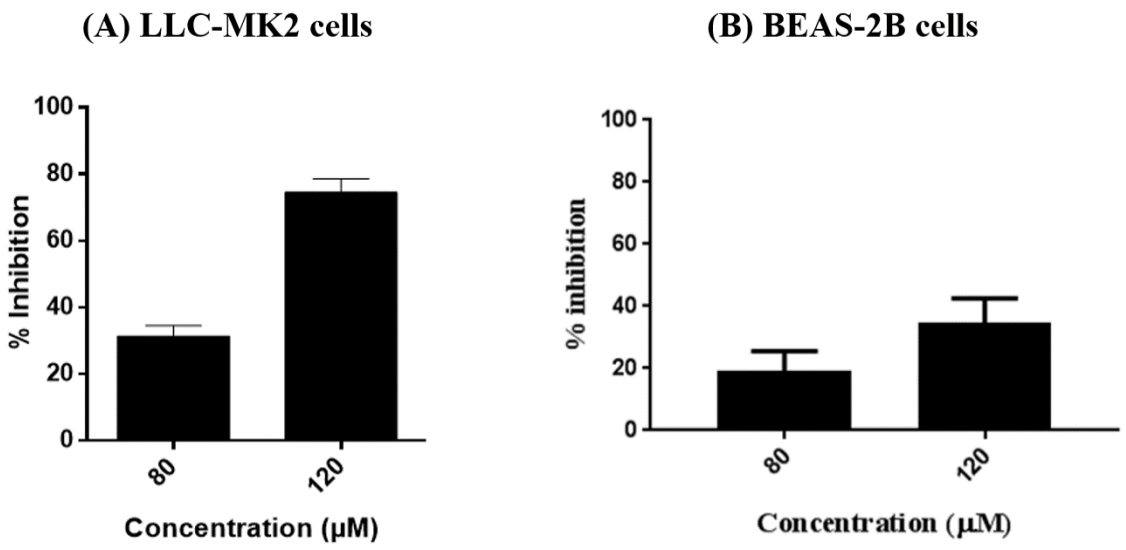

Figure 3.2.7: MBP-P_{1-29} inhibits viral progeny production. LLC-MK2 or BEAS-2B cells pre-treated with 80 μM and 120 μM of MBP-P_{1-29} were infected with RSV for 48 hours. The supernatants were then used to infect new LLC-MK2 or BEAS-2B cells for 48 hours and infection was visualized by indirect immunofluorescence microscopy using a mouse α-RSV fusion antibody and a goat α mouse-FITC antibody. The total number of virus-infected cells per monolayer were counted and percent inhibition, compared to a virus only control, was calculated and graphed. (A) Percent inhibition of progeny virus release in LLC-MK2 cells. The error bars represent one standard deviation from the mean. (B) Percent inhibition of progeny virus release in BEAS-2B cells. The error bars represent one standard deviation from the mean.

CHAPTER 4 – DISCUSSION

DISCUSSION

4.1.1 Interaction between hTrx-$P_{220-241}$ and N protein

Prior to the assessment of antiviral activity, it was crucial to verify that hTrx-$P_{220-241}$ can interact with RSV N protein. A previous graduate student demonstrated that $P_{220-241}$ conjugated to a MBP could interact with a full length N protein tagged with GST (GST-N). Thus, I hypothesized that hTrx-$P_{220-241}$ should also be able to specifically interact with full length N protein. GST-tagged proteins were bound to glutathione-agarose beads to act as bait proteins to test the interactions with MBP-$P_{220-241}$ and hTrx-$P_{220-241}$. Both MBP-$P_{220-241}$ and hTrx-$P_{220-241}$ interacted with GST-N, but did not interact with GST bound to beads. This suggested that the specific N-P interaction mediated the observed protein-protein interaction and that it was not a result of non-specific interactions between the GST and the prey proteins, MBP-$P_{220-214}$ and hTrx-$P_{220-241}$. Despite these GST pulldown results, it does not necessarily mean that hTrx-$P_{220-241}$ would be able to prevent the interaction between full length N and P protein and prevent the formation of the polymerase complex in infected cells.

4.1.2 Uptake of hTrx-$P_{220-241}$ into LLC-MK2 cells

Protein transduction across cell membranes has often been achieved by attaching cell penetrating peptides, also referred to as protein transduction domains, to therapeutic peptide mimetics to enable them to reach their intracellular targets (McGregor, 2008). Previously, it was demonstrated that MBP-$P_{220-241}$, which contained a HIV-1 Tat nuclear

localisation signal (YGRKKRRQRRR) could be taken up into cells as quickly as ten minutes. However, this result could not be replicated in my hands. In contrast, hTrx-$P_{220-241}$ peptide was successfully taken up into cells (**Figure 3.1.4.C**). The mechanism by which CPPs mediate cellular uptake is still widely debated and it is thought to be either accomplished through direct penetration or an endocytotic pathway (Madani, Lindberg, Langel, Futaki, & Gräslund, 2011). Direct penetration does not require any energy input and initiates with electrostatic interactions between the positively charged CPP and negatively charged cell surface components, such as heparan sulfate (Madani et al., 2011). The membrane is destabilized and the CPP is internalized (Madani et al., 2011). Meanwhile, endocytotic uptake is an energy-dependent pathway, which may facilitate uptake of CPPs through micropinocytosis or receptor-mediated endocytosis using clathrin or caveolin pits (Ferrari et al., 2003; Madani et al., 2011; Säälik et al., 2004). However, peptide concentration and cargo peptide attached to the CPPs have been shown to play a factor in which uptake mechanism is employed (Madani et al., 2011).

In this thesis, MBP-$P_{220-241}$ contained a HIV-1 Tat CPP while hTrx-$P_{220-241}$ had a 9R CPP. At high concentrations (approximately 50 μM), both of these hydrophilic, cationic CPP enter through cells through direct penetration (Guterstam et al., 2009; Madani et al., 2011). However, due to the low concentrations used for MBP-$P_{220-241}$ and hTrx-$P_{220-241}$ (less or equal to 20 μM), uptake was most likely mediated through endocytotic pathways, such as macropinocytosis for polyarginine-conjugated proteins (Guterstam et al., 2009; Madani et al., 2011). Nonetheless, it is difficult to explain why only the positive uptake control (hTrx Δcys5) and hTrx-$P_{220-241}$ were detected inside cells while MBP-$P_{220-241}$ was not. This

could be explained by the differences in CPPs employed as 9R has been shown to be more efficient than HIV-1 Tat in endosomal escape in the endocytotic pathway (Guterstam et al., 2009; Madani et al., 2011). Another possible explanation could be that the polyhistidine tag, used for Western Blot detection, on MBP-$P_{220-241}$ could have been degraded by proteases in the cytoplasm, therefore registering the result as a false negative.

4.1.3 Inhibition of RSV replication by hTrx-$P_{220-241}$

One of the central objectives was to assess the antiviral activity of hTrx-$P_{220-241}$ *in vitro* compared to MBP-$P_{220-241}$. A previous graduate student demonstrated that MBP-$P_{220-241}$ inhibited RSV replication *in vitro* in a dose-dependent manner. At a concentration of 20 μM, RSV replication was inhibited by up to 90%. After confirming that hTrx-$P_{220-241}$ could interact with the N protein and successfully translocate into cells, I hypothesized that it would be able to bind RSV N protein to inhibit the formation of the RdRp polymerase complex and inhibit RSV replication. Contrary to my expectations, hTrx-$P_{220-241}$ did not result in a statistically significant inhibition of RSV replication *in vitro*. At a maximal concentration of 20 μM, hTrx-$P_{220-241}$ only achieved an 7.6% reduction in RSV replication while 20 μM of the positive control, MBP-$P_{220-241}$, inhibited RSV replication by 50.7%. Concentrations above 20 μM of hTrx-$P_{220-241}$ could not be tested because of high levels of cytotoxicity destroying the LLC-MK2 monolayers.

One possible explanation is that the affinity between hTrx-$P_{220-241}$ and the N protein is not strong enough to displace full length P protein and interfere with the formation of the

polymerase complex. It was previously mentioned that the 9R CPP adjacent to $P_{220-241}$ was not sufficient to mediate cellular uptake of the peptide mimetic, which led to the addition of another 9R CPP at the N-terminus. It is plausible that the positively charged 9R CPP may form electrostatic interactions with the negatively charged $P_{220-241}$. This may induce a conformational change that interferes with the binding interface needed to stabilize F241 in the hydrophobic pocket of the N protein and lowers the affinity of hTrx-$P_{220-241}$ for the N protein. Another potential reason for the failure of hTrx-$P_{220-241}$ to inhibit RSV could be that it is degraded by proteases in the cytoplasm, thus reducing the amount of intracellular protein competing with full-length P protein for N binding.

4.2.1 The effect of MBP-P_{1-29} on cell viability

Prior to assessing the antiviral activity of MBP-P_{1-29}, it was important to assess its toxicity in cells. A PrestoBlue assay was used to acquire a quantitative measure of cell viability. PrestoBlue reagent is a non-fluorescent resazuirn-based dye that accepts electrons from NADPH, FADH, FMNH, NADH and cytochromes during cellular respiration in healthy cells (Al-Nasiry, Geusens, Hanssens, Luyten, & Pijnenborg, 2007; Xu et al., 2015). It is reduced to form fluorescent resorufin and its levels can be measured by fluorescence or absorbance, which is also directly proportional to the number of metabolically active cells (Fields & Lancaster, 1993; Xu et al., 2015). Using the PrestoBlue assay, LLC-MK2 and BEAS-2B cells treated for three days with MBP-P_{1-29} showed that 120 μM of MBP-P_{1-}

$_{29}$ was not cytotoxic while 160 μM was toxic to cells. Thus, the maximal safe concentration of MBP-P_{1-29} that could be used was 120 μM.

4.2.2 The inhibition of RSV replication by MBP-P_{1-29}

Following confirmation that MBP-P_{1-29} can successfully enter cells and the maximum concentration that could be safely tolerated, the antiviral activity of MBP-P_{1-29} was assessed. Once again, the controls used in this experiment were cells treated with virus only and cells that were not treated with peptide or virus. Compared to the virus only control, MBP-P_{1-29} significantly inhibited RSV A replication in a dose-dependent manner and achieved an approximately 80% reduction of viral replication at a maximal concentration of 120 μM in LLC-MK2 cells. The antiviral activity of MBP-P_{1-29} was also tested in a human lung epithelial cell line, BEAS-2B, which resulted in a 60% reduction in RSV replication at a maximal concentration of 120 μM. Thus, these results provide further evidence that a P_{1-29} peptide mimetic can inhibit RSV replication and it was consistent with the results achieved by Galloux and colleagues who used a minireplicon assay (Galloux et al., 2015). In addition, MBP-P_{1-29} also reduced progeny virus release by up to 70% and 34% in LLC-MK2 cells and BEAS-2B cells respectively compared to cells not treated with peptide. Thus, these progeny inhibition results are consistent and further corroborate the MBP-P_{1-29} peptide's inhibition of RSV replication.

4.3.1 Future directions – binding kinetics and immunoprecipitation of hTrx-$P_{220-241}$ and N

Although hTrx-$P_{220-241}$ was shown to be able to successfully interact with N protein and enter cells, it marginally inhibited RSV replication. It is important to fully investigate various parameters that may have potentially contributed to this result. One issue that needs to be explored is whether or not hTrx-$P_{220-241}$ is capable of blocking full length P protein interaction with N protein. This can be explored in a GST pulldown experiment where GST-N bound to glutathione-agarose beads are pre-incubated with hTrx-$P_{220-241}$ prior to incubation with full-length P protein. The protein binding affinity between hTrx-$P_{220-241}$ and N protein as well as full length N protein and P protein can also be investigated using surface plasmon resonance (SPR). SPR is a label-free method to measure the binding of a protein to another immobilized protein at the same time and place it occurs (Malmqvist, 1993). The association equilibrium constant (K_a) and the sensorgram produced from SPR can be used to further study the protein-protein interaction (Malmqvist, 1993).

Previously, it was discovered that a 9R CPP placed adjacent to $P_{220-241}$ on hTrx did not contribute to the successful uptake of hTrx-$P_{220-241}$ into cells. SPR can be used to assess the effect of this adjacent 9R CPP on the binding affinity between hTrx-$P_{220-241}$ and N protein. If it negatively affects the peptide binding affinity for the N protein, it can be removed from the construct and the resulting peptide mimetic could be re-assessed for antiviral activity. However, it is also plausible that other factors *in vitro* may interfere with hTrx-$P_{220-241}$ binding to N protein. In this case, an immunoprecipitation of hTrx-$P_{220-241}$, N protein, and full length P protein would be helpful in studying the behaviour of all three of these components in the cytoplasmic space.

4.3.2 Future directions – testing MBP-P_{1-29} in other RSV strains

In this thesis, the antiviral activity of MBP-P_{1-29} was tested only using RSV A Long strain. It would be interesting to test for inhibition against RSV B, which can co-circulate with RSV A during the RSV season. Between strains within the RSV A subtype, the amino acids in the phosphoprotein share 100% amino acid similarity. On the other hand, the amino acids of RSV A and RSV B phosphoproteins share a 91% similarity (**Section 6.4**). Furthermore, P_{1-29} on both RSV A and B are fairly well conserved with only slight amino acid differences in regions not required for mediating the nucleoprotein-phosphoprotein interaction. Thus, although MBP-P_{1-29} was initially designed to inhibit RSV A replication, it is highly possible that it can also inhibit other RSV A strains and RSV B replication as well.

4.3.3 Future directions – attaching MBP-P_{1-29} on a human carrier protein

For my experiments, P_{1-29} was conjugated to MBP, which serves as an effective carrier protein to produce high yields of soluble protein from *E. coli*. (Sun et al., 2011). MBP is also possesses chaperone activity preventing the formation of aggregates and ensure proper folding occurs (Reuten et al., 2016). However, due to its immunogenicity, a human carrier protein would be ideal to increase the half-life of the therapeutic peptide mimetic and prevent the drug from being degraded by host proteases. In this thesis, a mutated human thioredoxin was assessed as a potential carrier protein for the $P_{220-241}$ and hTrx remains a potential carrier candidate for P_{1-29}. However, concentrations above 20 μM

of human thioredoxin constructs were severely toxic to cells. This may pose an issue for $P_{1\text{-}29}$, which requires concentrations above 20 μM to yield a statistically significant reduction in RSV replication *in vitro*. Thus, another human carrier protein may be required. Some potential candidates are the monomeric CH2 and CH3 domain of the IgG Fc region, which are currently being investigated in Dr. Mahony's laboratory.

4.3.4 Future directions – mode of therapeutic drug delivery

One of the most challenging aspects of designing an anti-RSV therapeutic protein is the method by which the therapeutic is delivered (Amirav et al., 2002) to the lower respiratory tract. Aerosolized delivery of medicine is a common method used and possesses a number of advantages over intravenous administration including lower drug doses required to reach target site, quicker onset of action and fewer side effects (Goralski & Davis, 2014). However, in the pediatric population afflicted with RSV, aerosolized medication is poorly deposited in the lungs. A study found that only 1.5% ± 0.7% of administered aerosolized β-agonist bronchodilators reached the lungs and the majority accumulated in the central and intermediate airways (Amirav et al., 2002). This may partly due to the small airways in infants, which is further narrowed by mucosal edema and luminal plugging caused by alveolar inflammation (Amirav et al., 2002). However, it remains possible that small aerosol particles and a larger medication dose may reach their intended target site and bring about greater clinical benefit (Amirav et al., 2002).

One novel delivery method that has been gaining a lot of interest is using genetically modified bacteria as *in situ* drug delivery vehicles (Wegmann, Carvalho, Stocks, & Carding, 2017). This method has already been successfully tested in a Phase I human clinical trial with a genetically modified *Lactococcus lactis* in the gastrointestinal tract, which secreted interleukin-10 for the long term management of Crohn's disease (Braat et al., 2006). Furthermore, it appears to be a relatively safe method due to the various restraints imposed to prevent environmental spread (Braat et al., 2006). Some methods include the use of a non-pathogenic food derived commensal, *L. lactis*, and then it was also engineered to be unable to reproduce in environments lacking thymine or thymidine (Braat et al., 2006). Owing to novelty and its recent success, Dr. Mahony's laboratory is also working on developing a genetically modified *Streptococcus gordonii* that can secrete various antiviral peptide mimetics.

4.4 Closing remarks

Globally, RSV is a leading cause of childhood hospitalization for acute lower respiratory tract infection and can repeatedly infect people throughout their lives. To date, there has been little success in developing vaccines or antiviral treatments for the prevention, management, and treatment of RSV. Meanwhile, infants at risk of severe RSV infection are treated prophylactically with palivizumab. Thus, there remains a pressing need for the development of new antivirals for RSV. One potential strategy is the use of therapeutic mimetic peptides to disrupt the essential interaction between the nucleoprotein

and phosphoprotein of RSV, which is required for the formation of the RNA-dependent RNA polymerase complex and subsequent replication of the RNA genome. Expanding on previous studies, a $P_{1\text{-}29}$ peptide mimetic demonstrates potential as a novel anti-RSV therapeutic with its ability to inhibit RSV A replication *in vitro*. However, further research is required to select an optimal carrier protein before moving it into animal models and subsequently, into human clinical trials.

CHAPTER 5 - REFERENCES

REFERENCES

Afonso, C. L., Amarasinghe, G. K., Bányai, K., Bào, Y., Basler, C. F., Bavari, S., … Kuhn, J. H. (2016). Taxonomy of the order Mononegavirales: update 2016. *Archives of Virology*, *161*(8), 2351–2360. https://doi.org/10.1007/s00705-016-2880-1

Al-Nasiry, S., Geusens, N., Hanssens, M., Luyten, C., & Pijnenborg, R. (2007). The use of Alamar Blue assay for quantitative analysis of viability, migration and invasion of choriocarcinoma cells. *Human Reproduction (Oxford, England)*, *22*(5), 1304–9. https://doi.org/10.1093/humrep/dem011

American Academy of Pediatrics Subcommittee on Diagnosis and Management of Bronchiolitis. (2006). Diagnosis and Management of Bronchiolitis. *PEDIATRICS*, *118*(4), 1774–1793. https://doi.org/10.1542/peds.2006-2223

Amirav, I., Balanov, I., Gorenberg, M., Luder, A. S., Newhouse, M. T., & Groshar, D. (2002). Beta-agonist aerosol distribution in respiratory syncytial virus bronchiolitis in infants. *Journal of Nuclear Medicine : Official Publication, Society of Nuclear Medicine*, *43*(4), 487–91. Retrieved from http://www.ncbi.nlm.nih.gov/pubmed/11937592

Anderson, L. J. (2013). Respiratory syncytial virus vaccine development. *Seminars in Immunology*, *25*(2), 160–171. https://doi.org/10.1016/j.smim.2013.04.011

Araujo, G. C., Silva, R. H. T., Scott, L. P. B., Araujo, A. S., Souza, F. P., & de Oliveira, R. J. (2016). Structure and functional dynamics characterization of the ion channel of the human respiratory syncytial virus (hRSV) small hydrophobic protein (SH) transmembrane domain by combining molecular dynamics with excited normal modes. *Journal of Molecular Modeling*, *22*(12), 286. https://doi.org/10.1007/s00894-016-3150-6

Baviskar, P. S., Hotard, A. L., Moore, M. L., & Oomens, A. G. P. (2013). The respiratory syncytial virus fusion protein targets to the perimeter of inclusion bodies and facilitates filament formation by a cytoplasmic tail-dependent mechanism. *Journal of Virology*, *87*(19), 10730–41. https://doi.org/10.1128/JVI.03086-12

Bawage, S. S., Tiwari, P. M., Pillai, S., Dennis, V., & Singh, S. R. (2013). Recent Advances in Diagnosis, Prevention, and Treatment of Human Respiratory Syncytial Virus. *Advances in Virology*, *2013*, 1–26. https://doi.org/10.1155/2013/595768

Beaucourt, S., & Vignuzzi, M. (2014). Ribavirin: a drug active against many viruses with multiple effects on virus replication and propagation. Molecular basis of ribavirin resistance. *Current Opinion in Virology*, *8*, 10–5. https://doi.org/10.1016/j.coviro.2014.04.011

Bermingham, A., & Collins, P. L. (1999). The M2-2 protein of human respiratory syncytial virus is a regulatory factor involved in the balance between RNA replication and transcription. *Proceedings of the National Academy of Sciences of the United States of America*, *96*(20), 11259–64. Retrieved from http://www.ncbi.nlm.nih.gov/pubmed/10500164

Bitko, V., Shulyayeva, O., Mazumder, B., Musiyenko, A., Ramaswamy, M., Look, D. C., & Barik, S. (2007). Nonstructural proteins of respiratory syncytial virus suppress

premature apoptosis by an NF-kappaB-dependent, interferon-independent mechanism and facilitate virus growth. *Journal of Virology*, *81*(4), 1786–95. https://doi.org/10.1128/JVI.01420-06

Blount, R. E., Morris, J. A., & Savage, R. E. (1956). Recovery of cytopathogenic agent from chimpanzees with coryza. *Proceedings of the Society for Experimental Biology and Medicine. Society for Experimental Biology and Medicine (New York, N.Y.)*, *92*(3), 544–9. Retrieved from http://www.ncbi.nlm.nih.gov/pubmed/13359460

Bolt, G., Pedersen, L. O., & Birkeslund, H. H. (2000). Cleavage of the respiratory syncytial virus fusion protein is required for its surface expression: role of furin. *Virus Research*, *68*(1), 25–33. Retrieved from http://www.ncbi.nlm.nih.gov/pubmed/10930660

Bont, L. (2009). Nosocomial RSV infection control and outbreak management. *Paediatric Respiratory Reviews*, *10*, 16–17. https://doi.org/10.1016/S1526-0542(09)70008-9

Borghouts, C., Kunz, C., Delis, N., & Groner, B. (2008). Monomeric recombinant peptide aptamers are required for efficient intracellular uptake and target inhibition. *Molecular Cancer Research : MCR*, *6*(2), 267–81. https://doi.org/10.1158/1541-7786.MCR-07-0245

Braat, H., Rottiers, P., Hommes, D. W., Huyghebaert, N., Remaut, E., Remon, J.-P., … Steidler, L. (2006). A phase I trial with transgenic bacteria expressing interleukin-10 in Crohn's disease. *Clinical Gastroenterology and Hepatology : The Official Clinical Practice Journal of the American Gastroenterological Association*, *4*(6), 754–9. https://doi.org/10.1016/j.cgh.2006.03.028

Brealey, J. C., Sly, P. D., Young, P. R., & Chappell, K. J. (2015). Viral bacterial co-infection of the respiratory tract during early childhood. *FEMS Microbiology Letters*, *362*(10). https://doi.org/10.1093/femsle/fnv062

Bukreyev, A., Yang, L., & Collins, P. L. (2012). The Secreted G Protein of Human Respiratory Syncytial Virus Antagonizes Antibody-Mediated Restriction of Replication Involving Macrophages and Complement. *Journal of Virology*, *86*(19), 10880–10884. https://doi.org/10.1128/JVI.01162-12

Burrows, F. S., Carlos, L. M., Benzimra, M., Marriott, D. J. E., Havryk, A. P., Plit, M. L., … Glanville, A. R. (2015). Oral ribavirin for respiratory syncytial virus infection after lung transplantation: Efficacy and cost-efficiency. *The Journal of Heart and Lung Transplantation*, *34*(7), 958–962. https://doi.org/10.1016/j.healun.2015.01.009

Cane, P. A., Matthews, D. A., & Pringle, C. R. (1994). Analysis of respiratory syncytial virus strain variation in successive epidemics in one city. *Journal of Clinical Microbiology*, *32*(1), 1–4. Retrieved from http://www.ncbi.nlm.nih.gov/pubmed/8126162

Carbonell-Estrany, X., Simões, E. A. F., Dagan, R., Hall, C. B., Harris, B., Hultquist, M., … Motavizumab Study Group. (2010). Motavizumab for prophylaxis of respiratory syncytial virus in high-risk children: a noninferiority trial. *Pediatrics*, *125*(1), e35-51. https://doi.org/10.1542/peds.2008-1036

Chang, A., & Dutch, R. E. (2012). Paramyxovirus fusion and entry: multiple paths to a common end. *Viruses*, *4*(4), 613–36. https://doi.org/10.3390/v4040613

Chanock, R. M., Parrott, R. H., Vargosko, A. J., Kapikian, A. Z., Knight, V., & Johnson, K. M. (1962). Acute respiratory diseases of viral etiology. IV. Respiratory syncytial virus. *American Journal of Public Health and the Nation's Health*, *52*(6), 918–25. Retrieved from http://www.ncbi.nlm.nih.gov/pubmed/13878129

Cochran, A. G. (2000). Antagonists of protein-protein interactions. *Chemistry & Biology*, *7*(4), R85-94. Retrieved from http://www.ncbi.nlm.nih.gov/pubmed/10779412

Collins, P., Fearns, R., & Graham, B. S. (2013). Respiratory Syncytial Virus: Virology, Reverse Genetics, and Pathogenesis of Disease. In *Challenges and Opportunities for Respiratory Syncytial Virus Vaccines* (Vol. 372, pp. 3–38). https://doi.org/10.1007/978-3-642-38919-1_1

Collins, P. L., Huang, Y. T., & Wertz, G. W. (1984). Nucleotide sequence of the gene encoding the fusion (F) glycoprotein of human respiratory syncytial virus. *Proceedings of the National Academy of Sciences of the United States of America*, *81*(24), 7683–7. Retrieved from http://www.ncbi.nlm.nih.gov/pubmed/6096849

Corneli, H. M., Zorc, J. J., Mahajan, P., Shaw, K. N., Holubkov, R., Reeves, S. D., … Bronchiolitis Study Group of the Pediatric Emergency Care Applied Research Network (PECARN). (2007). A Multicenter, Randomized, Controlled Trial of Dexamethasone for Bronchiolitis. *New England Journal of Medicine*, *357*(4), 331–339. https://doi.org/10.1056/NEJMoa071255

Cowton, V. M., McGivern, D. R., & Fearns, R. (2006). Unravelling the complexities of respiratory syncytial virus RNA synthesis. *The Journal of General Virology*, *87*(Pt 7), 1805–21. https://doi.org/10.1099/vir.0.81786-0

DeVincenzo, J. P., McClure, M. W., Symons, J. A., Fathi, H., Westland, C., Chanda, S., … Fry, J. (2015). Activity of Oral ALS-008176 in a Respiratory Syncytial Virus Challenge Study. *The New England Journal of Medicine*, *373*(21), 2048–58. https://doi.org/10.1056/NEJMoa1413275

DeVincenzo, J. P., Whitley, R. J., Mackman, R. L., Scaglioni-Weinlich, C., Harrison, L., Farrell, E., … Chien, J. W. (2014). Oral GS-5806 activity in a respiratory syncytial virus challenge study. *The New England Journal of Medicine*, *371*(8), 711–22. https://doi.org/10.1056/NEJMoa1401184

Dobson, J. V, Stephens-Groff, S. M., McMahon, S. R., Stemmler, M. M., Brallier, S. L., & Bay, C. (1998). The use of albuterol in hospitalized infants with bronchiolitis. *Pediatrics*, *101*(3 Pt 1), 361–8. Retrieved from http://www.ncbi.nlm.nih.gov/pubmed/9480998

Drysdale, S. B., Green, C. A., & Sande, C. J. (2016). Best practice in the prevention and management of paediatric respiratory syncytial virus infection. *Therapeutic Advances in Infectious Disease*, *3*(2), 63–71. https://doi.org/10.1177/2049936116630243

Eiland, L. S. (2009). Respiratory syncytial virus: diagnosis, treatment and prevention. *The Journal of Pediatric Pharmacology and Therapeutics : JPPT : The Official Journal of PPAG*, *14*(2), 75–85. https://doi.org/10.5863/1551-6776-14.2.75

Falsey, A. R., Hennessey, P. A., Formica, M. A., Cox, C., & Walsh, E. E. (2005). Respiratory Syncytial Virus Infection in Elderly and High-Risk Adults. *New England Journal of Medicine*, *352*(17), 1749–1759.

https://doi.org/10.1056/NEJMoa043951

Fearns, R., & Collins, P. L. (1999). Model for polymerase access to the overlapped L gene of respiratory syncytial virus. *Journal of Virology*, *73*(1), 388–97. Retrieved from http://www.ncbi.nlm.nih.gov/pubmed/9847343

Feldman, S. A., Audet, S., & Beeler, J. A. (2000). The fusion glycoprotein of human respiratory syncytial virus facilitates virus attachment and infectivity via an interaction with cellular heparan sulfate. *Journal of Virology*, *74*(14), 6442–7. Retrieved from http://www.ncbi.nlm.nih.gov/pubmed/10864656

Feldman, S. A., Hendry, R. M., & Beeler, J. A. (1999). Identification of a linear heparin binding domain for human respiratory syncytial virus attachment glycoprotein G. *Journal of Virology*, *73*(8), 6610–7. Retrieved from http://www.ncbi.nlm.nih.gov/pubmed/10400758

Feltes, T. F., Cabalka, A. K., Meissner, H. C., Piazza, F. M., Carlin, D. A., Top, F. H., … Cardiac Synagis Study Group. (2003). Palivizumab prophylaxis reduces hospitalization due to respiratory syncytial virus in young children with hemodynamically significant congenital heart disease. *The Journal of Pediatrics*, *143*(4), 532–40. Retrieved from http://www.ncbi.nlm.nih.gov/pubmed/14571236

Fernandes, R. M., Bialy, L. M., Vandermeer, B., Tjosvold, L., Plint, A. C., Patel, H., … Hartling, L. (2013). Glucocorticoids for acute viral bronchiolitis in infants and young children. In R. M. Fernandes (Ed.), *Cochrane Database of Systematic Reviews* (p. CD004878). Chichester, UK: John Wiley & Sons, Ltd. https://doi.org/10.1002/14651858.CD004878.pub4

Ferrari, A., Pellegrini, V., Arcangeli, C., Fittipaldi, A., Giacca, M., & Beltram, F. (2003). Caveolae-mediated internalization of extracellular HIV-1 tat fusion proteins visualized in real time. *Molecular Therapy : The Journal of the American Society of Gene Therapy*, *8*(2), 284–94. Retrieved from http://www.ncbi.nlm.nih.gov/pubmed/12907151

Fields, R. D., & Lancaster, M. V. (1993). Dual-attribute continuous monitoring of cell proliferation/cytotoxicity. *American Biotechnology Laboratory*, *11*(4), 48–50. Retrieved from http://www.ncbi.nlm.nih.gov/pubmed/7763491

Förster, A., Maertens, G. N., Farrell, P. J., & Bajorek, M. (2015). Dimerization of matrix protein is required for budding of respiratory syncytial virus. *Journal of Virology*, *89*(8), 4624–35. https://doi.org/10.1128/JVI.03500-14

Franchetti, P., & Grifantini, M. (1999). Nucleoside and non-nucleoside IMP dehydrogenase inhibitors as antitumor and antiviral agents. *Current Medicinal Chemistry*, *6*(7), 599–614. Retrieved from http://www.ncbi.nlm.nih.gov/pubmed/10390603

Gadomski, A. M., Lichenstein, R., Horton, L., King, J., Keane, V., & Permutt, T. (1994). Efficacy of albuterol in the management of bronchiolitis. *Pediatrics*, *93*(6 Pt 1), 907–12. Retrieved from http://www.ncbi.nlm.nih.gov/pubmed/8190575

Galloux, M., Gabiane, G., Sourimant, J., Richard, C.-A., England, P., Moudjou, M., … Eléouët, J.-F. (2015). Identification and Characterization of the Binding Site of the Respiratory Syncytial Virus Phosphoprotein to RNA-Free Nucleoprotein. *Journal of Virology*, *89*(7), 3484–3496. https://doi.org/10.1128/JVI.03666-14

García-Barreno, B., Delgado, T., & Melero, J. A. (1996). Identification of protein regions involved in the interaction of human respiratory syncytial virus phosphoprotein and nucleoprotein: significance for nucleocapsid assembly and formation of cytoplasmic inclusions. *Journal of Virology*, *70*(2), 801–8. Retrieved from http://www.ncbi.nlm.nih.gov/pubmed/8551618

Ghildyal, R., Jans, D. A., Bardin, P. G., & Mills, J. (2012). Protein-protein interactions in RSV assembly: potential targets for attenuating RSV strains. *Infectious Disorders Drug Targets*, *12*(2), 103–9. Retrieved from http://www.ncbi.nlm.nih.gov/pubmed/22335497

Glezen, W. P., Taber, L. H., Frank, A. L., & Kasel, J. A. (1986). Risk of primary infection and reinfection with respiratory syncytial virus. *American Journal of Diseases of Children (1960)*, *140*(6), 543–6. Retrieved from http://www.ncbi.nlm.nih.gov/pubmed/3706232

González, P. A., Bueno, S. M., Carreño, L. J., Riedel, C. A., & Kalergis, A. M. (2012). Respiratory syncytial virus infection and immunity. *Reviews in Medical Virology*, *22*(4), 230–244. https://doi.org/10.1002/rmv.1704

Goralski, J. L., & Davis, S. D. (2014). Breathing easier: addressing the challenges of aerosolizing medications to infants and preschoolers. *Respiratory Medicine*, *108*(8), 1069–74. https://doi.org/10.1016/j.rmed.2014.06.004

Graci, J. D., & Cameron, C. E. (2006). Mechanisms of action of ribavirin against distinct viruses. *Reviews in Medical Virology*, *16*(1), 37–48. https://doi.org/10.1002/rmv.483

Guterstam, P., Madani, F., Hirose, H., Takeuchi, T., Futaki, S., El Andaloussi, S., … Langel, U. (2009). Elucidating cell-penetrating peptide mechanisms of action for membrane interaction, cellular uptake, and translocation utilizing the hydrophobic counter-anion pyrenebutyrate. *Biochimica et Biophysica Acta*, *1788*(12), 2509–17. https://doi.org/10.1016/j.bbamem.2009.09.014

Hall, C. B., & Douglas, R. G. (1981). Modes of transmission of respiratory syncytial virus. *The Journal of Pediatrics*, *99*(1), 100–3. Retrieved from http://www.ncbi.nlm.nih.gov/pubmed/7252646

Hall, C. B., Geiman, J. M., Douglas, R. G., & Meagher, M. P. (1978). Control of nosocomial respiratory syncytial viral infections. *Pediatrics*, *62*(5), 728–32. Retrieved from http://www.ncbi.nlm.nih.gov/pubmed/724317

Hall, C. B., Simőes, E. A. F., & Anderson, L. J. (2013). Clinical and Epidemiologic Features of Respiratory Syncytial Virus. In *Current topics in microbiology and immunology* (Vol. 372, pp. 39–57). https://doi.org/10.1007/978-3-642-38919-1_2

Haynes, L. M. (2013). Progress and challenges in RSV prophylaxis and vaccine development. *The Journal of Infectious Diseases*, *208 Suppl 3*(suppl 3), S177-83. https://doi.org/10.1093/infdis/jit512

Hishiki, H., Ishiwada, N., Fukasawa, C., Kohno, Y., Abe, K., Hoshino, T., … Ishikawa, N. (2011). Incidence of bacterial coinfection with respiratory syncytial virus bronchopulmonary infection in pediatric inpatients. *Journal of Infection and Chemotherapy*, *17*(1), 87–90. https://doi.org/10.1007/s10156-010-0097-x

Hussell, T., & Cavanagh, M. M. (2009). The innate immune rheostat: influence on lung inflammatory disease and secondary bacterial pneumonia. *Biochemical Society*

Transactions, *37*(Pt 4), 811–3. https://doi.org/10.1042/BST0370811

Jacobs, P., Lier, D., Gooch, K., Buesch, K., Lorimer, M., & Mitchell, I. (2013). A model of the costs of community and nosocomial pediatric respiratory syncytial virus infections in Canadian hospitals. *The Canadian Journal of Infectious Diseases & Medical Microbiology = Journal Canadien Des Maladies Infectieuses et de La Microbiologie Medicale*, *24*(1), 22–6. Retrieved from http://www.ncbi.nlm.nih.gov/pubmed/24421788

Jafri, H. S., Wu, X., Makari, D., & Henrickson, K. J. (2013). Distribution of respiratory syncytial virus subtypes A and B among infants presenting to the emergency department with lower respiratory tract infection or apnea. *The Pediatric Infectious Disease Journal*, *32*(4), 335–40. https://doi.org/10.1097/INF.0b013e318282603a

Jeffree, C. E., Brown, G., Aitken, J., Su-Yin, D. Y., Tan, B.-H., & Sugrue, R. J. (2007). Ultrastructural analysis of the interaction between F-actin and respiratory syncytial virus during virus assembly. *Virology*, *369*(2), 309–23. https://doi.org/10.1016/j.virol.2007.08.007

Johnson, P. R., Spriggs, M. K., Olmsted, R. A., & Collins, P. L. (1987). The G glycoprotein of human respiratory syncytial viruses of subgroups A and B: extensive sequence divergence between antigenically related proteins. *Proceedings of the National Academy of Sciences of the United States of America*, *84*(16), 5625–9. Retrieved from http://www.ncbi.nlm.nih.gov/pubmed/2441388

Karanfil, L. V, Conlon, M., Lykens, K., Masters, C. F., Forman, M., Griffith, M. E., … Perl, T. M. (1999). Reducing the rate of nosocomially transmitted respiratory syncytial virus. *American Journal of Infection Control*, *27*(2), 91–6. Retrieved from http://www.ncbi.nlm.nih.gov/pubmed/10196485

Karron, R. A., Buonagurio, D. A., Georgiu, A. F., Whitehead, S. S., Adamus, J. E., Clements-Mann, M. L., … Sidhu, M. S. (1997). Respiratory syncytial virus (RSV) SH and G proteins are not essential for viral replication in vitro: clinical evaluation and molecular characterization of a cold-passaged, attenuated RSV subgroup B mutant. *Proceedings of the National Academy of Sciences of the United States of America*, *94*(25), 13961–6. Retrieved from http://www.ncbi.nlm.nih.gov/pubmed/9391135

Killikelly, A. M., Kanekiyo, M., & Graham, B. S. (2016). Pre-fusion F is absent on the surface of formalin-inactivated respiratory syncytial virus. *Scientific Reports*, *6*(1), 34108. https://doi.org/10.1038/srep34108

Kim, H. W., Canchola, J. G., Brandt, C. D., Pyles, G., Chanock, R. M., Jensen, K., & Parrott, R. H. (1969). Respiratory syncytial virus disease in infants despite prior administration of antigenic inactivated vaccine. *American Journal of Epidemiology*, *89*(4), 422–34. Retrieved from http://www.ncbi.nlm.nih.gov/pubmed/4305198

Kneyber, M. C. J., Blussé van Oud-Alblas, H., van Vliet, M., Uiterwaal, C. S. P. M., Kimpen, J. L. L., & van Vught, A. J. (2005). Concurrent bacterial infection and prolonged mechanical ventilation in infants with respiratory syncytial virus lower respiratory tract disease. *Intensive Care Medicine*, *31*(5), 680–5. https://doi.org/10.1007/s00134-005-2614-4

Krilov, L. R. (2011). Respiratory syncytial virus disease: update on treatment and

prevention. *Expert Review of Anti-Infective Therapy*, *9*(1), 27–32. https://doi.org/10.1586/eri.10.140

Kristjánsson, S., Lødrup Carlsen, K. C., Wennergren, G., Strannegård, I. L., & Carlsen, K. H. (1993). Nebulised racemic adrenaline in the treatment of acute bronchiolitis in infants and toddlers. *Archives of Disease in Childhood*, *69*(6), 650–4. Retrieved from http://www.ncbi.nlm.nih.gov/pubmed/8285776

Kuo, L., Grosfeld, H., Cristina, J., Hill, M. G., & Collins, P. L. (1996). Effects of mutations in the gene-start and gene-end sequence motifs on transcription of monocistronic and dicistronic minigenomes of respiratory syncytial virus. *Journal of Virology*, *70*(10), 6892–901. Retrieved from http://www.ncbi.nlm.nih.gov/pubmed/8794332

Kwong, J. A., Dorfman, T., Quinlan, B. D., Chiang, J. J., Ahmed, A. A., Choe, H., & Farzan, M. (2011). A tyrosine-sulfated CCR5-mimetic peptide promotes conformational transitions in the HIV-1 envelope glycoprotein. *Journal of Virology*, *85*(15), 7563–71. https://doi.org/10.1128/JVI.00630-11

La Via, W. V, Marks, M. I., & Stutman, H. R. (1992). Respiratory syncytial virus puzzle: clinical features, pathophysiology, treatment, and prevention. *The Journal of Pediatrics*, *121*(4), 503–10. Retrieved from http://www.ncbi.nlm.nih.gov/pubmed/1403380

Leader, S., & Kohlhase, K. (2003). Recent trends in severe respiratory syncytial virus (RSV) among US infants, 1997 to 2000. *The Journal of Pediatrics*, *143*(5 Suppl), S127-32. Retrieved from http://www.ncbi.nlm.nih.gov/pubmed/14615711

Lindsley, W. G., Blachere, F. M., Davis, K. A., Pearce, T. A., Fisher, M. A., Khakoo, R., … Beezhold, D. H. (2010). Distribution of airborne influenza virus and respiratory syncytial virus in an urgent care medical clinic. *Clinical Infectious Diseases : An Official Publication of the Infectious Diseases Society of America*, *50*(5), 693–8. https://doi.org/10.1086/650457

Madani, F., Lindberg, S., Langel, Ü., Futaki, S., & Gräslund, A. (2011). Mechanisms of Cellular Uptake of Cell-Penetrating Peptides. *Journal of Biophysics*, *2011*, 1–10. https://doi.org/10.1155/2011/414729

Malmqvist, M. (1993). Surface plasmon resonance for detection and measurement of antibody-antigen affinity and kinetics. *Current Opinion in Immunology*, *5*(2), 282–6. Retrieved from http://www.ncbi.nlm.nih.gov/pubmed/8507407

Marty, A., Meanger, J., Mills, J., Shields, B., & Ghildyal, R. (2003). Association of matrix protein of respiratory syncytial virus with the host cell membrane of infected cells. *Archives of Virology*, *149*(1), 199–210. https://doi.org/10.1007/s00705-003-0183-9

Mason, J. M. (2010). Design and development of peptides and peptide mimetics as antagonists for therapeutic intervention. *Future Medicinal Chemistry*, *2*(12), 1813–22. https://doi.org/10.4155/fmc.10.259

Mastrangelo, P., & Hegele, R. (2013). RSV Fusion: Time for a New Model. *Viruses*, *5*(3), 873–885. https://doi.org/10.3390/v5030873

Mazumder, B., & Barik, S. (1994). Requirement of casein kinase II-mediated phosphorylation for the transcriptional activity of human respiratory syncytial viral

phosphoprotein P: transdominant negative phenotype of phosphorylation-defective P mutants. *Virology*, *205*(1), 104–11. https://doi.org/10.1006/viro.1994.1624

McElhaney, J. E. (2009). Prevention of infectious diseases in older adults through immunization: the challenge of the senescent immune response. *Expert Review of Vaccines*, *8*(5), 593–606. https://doi.org/10.1586/erv.09.12

McGregor, D. (2008). Discovering and improving novel peptide therapeutics. *Current Opinion in Pharmacology*, *8*(5), 616–619. https://doi.org/10.1016/j.coph.2008.06.002

McLellan, J. S., Ray, W. C., & Peeples, M. E. (2013). Structure and Function of Respiratory Syncytial Virus Surface Glycoproteins. In *Current topics in microbiology and immunology* (Vol. 372, pp. 83–104). https://doi.org/10.1007/978-3-642-38919-1_4

Mejias, A., Garcia-Maurino, C., Rodriguez-Fernandez, R., Peeples, M. E., & Ramilo, O. (2017). Development and clinical applications of novel antibodies for prevention and treatment of respiratory syncytial virus infection. *Vaccine*, *35*(3), 496–502. https://doi.org/10.1016/j.vaccine.2016.09.026

Mejias, A., & Ramilo, O. (2015). New options in the treatment of respiratory syncytial virus disease. *Journal of Infection*, *71*, S80–S87. https://doi.org/10.1016/j.jinf.2015.04.025

Menon, K., Sutcliffe, T., & Klassen, T. P. (1995). A randomized trial comparing the efficacy of epinephrine with salbutamol in the treatment of acute bronchiolitis. *The Journal of Pediatrics*, *126*(6), 1004–7. Retrieved from http://www.ncbi.nlm.nih.gov/pubmed/7776075

Mink, M. A., Stec, D. S., & Collins, P. L. (1991). Nucleotide sequences of the 3' leader and 5' trailer regions of human respiratory syncytial virus genomic RNA. *Virology*, *185*(2), 615–24. Retrieved from http://www.ncbi.nlm.nih.gov/pubmed/1840712

Moses, E, Zeldin, R.K., De Fougerolles, A. . . (2016). Results from the first-in-infant Phase I/IIastudy with the anti-RSV Nanobody, ALX-0171. Retrieved from http://www.ablynx.com/uploads/data/files/ablynx_alx-0171_first-in-infant study results_webcast presentation.pdf

Mullins, J. A., Lamonte, A. C., Bresee, J. S., & Anderson, L. J. (2003). Substantial variability in community respiratory syncytial virus season timing. *The Pediatric Infectious Disease Journal*, *22*(10), 857–62. https://doi.org/10.1097/01.inf.0000090921.21313.d3

Murata, Y. (2009). Respiratory Syncytial Virus Vaccine Development. *Clinics in Laboratory Medicine*, *29*(4), 725–739. https://doi.org/10.1016/j.cll.2009.07.004

Murphy, B. R., & Walsh, E. E. (1988). Formalin-inactivated respiratory syncytial virus vaccine induces antibodies to the fusion glycoprotein that are deficient in fusion-inhibiting activity. *Journal of Clinical Microbiology*, *26*(8), 1595–7. Retrieved from http://www.ncbi.nlm.nih.gov/pubmed/2459154

Nair, H., Nokes, D. J., Gessner, B. D., Dherani, M., Madhi, S. A., Singleton, R. J., … Campbell, H. (2010). Global burden of acute lower respiratory infections due to respiratory syncytial virus in young children: a systematic review and meta-analysis. *The Lancet*, *375*(9725), 1545–1555. https://doi.org/10.1016/S0140-6736(10)60206-1

Noveroske, D. B., Warren, J. L., Pitzer, V. E., & Weinberger, D. M. (2016). Local variations in the timing of RSV epidemics. *BMC Infectious Diseases*, *16*(1), 674. https://doi.org/10.1186/s12879-016-2004-2

Ogra, P. L. (2004). Respiratory syncytial virus: the virus, the disease and the immune response. *Paediatric Respiratory Reviews*, *5 Suppl A*, S119-26. Retrieved from http://www.ncbi.nlm.nih.gov/pubmed/14980256

Olson, G. L., Bolin, D. R., Bonner, M. P., Bös, M., Cook, C. M., Fry, D. C., … Kahn, M. (1993). Concepts and progress in the development of peptide mimetics. *Journal of Medicinal Chemistry*, *36*(21), 3039–49. Retrieved from http://www.ncbi.nlm.nih.gov/pubmed/8230089

Ouizougun-Oubari, M., Pereira, N., Tarus, B., Galloux, M., Lassoued, S., Fix, J., … Duquerroy, S. (2015). A Druggable Pocket at the Nucleocapsid/Phosphoprotein Interaction Site of Human Respiratory Syncytial Virus. *Journal of Virology*, *89*(21), 11129–43. https://doi.org/10.1128/JVI.01612-15

Palivizumab, a humanized respiratory syncytial virus monoclonal antibody, reduces hospitalization from respiratory syncytial virus infection in high-risk infants. The IMpact-RSV Study Group. (1998). *Pediatrics*, *102*(3 Pt 1), 531–7. Retrieved from http://www.ncbi.nlm.nih.gov/pubmed/9738173

Paramore, L. C., Ciuryla, V., Ciesla, G., & Liu, L. (2004). Economic impact of respiratory syncytial virus-related illness in the US: an analysis of national databases. *PharmacoEconomics*, *22*(5), 275–84. Retrieved from http://www.ncbi.nlm.nih.gov/pubmed/15061677

Porter, D. D., Prince, G. A., Yim, K. C., & Curtis, S. J. (2001). Vaccine-enhanced respiratory syncytial virus disease in cotton rats following immunization with Lot 100 or a newly prepared reference vaccine. *Journal of General Virology*, *82*(12), 2881–2888. https://doi.org/10.1099/0022-1317-82-12-2881

Ralston, S., & Hill, V. (2009). Incidence of Apnea in Infants Hospitalized with Respiratory Syncytial Virus Bronchiolitis: A Systematic Review. *The Journal of Pediatrics*, *155*(5), 728–733. https://doi.org/10.1016/j.jpeds.2009.04.063

Raman, M., Martin, K. (2014). One solution for cloning and mutagenesis: In-Fusion [reg] HD Cloning Plus. *Nature Methods*, *11*(9).

Resch, B., Gusenleitner, W., & Mueller, W. D. (2007). Risk of concurrent bacterial infection in preterm infants hospitalized due to respiratory syncytial virus infection. *Acta Paediatrica (Oslo, Norway : 1992)*, *96*(4), 495–8. https://doi.org/10.1111/j.1651-2227.2007.00226.x

Reuten, R., Nikodemus, D., Oliveira, M. B., Patel, T. R., Brachvogel, B., Breloy, I., … Koch, M. (2016). Maltose-Binding Protein (MBP), a Secretion-Enhancing Tag for Mammalian Protein Expression Systems. *PloS One*, *11*(3), e0152386. https://doi.org/10.1371/journal.pone.0152386

Ruuskanen, O., & Ogra, P. L. (1993). Respiratory syncytial virus. *Current Problems in Pediatrics*, *23*(2), 50–79. Retrieved from http://www.ncbi.nlm.nih.gov/pubmed/7681743

Säälik, P., Elmquist, A., Hansen, M., Padari, K., Saar, K., Viht, K., … Pooga, M. (2004). Protein Cargo Delivery Properties of Cell-Penetrating Peptides. A Comparative

Study. *Bioconjugate Chemistry*, *15*(6), 1246–1253. https://doi.org/10.1021/bc049938y

Samuel, D., Xing, W., Niedziela-Majka, A., Wong, J. S., Hung, M., Brendza, K. M., … Sakowicz, R. (2015). GS-5806 Inhibits Pre- to Postfusion Conformational Changes of the Respiratory Syncytial Virus Fusion Protein. *Antimicrobial Agents and Chemotherapy*, *59*(11), 7109–7112. https://doi.org/10.1128/AAC.00761-15

Sawada, A., & Nakayama, T. (2016). Experimental animal model for analyzing immunobiological responses following vaccination with formalin-inactivated respiratory syncytial virus. *Microbiology and Immunology*, *60*(4), 234–242. https://doi.org/10.1111/1348-0421.12365

Schickli, J. H., Dubovsky, F., & Tang, R. S. (2009). Challenges in developing a pediatric RSV vaccine. *Human Vaccines*, *5*(9), 582–91. Retrieved from http://www.ncbi.nlm.nih.gov/pubmed/19556888

Schneider-Poetsch, T., Ju, J., Eyler, D. E., Dang, Y., Bhat, S., Merrick, W. C., … Liu, J. O. (2010). Inhibition of eukaryotic translation elongation by cycloheximide and lactimidomycin. *Nature Chemical Biology*, *6*(3), 209–217. https://doi.org/10.1038/nchembio.304

Shah, J. N., & Chemaly, R. F. (2011). Management of RSV infections in adult recipients of hematopoietic stem cell transplantation. *Blood*, *117*(10), 2755–2763. https://doi.org/10.1182/blood-2010-08-263400

Simon, A., Müller, A., Khurana, K., Engelhart, S., Exner, M., Schildgen, O., … DSM RSV Paed Study Group. (2008). Nosocomial infection: a risk factor for a complicated course in children with respiratory syncytial virus infection--results from a prospective multicenter German surveillance study. *International Journal of Hygiene and Environmental Health*, *211*(3–4), 241–50. https://doi.org/10.1016/j.ijheh.2007.07.020

Sourimant, J., Rameix-Welti, M.-A., Gaillard, A.-L., Chevret, D., Galloux, M., Gault, E., & Eléouët, J.-F. (2015). Fine mapping and characterization of the L-polymerase-binding domain of the respiratory syncytial virus phosphoprotein. *Journal of Virology*, *89*(8), 4421–33. https://doi.org/10.1128/JVI.03619-14

Spann, K. M., Tran, K. C., & Collins, P. L. (2005). Effects of nonstructural proteins NS1 and NS2 of human respiratory syncytial virus on interferon regulatory factor 3, NF-kappaB, and proinflammatory cytokines. *Journal of Virology*, *79*(9), 5353–62. https://doi.org/10.1128/JVI.79.9.5353-5362.2005

Stensballe, L. G., Devasundaram, J. K., & Simoes, E. A. F. (2003). Respiratory syncytial virus epidemics: the ups and downs of a seasonal virus. *The Pediatric Infectious Disease Journal*, *22*(Supplement), S21–S32. https://doi.org/10.1097/01.inf.0000053882.70365.c9

Sullender, W. M. (2000). Respiratory syncytial virus genetic and antigenic diversity. *Clinical Microbiology Reviews*, *13*(1), 1–15, table of contents. Retrieved from http://www.ncbi.nlm.nih.gov/pubmed/10627488

Sun, P., Tropea, J. E., & Waugh, D. S. (2011). Enhancing the solubility of recombinant proteins in Escherichia coli by using hexahistidine-tagged maltose-binding protein as a fusion partner. *Methods in Molecular Biology (Clifton, N.J.)*, *705*, 259–74.

https://doi.org/10.1007/978-1-61737-967-3_16

Tawar, R. G., Duquerroy, S., Vonrhein, C., Varela, P. F., Damier-Piolle, L., Castagne, N., … Rey, F. A. (2009). Crystal Structure of a Nucleocapsid-Like Nucleoprotein-RNA Complex of Respiratory Syncytial Virus. *Science*, *326*(5957), 1279–1283. https://doi.org/10.1126/science.1177634

Techaarpornkul, S., Barretto, N., & Peeples, M. E. (2001). Functional Analysis of Recombinant Respiratory Syncytial Virus Deletion Mutants Lacking the Small Hydrophobic and/or Attachment Glycoprotein Gene. *Journal of Virology*, *75*(15), 6825–6834. https://doi.org/10.1128/JVI.75.15.6825-6834.2001

Techaarpornkul, S., Collins, P. L., & Peeples, M. E. (2002). Respiratory Syncytial Virus with the Fusion Protein as Its only Viral Glycoprotein Is Less Dependent on Cellular Glycosaminoglycans for Attachment than Complete Virus. *Virology*, *294*(2), 296–304. https://doi.org/10.1006/viro.2001.1340

Teng, M. N., Whitehead, S. S., & Collins, P. L. (2001). Contribution of the Respiratory Syncytial Virus G Glycoprotein and Its Secreted and Membrane-Bound Forms to Virus Replication in Vitro and in Vivo. *Virology*, *289*(2), 283–296. https://doi.org/10.1006/viro.2001.1138

Thomas, E., Ghany, M. G., & Liang, T. J. (2012). The application and mechanism of action of ribavirin in therapy of hepatitis C. *Antiviral Chemistry & Chemotherapy*, *23*(1), 1–12. https://doi.org/10.3851/IMP2125

Thorburn, K., Harigopal, S., Reddy, V., Taylor, N., & van Saene, H. K. F. (2006). High incidence of pulmonary bacterial co-infection in children with severe respiratory syncytial virus (RSV) bronchiolitis. *Thorax*, *61*(7), 611–5. https://doi.org/10.1136/thx.2005.048397

Tran, T.-L., Castagné, N., Bhella, D., Varela, P. F., Bernard, J., Chilmonczyk, S., … Eléouët, J.-F. (2007). The nine C-terminal amino acids of the respiratory syncytial virus protein P are necessary and sufficient for binding to ribonucleoprotein complexes in which six ribonucleotides are contacted per N protein protomer. *The Journal of General Virology*, *88*(Pt 1), 196–206. https://doi.org/10.1099/vir.0.82282-0

Tuan, T. A., Thanh, T. T., Hai, N. thi T., Tinh, L. B. B., Kim, L. thi N., Do, L. A. H., … van Doorn, H. R. (2015). Characterization of hospital and community-acquired respiratory syncytial virus in children with severe lower respiratory tract infections in Ho Chi Minh City, Vietnam, 2010. *Influenza and Other Respiratory Viruses*, *9*(3), 110–119. https://doi.org/10.1111/irv.12307

Ulloa, L., Serra, R., Asenjo, A., & Villanueva, N. (1998). Interactions between cellular actin and human respiratory syncytial virus (HRSV). *Virus Research*, *53*(1), 13–25. Retrieved from http://www.ncbi.nlm.nih.gov/pubmed/9617766

Wainwright, C., Altamirano, L., Cheney, M., Cheney, J., Barber, S., Price, D., … Francis, P. (2003). A Multicenter, Randomized, Double-Blind, Controlled Trial of Nebulized Epinephrine in Infants with Acute Bronchiolitis. *New England Journal of Medicine*, *349*(1), 27–35. https://doi.org/10.1056/NEJMoa022226

Weber, A., Weber, M., & Milligan, P. (2001). Modeling epidemics caused by respiratory syncytial virus (RSV). *Mathematical Biosciences*, *172*(2), 95–113. Retrieved from

http://www.ncbi.nlm.nih.gov/pubmed/11520501

Weber, M. W., Mulholland, E. K., & Greenwood, B. M. (1998). Respiratory syncytial virus infection in tropical and developing countries. *Tropical Medicine & International Health : TM & IH*, *3*(4), 268–80. Retrieved from http://www.ncbi.nlm.nih.gov/pubmed/9623927

Wegmann, U., Carvalho, A. L., Stocks, M., & Carding, S. R. (2017). Use of genetically modified bacteria for drug delivery in humans: Revisiting the safety aspect. *Scientific Reports*, *7*(1), 2294. https://doi.org/10.1038/s41598-017-02591-6

Werle, M., & Bernkop-Schnürch, A. (2006). Strategies to improve plasma half life time of peptide and protein drugs. *Amino Acids*, *30*(4), 351–367. https://doi.org/10.1007/s00726-005-0289-3

Wu, P., & Hartert, T. V. (2011). Evidence for a causal relationship between respiratory syncytial virus infection and asthma. *Expert Review of Anti-Infective Therapy*, *9*(9), 731–745. https://doi.org/10.1586/eri.11.92

Xu, M., McCanna, D. J., & Sivak, J. G. (2015). Use of the viability reagent PrestoBlue in comparison with alamarBlue and MTT to assess the viability of human corneal epithelial cells. *Journal of Pharmacological and Toxicological Methods*, *71*, 1–7. https://doi.org/10.1016/j.vascn.2014.11.003

Yu, Q., Hardy, R. W., & Wertz, G. W. (1995). Functional cDNA clones of the human respiratory syncytial (RS) virus N, P, and L proteins support replication of RS virus genomic RNA analogs and define minimal trans-acting requirements for RNA replication. *Journal of Virology*, *69*(4), 2412–9. Retrieved from http://www.ncbi.nlm.nih.gov/pubmed/7884888

CHAPTER 6 – APPENDIX

APPENDIX

Primer Set	Construct	Forward Primer (5' – 3')	Reverse Primer (5' – 3')
A	His_6-S-hTrx-9R-$RSVP_{220-241}$	GGCAATGATTCAGATA ACGATTTGTCTTTGGAG GATTTTTAACTCGAGCA CCACCACC	ATC TGA ATC ATT GCC CTC GAG GAG ATT GTT CAG CTT TTC ACC TCT TCT TCT TCT TCT TCT T
B	His_{10}-9R-S-hTrx-9R-$RSVP_{220-241}$	CGC CGT AGA AGA CGT AGA CGT AGA CGC GGT TCT TCT GGT CTG GTG CCA C	ACG TCT TCT ACG GCG TCC GTG ATG GTG GTG ATG ATG ATG ATG GTG CAT
C	HisMBP-NLS-P_{1-29}	ACC GCA CGT AAC AAT GCG GAT GAA GGT CAT TTT GAA CCA GCT TTC AAG GAA ATG TAA GAC CCA GCT TTC TTG TAC AA	ATT GTT ACG TGC GGT TTT AAA CAG TTC GGA TAT TTT TCC CTT GAA TGT ACG ACG TCG TTG ACG GCG

Table 6.1: Forward and Reverse Primers used in Inverse PCR. All of the primers used in this study are listed above and were designed to be compatible with the In-Fusion® Cloning System. The first 15 nucleotides of the forward primer at their 5' was designed to be complementary to the first 15 nucleotides at the 5' end on the reverse primer and vice versa.

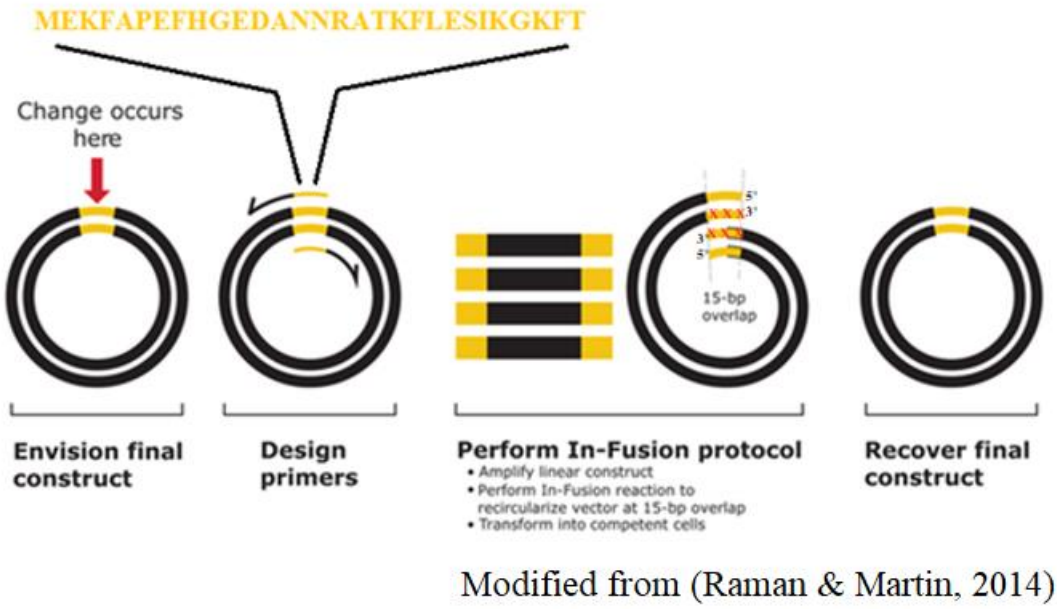

Figure 6.2 Overview of the Inverse PCR and In-Fusion® Cloning System Process Using $P_{220-241}$ as an example. The method is a modified description of the protocol described in Raman & Martin (2014). The first step was to choose an appropriate plasmid, hTrx Δcys5 and MBP-$P_{220-241}$ plasmids. The second step was to design primers that have 15 nucleotides that are complementary to each other at their 5' end so that they can overlap with each other. The yellow part of the primer correspond to the nucleotide sequence of the amino acids of $P_{220-241}$, His_{10}-9R or P_{1-29} to be inserted and the black part of the primer correspond to the nucleotide sequence complementary to the plasmid. Inverse PCR was used to amplify the template vector with the appropriate primers to generate a linearized plasmid containing the inserted DNA, which was then purified by gel extraction. Next, the linearized plasmid was incubated with the In-Fusion HD enzyme premix, which functions as a 3'-5' exonuclease to generate single-stranded 5' overhangs at the termini. These loose overhangs annealed together and circularized the plasmid, which was then transformed into *E. coli* DH5α chemically competent cells and plated on LB agar plates with the appropriate antibiotic. The colonies were grown, plasmid preparations were conducted, and the resulting plasmids were sent to MOBIX laboratory to confirm their sequences using T7 promoter forward and reverse primers (Raman, M., Martin, 2014).

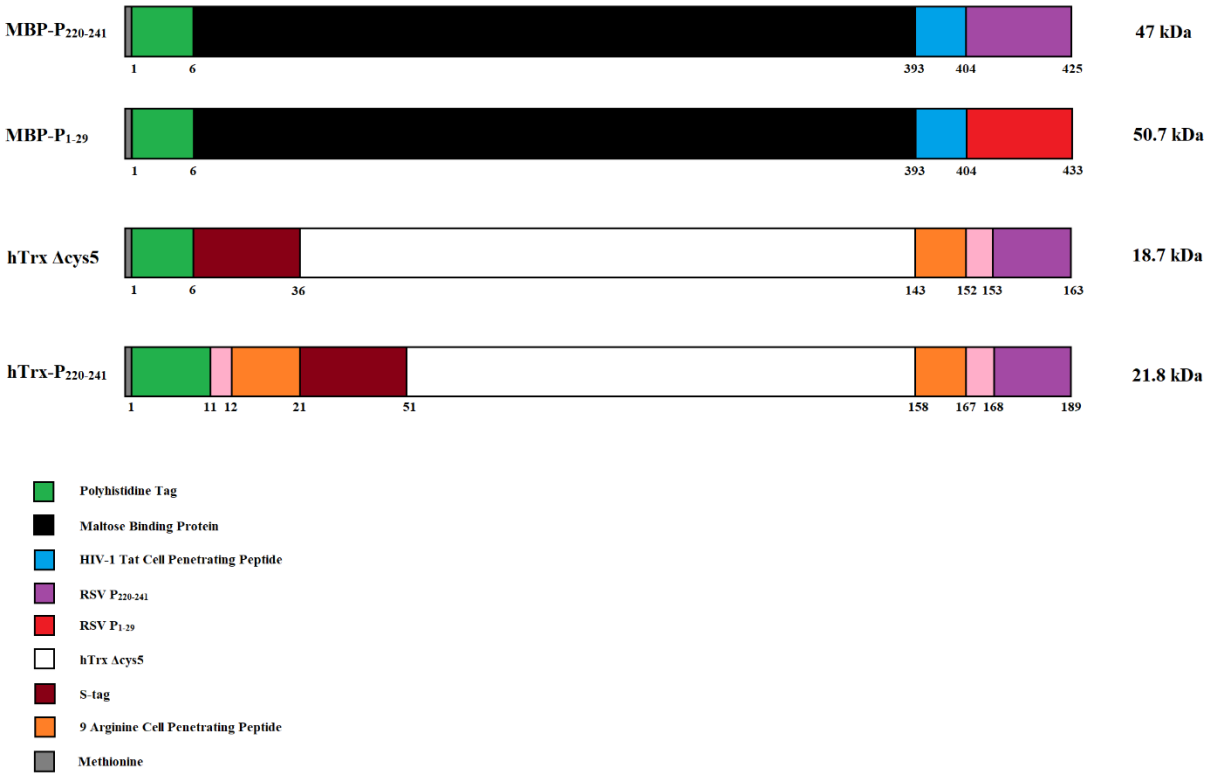

Figure 6.3 Boxcar diagrams of recombinant proteins used in this study. Boxcar diagrams depicting visually the components of the various recombinant peptide mimetics used in this study. The numbers underneath each construct represent the number of amino acids.

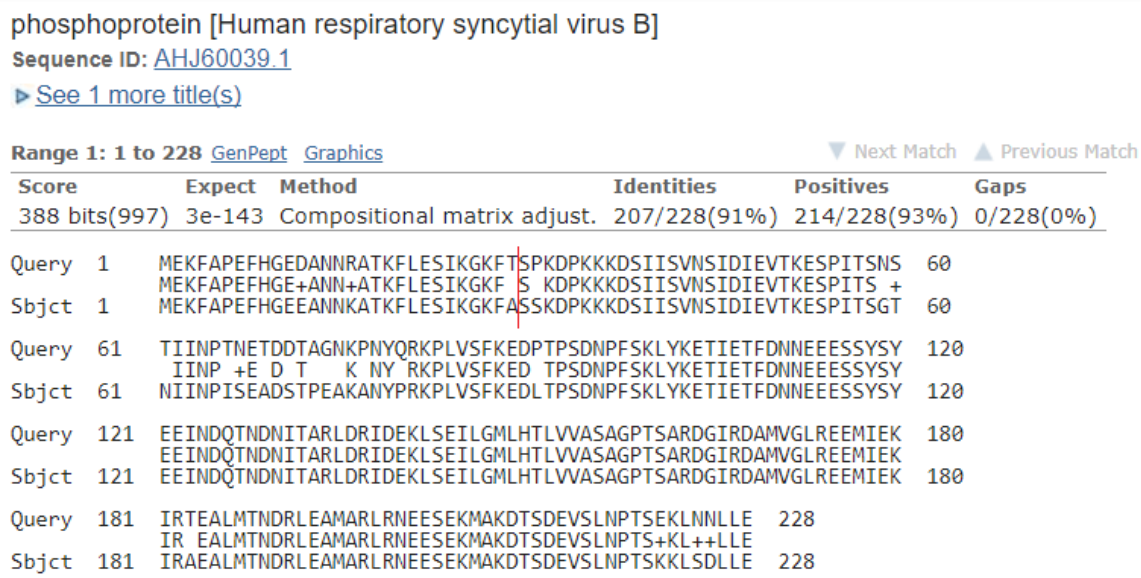
phosphoprotein [Human respiratory syncytial virus B]
Sequence ID: AHJ60039.1
See 1 more title(s)

Range 1: 1 to 228 GenPept Graphics Next Match Previous Match

Score	Expect	Method	Identities	Positives	Gaps
388 bits(997)	3e-143	Compositional matrix adjust.	207/228(91%)	214/228(93%)	0/228(0%)

```
Query  1    MEKFAPEFHGEDANNRATKFLESIKGKFTSPKDPKKKDSIISVNSIDIEVTKESPITSNS  60
            MEKFAPEFHGE+ANN+ATKFLESIKGKF S KDPKKKDSIISVNSIDIEVTKESPITS +
Sbjct  1    MEKFAPEFHGEEANNKATKFLESIKGKFASSKDPKKKDSIISVNSIDIEVTKESPITSGT  60

Query  61   TIINPTNETDDTAGNKPNYQRKPLVSFKEDPTPSDNPFSKLYKETIETFDNNEEESSYSY  120
             IINP +E D T   K NY RKPLVSFKED TPSDNPFSKLYKETIETFDNNEEESSYSY
Sbjct  61   NIINPISEADSTPEAKANYPRKPLVSFKEDLTPSDNPFSKLYKETIETFDNNEEESSYSY  120

Query  121  EEINDQTNDNITARLDRIDEKLSEILGMLHTLVVASAGPTSARDGIRDAMVGLREEMIEK  180
            EEINDQTNDNITARLDRIDEKLSEILGMLHTLVVASAGPTSARDGIRDAMVGLREEMIEK
Sbjct  121  EEINDQTNDNITARLDRIDEKLSEILGMLHTLVVASAGPTSARDGIRDAMVGLREEMIEK  180

Query  181  IRTEALMTNDRLEAMARLRNEESEKMAKDTSDEVSLNPTSEKLNNLLE  228
            IR EALMTNDRLEAMARLRNEESEKMAKDTSDEVSLNPTS+KL++LLE
Sbjct  181  IRAEALMTNDRLEAMARLRNEESEKMAKDTSDEVSLNPTSKKLSDLLE  228
```

Figure 6.4 Amino Acid Alignment of RSV A and RSV B Phosphoproteins. ProteinBlast was used to align the amino acid sequence of RSV A phosphoprotein (GenBank: AHV80722.1) and RSV B phosphoprotein (AHJ60039.1). There is 93% total amino acid similarity between the two proteins. To the left of the red line, the first 29 amino acids of the RSV A and RSV B phosphoprotein are aligned. The differences in amino acids between RSV A and B are in regions not essential for the N°-P interaction.